

DEEP DRILLING IN THE HIGHLY LAMINATED PINEDALE ANTICLINE:  
DOWNHOLE VIBRATIONS STUDY AND BIT DYSFUNCTION DIAGNOSIS

A Thesis

by

CHARLES BRANDON MANN

Submitted to the Office of Graduate and Professional Studies of  
Texas A&M University  
in partial fulfillment of the requirements for the degree of

MASTER OF SCIENCE

Chair of Committee, Samuel F. Noynaert  
Committee Members, Eduardo Gildin  
Satish T.S. Bukkapatnam  
Head of Department, A. Daniel Hill

December 2015

Major Subject: Petroleum Engineering

Copyright 2015 Charles Brandon Mann

## ABSTRACT

Ultra Petroleum has been drilling in the Pinedale Anticline in Wyoming since 2003. At that point in time, wells could take as much as 75 days to reach target depth. In the first quarter of 2015, Ultra Petroleum, has greatly reduced their spud to target depth time to 9 days. However, despite their drastic improvement in performance over the years, Ultra's current performance has seemed to have plateaued due to consistently occurring non-productive time on each well resulting from as many as three bit trips to replace damaged drill bits, while drilling the 6 inch production hole. Hours spent tripping in and out of the hole to replace worn drill bits is extremely costly. In the third quarter of 2014, Ultra in an effort to improve performance, began a concerted effort to target this problem area and improve performance. After training Ultra Petroleum personnel on a physics-based, continuous improvement set of practices, Ultra Petroleum's performance increased significantly. In addition to the training, Ultra Petroleum and Texas A&M University examined their operations performance and practices using downhole drilling dynamics data. After the analysis, suggestions were made for engineering redesign possibilities. The objective of this study is to determine the in-situ dynamics state of the bottom hole assembly and drill bit, and how this excited vibrational state contributes to the bit damage seen from the drill bits pulled out of the well. This thesis will document that students work and findings. In order to accomplish this goal downhole dynamics measurements were studied to determine the specific vibrations present in the drilling of these wells. In addition these measurements were

used to determining the severity of each vibration type and the effectiveness of specific drilling equipment at mitigating their negative effects on performance and tool life. Meaningful results were obtained from the downhole dynamics measurements that provide both knowledge to the operator and suggestions for ways to improve performance and tool life, and include conclusions regarding the effectiveness of roller reamers and depth of cut control bits in reducing torsional oscillation, the effectiveness of full-gauge stabilization and extended gauge bits at reducing lateral vibrations, and hypotheses about the effectiveness of incorporating some specific tools and techniques for performance improvement.

## ACKNOWLEDGEMENTS

The author would like to thank Ultra Petroleum, its vendors, rig crews, and contractor personnel who have worked hard to develop and implement new practices to extend well performance in Pinedale, Wyoming. Their insights, encouragement, and assistance were crucial to this research.

The author would also like to thank Fred E. Dupriest, P.E. for helping him establish a relationship with Ultra Petroleum, arranging for this research to be performed, and for his continuous guidance and willingness to discuss the physics behind the dynamic dysfunctions present in this study throughout the research process. The knowledge he shared in his courses at Texas A&M University and in one-on-one discussions fostered the author's development as a Drilling Engineer. He has been a wonderful mentor throughout the author's graduate studies.

The author wishes to thank Eric van Oort, Ph.D. for inspiring him to become a Drilling Engineer, serving as a mentor during his undergraduate work at the University of Texas at Austin, introducing him to the field of Drilling Engineering, and recommending him for entry into the graduate program.

In addition the author would like to thank Samuel F. Noynaert, Ph.D., Committee Chair, for his steady support and unwavering patience throughout the completion of this study and thesis as well as Eduardo Gildin, Ph.D. and Satish T.S. Bukkapatnam, Ph.D., Committee Members, for their support throughout this study. Also the author wishes to thank Jerome Schubert, Ph.D. for kindly serving as a substitute committee member during his final examination.

Finally, the author wishes to thank his family and friends for their love, inspiration, and encouragement during his graduate studies.

## TABLE OF CONTENTS

	Page
ABSTRACT .....	ii
ACKNOWLEDGEMENTS .....	iv
TABLE OF CONTENTS .....	vi
LIST OF FIGURES.....	viii
LIST OF TABLES .....	xvi
1. INTRODUCTION.....	1
1.1 Literature review .....	1
Stick-slip.....	1
Buckling .....	8
Whirl.....	9
Coupled stick-slip and whirl .....	18
Mechanical specific energy.....	34
Pinedale Anticline lithology and drilling considerations.....	41
1.2 Provided information.....	60
2. PROBLEM STATEMENT .....	61
3. METHODS.....	62
3.1. Mechanical specific energy.....	62
3.2. Drill bit forensics analysis.....	62
3.3. Memory-based vibration recording subs.....	64
3.4. Measurement while drilling (MWD) and open hole well logging ....	67
4. OBJECTIVES AND PROCEDURES .....	69
4.1. Physics-based continuous improvement practices.....	70
4.2. Roller reamers .....	72
4.3. Extended gauge length bits .....	73
4.4. Depth of cut control bits.....	75
4.5. Active torque control.....	77
4.6. Larger diameter drill pipe .....	77
4.7. Procedure.....	78

5.	RESULTS.....	83
5.1.	High level vibrations overview.....	83
5.2.	Equipment involved in each well.....	89
5.3.	Early observations.....	92
5.4.	Effectiveness of lateral stability.....	96
5.5.	Discovery of resonance speeds.....	111
5.6.	Finding the onset of torsional oscillation.....	113
5.7.	Closer look at STO.....	130
6.	DISCUSSION AND SUMMARY.....	144
6.1.	Bit wear and modes of failure.....	144
6.2.	Stick-slip, STO, and operations management.....	151
6.3.	Roller reamers.....	156
6.4.	Extending the gauge on drill bits.....	157
6.5.	Larger diameter drill pipe.....	158
6.6.	Soft-Speed™ response system.....	162
6.7.	Depth of cut control effectiveness.....	163
6.8.	Managing vibrations levels.....	168
6.9.	Further research.....	170
	NOMENCLATURE.....	174
	REFERENCES.....	177
	APPENDIX A: INFORMATION PROVIDED BY ULTRA PETROLEUM.....	185

## LIST OF FIGURES

	Page
Fig. 1.1 – Drillstring vibration types .....	1
Fig. 1.2 – Fully developed stick-slip showing periods where the bit and BHA completely stop (Drillstring Vibrations and Vibration Modeling 2010).....	3
Fig. 1.3 – PDC cutter damage from stick-slip (Robnett et al. 1999).....	4
Fig. 1.4 – Torque and rotary speed response to fully developed stick-slip (Fear et al. 1997).....	5
Fig. 1.5 – Depth of cut element limits cutter indentation (Davis et al. 2012).....	7
Fig. 1.6 – Active damping eliminates stick-slip in two cycles (Kriesels et al. 1999) .....	8
Fig. 1.7 – PDC cutter wear on bit that stopped drilling (Warren et al. 1990).....	10
Fig. 1.8 - PDC drill bits with smooth, non-active gauge profiles of increasing length (Pastusek et al. 2005) .....	11
Fig. 1.9 – Types of oscillating borehole patterns including the rippling 2D oscillation (a), spiraling 3D corkscrew (b), and hour-glassing cyclic hole enlargement (c) (Pastusek and Brackin 2003).....	15
Fig. 1.10 – Vibration index decreases with increasing rotary speed during BHA flexing or buckling (a), while it increases with increasing rotary speed during “twirl” or forward synchronous whirl (b) (Bailey et al. 2010).....	16
Fig. 1.11 – Measured downhole angular velocity versus time shows the dysfunction type as a function of downhole rotational speed (Leine and van Campen 2002).....	19
Fig. 1.12 – Measured downhole bending moment versus surface angular velocity showing the sweep-up trend of stick-slip followed by sweep down trend of whirl (Leine and van Campen 2002) .....	20



Fig. 1.13 – Measured downhole friction curve showing the torque losses associated with both stick-slip and whirl (Leine and van Campen 2002).....	20
Fig. 1.14 – MWD failure rate versus 1sRMS acceleration and time, fitted with a parametrical model (Reckmann et al. 2010) .....	22
Fig. 1.15 – Data distribution and ROP versus Stick-Slip Index and 1sRMS Lateral Acceleration (Reckmann et al. 2010).....	23
Fig. 1.16 – In-bit device measurement of accelerations during backward whirl (Ledgerwood et al. 2013) .....	25
Fig. 1.17 – Downhole measurement of rotational speed during stick-slip (Ledgerwood et al. 2013) .....	26
Fig. 1.18 – Bit rpm measured in-bit-device and commercial MWD tool during drill-collar torsional resonance (Ledgerwood et al. 2013) .....	27
Fig. 1.19 – Downhole measurements showing the coupling of whirl with stick-slip (Ledgerwood et al. 2013) .....	28
Fig. 1.20 – Stability diagram including the regime of HFTO (Jain et al. 2014) .....	32
Fig. 1.21 – An instance where both unstable stick-slip and first-harmonic resonance is observed in the downhole RPM and Fourier Transform (Ertas et al. 2013) .....	34
Fig. 1.22 – ROP versus WOB plots showing bit operating regions and bit founder (Dupriest and Koederitz 2005).....	37
Fig. 1.23 – Mechanical specific energy equation (Dupriest and Koederitz 2005).....	38
Fig. 1.24 – The Greater Green River Basin Geologic Structure (Gibson 1997).....	42
Fig. 1.25 – Pinedale Anticline Map (Gray et al. 2002) .....	44
Fig. 1.26 – Pinedale Anticline Formations (Bowker and Robinson 1997) .....	44
Fig. 1.27 – Pinedale Anticline Geological Cross Section (Gray et al. 2002).....	45
Fig. 1.28 – Structural Time-Interpretation of the Lower Lance (Gray et al. 2002).....	46

Fig. 1.29 – Map-view of the migrated fracture intensity Lower Lance horizon (Gray et al. 2002) .....	46
Fig. 1.30 – P-waves show high intensity fracturing in zones of high stress (on west side and on crest of anticline) (Gray et al. 2002) .....	47
Fig. 1.31 – S-waves confirm high intensity fracturing using amplitude versus offset (AVO) methods (Gray, David et al. 2003).....	47
Fig. 1.32 – Multiple reservoirs with high density natural fractures around a good gas well in the Pinedale Anticline (Gray, David et al. 2003).....	48
Fig. 1.33 – Visualization of geobodies with high natural fracture density between Upper Lance and Mesaverde formations (Gray, David et al. 2003) .....	48
Fig. 1.34 – Slim-hole well plan for Pinedale Anticline (courtesy of Ultra Petroleum) .....	50
Fig. 1.35 – Diagram of a PDC drill bit (Gent et al. 2009).....	54
Fig. 1.36 – Enhanced lateral stability feature development (Gent et al. 2009).....	55
Fig. 1.37 – Baker Hughes 2-cone/4-blade Kymera FSR Hybrid Drill Bit showing.....	57
Fig. 1.38 – Multidimensional non-planar cutter (DiGiovanni et al. 2014).....	59
Fig. 3.1 – Bit forensics diagram (courtesy of Halliburton).....	64
Fig. 3.2 – Capabilities of NOV downhole dynamics tools (courtesy of NOV).....	66
Fig. 3.3 – Spectral gamma ray logging shows increased total organic carbon Courtesy of Texas A&M University).....	68
Fig. 4.1 – Example ROP versus WOB plot showing bit founder and redesign opportunities for the operator.....	71
Fig. 4.2 – Bit tilt, which is the angle measured between the bit axis and bore axis, can be reduced with extended gauge bits by reducing the amount of distance a bit can rotate or tilt off center before making contact with the borehole wall (Pastusek et al. 2005).....	74

Fig. 4.3 – Reduced gauge activity reduces side cutting, severity of lateral vibrations, and borehole patterns (Dupriest and Sowers 2010).....	75
Fig. 4.4 – When the rubbing surfaces make contact with the bottom of the hole they prevent over-engagement of the cutters into the formation being drilled by carrying some of the applied axial load (Davis et al. 2012).....	76
Fig. 4.5 – Bit forensic pictures from Wells 1, 2, and 3 respectively.....	79
Fig. 5.1 – Surface and downhole measurements versus time Well 1 Bit Run 2.....	83
Fig. 5.2 – Asymmetric torque signature during full stick-slip.....	86
Fig. 5.3 – Stick-slip observed by MSE.....	87
Fig. 5.4 – Synchronous Torsional Oscillation observed by MSE.....	88
Fig. 5.5 – Standard BHA design (Courtesy of NOV).....	92
Fig. 5.6 – Lateral bit acceleration versus DOC in the upper production interval.....	93
Fig. 5.7 - Lateral bit acceleration versus DOC in the lower production interval.....	95
Fig. 5.8 – Lateral bit acceleration versus DOC Well 1 Bit Run 1.....	97
Fig. 5.9 – Lateral bit acceleration versus DOC Well 2 Bit Run 1.....	98
Fig. 5.10 – Lateral bit acceleration versus DOC Well 3 Bit Run 1.....	98
Fig. 5.11 – Tangential bit acceleration versus DOC for Well 1 Bit Run 1.....	100
Fig. 5.12 – Tangential bit acceleration versus DOC for Well 2 Bit Run 1.....	101
Fig. 5.13 – Tangential bit acceleration versus DOC for Well 3 Bit Run 1.....	101
Fig. 5.14 – Lateral BHA acceleration versus downhole WOB showing whirl pattern.....	104
Fig. 5.15 – Lateral BHA acceleration versus surface WOB showing whirl pattern.....	106
Fig. 5.16 – Lateral BHA acceleration versus downhole WOB Well 1 Bit Run 1.....	107
Fig. 5.17 – Lateral BHA acceleration versus surface WOB Well 1 Bit Run 1.....	108

Fig. 5.18 – Lateral BHA acceleration versus surface WOB Well 2 Bit Run 1.....	108
Fig. 5.19 – Lateral BHA acceleration versus surface WOB Well 3 Bit Run 1.....	109
Fig. 5.20 – Lateral BHA accelerations versus rotary speed Well 1 Bit Run 1.....	111
Fig. 5.21 – Lateral BHA accelerations versus rotary speed Well 2 Bit Run 1.....	112
Fig. 5.22 – Lateral BHA accelerations versus rotary speed Well 3 Bit Run 1.....	112
Fig. 5.23 – Lateral bit acceleration versus downhole torque for Well 1 Bit Run 1.....	115
Fig. 5.24 – Lateral bit acceleration versus surface torque for Well 1 Bit Run 1.....	115
Fig. 5.25 – Lateral bit acceleration versus downhole torque for Well 1 Bit Run 2.....	116
Fig. 5.26 – Lateral bit acceleration versus surface torque for Well 1 Bit Run 2.....	116
Fig. 5.27 – Lateral bit acceleration versus surface torque for Well 2 Bit Run 1.....	119
Fig. 5.28 – Lateral bit acceleration versus surface torque for Well 3 Bit Run 1.....	120
Fig. 5.29 – DSSI versus downhole torque for Well 1 Bit Run 2.....	122
Fig. 5.30 – DSSI versus surface torque for Well 1 Bit Run.....	123
Fig. 5.31 – DSSI versus surface torque for Well 2 Bit Run 1.....	125
Fig. 5.32 – DSSI versus surface torque for Well 3 Bit Run 1.....	125
Fig. 5.33 – Bit RPM versus downhole torque for Well 1 Bit Run 2.....	127
Fig. 5.34 – Bit RPM versus surface torque for Well 1 Bit Run 2.....	128
Fig. 5.35 – Bit RPM versus surface torque for Well 2 Bit Run 1.....	129
Fig. 5.36 – Bit RPM versus surface torque for Well 3 Bit Run 1.....	129
Fig. 5.37 – Vibrational state of the bit during a period of STO.....	130
Fig. 5.38 – DOC versus time for a period of STO.....	132
Fig. 5.39 – Well-developed full stick-slip preceding a period of STO.....	133

Fig. 5.40 – Onset and periods of STO between periods of stick-slip.....	135
Fig. 5.41 – Sustained period of STO.....	136
Fig. 5.42 – STO and its relationship with WOB (Courtesy of NOV).....	138
Fig. 5.43 – Fast Fourier Transform analysis of a period of STO.....	140
Fig. 5.44 – Period in which various dysfunction occurs.....	142
Fig. 6.1 – Unique location of bit wear.....	145
Fig. 6.2 – Close up of lateral impact damage.....	146
Fig. 6.3 – Close up of thermal wear and degradation on PDC cutters from Well 2 (Courtesy of Ultra Petroleum).....	150
Fig. 6.4 – Thermal damage starting on PDC cutter (Courtesy of Ultra Petroleum).....	151
Fig. 6.5 – MSE response to full stick-slip (a) and STO (b).....	154
Fig. 6.6 – Torsional deflection and polar moment of inertia equations for a hollow circular shaft (Davis et al. 2012).....	159
Fig. 6.7 – Polar moment of inertia results for various drill pipe sizes and weights.....	160
Fig. 6.8 – Results of fourth-order diameter ratio calculation.....	161
Fig. 6.9 – DOC versus time Well 1 Bit Run 1 (a) and Bit Run 2 (b).....	165
Fig. 6.10 – DOC versus time Well 2 Bit Run 1 (a) and Well 3 Bit Run 1 (b).....	166
Fig. 6.11 – BHA lateral accelerations versus DSSI.....	169

## LIST OF TABLES

	Page
Table 5.1 – Differences between BHA designs in each well.....	90
Table 5.2 – Peak RMS Lateral BHA Accelerations for each well.....	110

# 1. INTRODUCTION

## 1.1 Literature review

### Stick-slip

There are various vibrational frequencies that exist in the drillstring as a part of the drilling process, but it is common to group them into three types of vibration, torsional (rotation), axial (bit bounce), and lateral (sideways/circular whirl) (Reckmann et al. 2010). These vibrations types can be visualized as shown in **Fig. 1.1** below.

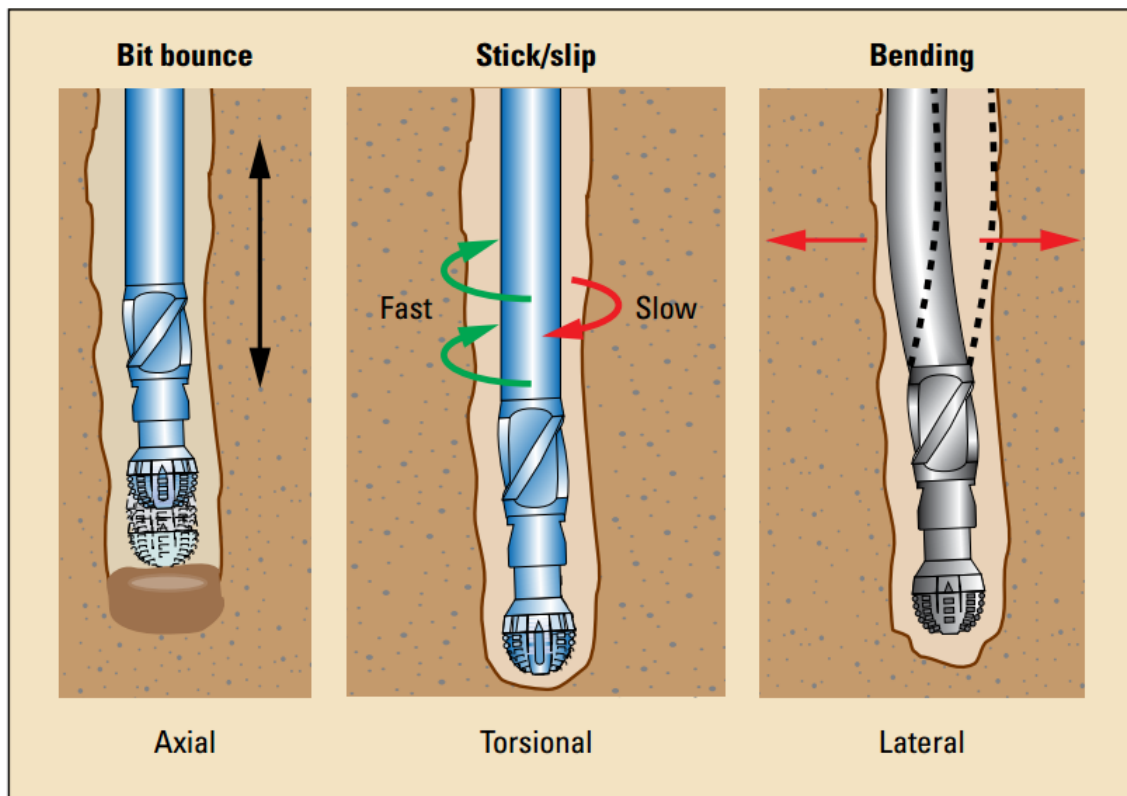


**Fig. 1.1 – Drillstring vibration types**

**(Drillstring Vibrations and Vibration Modeling 2010)**

Stick-slip is a severe type of torsional vibration that can be experienced during the drilling process that causes accelerated degradation and destruction of polycrystalline diamond compact (PDC) drill bits (Fear et al. 1997); and can be of two types: transient vibrations, which correspond to changes in the drilling condition such as heterogeneities in the rock, or stationary vibrations, that are self-induced by the components of the drillstring (Dufeyte and Henneuse 1991). Stick-slip is more widely known for its self-induced torsional vibrations, which occur periodically and are generated by frictional forces on the borehole walls, or by an inadequate drive system that is unable to break out of the cycles of torsional oscillation (Dufeyte and Henneuse 1991). It should be noted that it is not necessary for these frictional forces to be purely static in nature for these self-excited torsional drillstring vibrations to occur (Brett 1992). Stick-slip can often be observed when combining a limber bottomhole assembly (BHA) with a PDC bit that does not incorporate anti-whirl stabilization features, or if the bit is not well balanced (Fear et al. 1997);

The torsional vibrations have a period which depends on the mechanical properties of the entire drilling system, including the length of the drill string, the rotational speed of the surface rotary system, and the nature and location of the wellbore friction (Dufeyte and Henneuse 1991). These torsional vibrations can range from simple torsional oscillation where the bit does not completely stop rotating, to a more extreme condition, in which the bit and BHA completely stop and then start, which by its nature is a stick-slip motion (Detournay and Defourny 1992). The characteristic downhole RPM signature of fully developed stick-slip can be observed in **Fig. 1.2**.



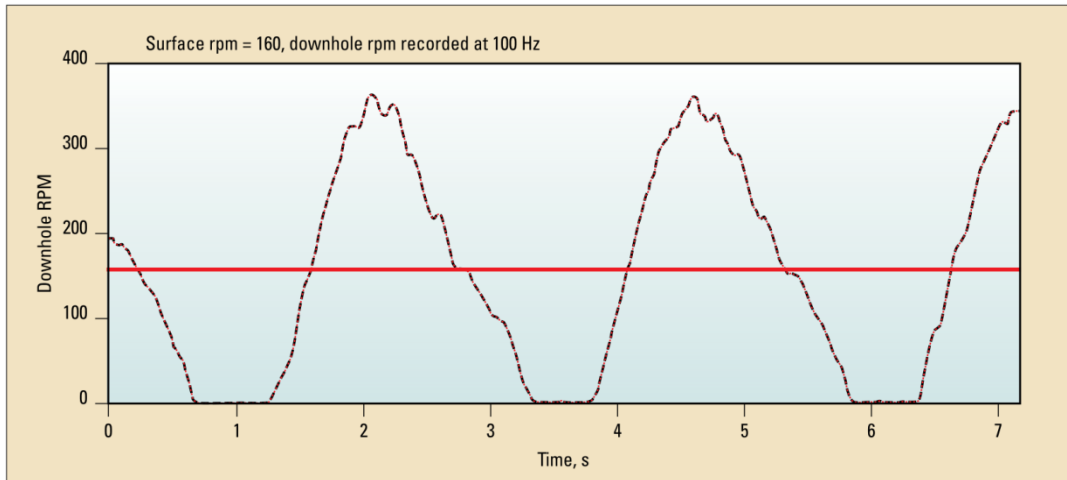


**Fig. 1.2 – Fully developed stick-slip showing periods where the bit and BHA completely stop (Drillstring Vibrations and Vibration Modeling 2010)**

“Stick-slip vibrations induced in the drilling assembly increase bit wear and can results in premature fatigue failure of the string or breakage of the bit itself” (Richard and Detournay 2000). This breakage of the bit, comes in the form of cutter damage occurring “after only short periods of time if a PDC bit spins backwards in relatively hard rock” (Robnett et al. 1999), and these cutters are torn off from the backside (Dufeyte and Henneuse 1991). **Fig. 1.3**, shows a representation of what this cutter damage looks like.

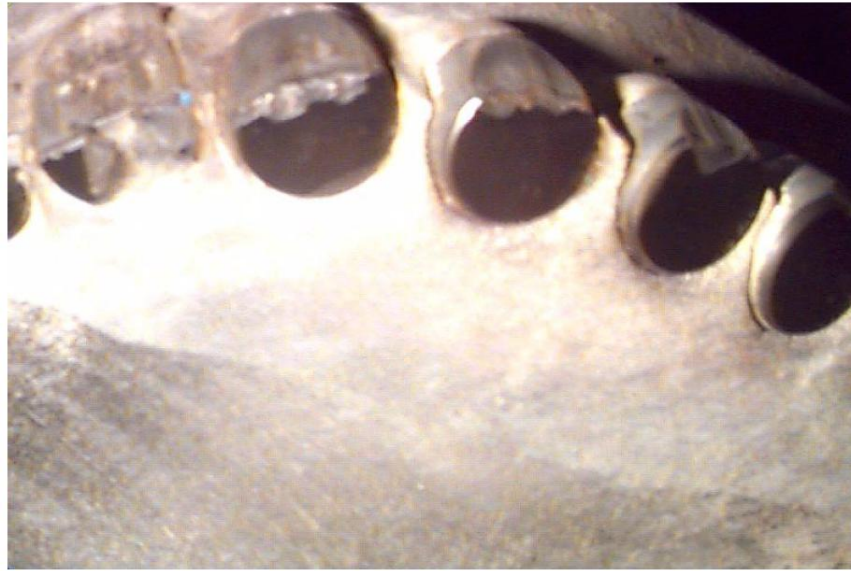


**Fig. 1.3 – PDC cutter damage from stick-slip (Robnett et al. 1999)**

While this backwards rotation can be non-damaging in softer rocks such as the Catoosa shale (1,000 psi compressive strength), it can be catastrophic in harder rocks such as the Carthage limestone (16,000 psi compressive strength), where during laboratory testing, PDC cutter damage was observed with as little as 1,000 pounds WOB (Brett 1992). Brett (1992) also noted in his experiments, that the “spalling generated by rotating backward in the laboratory is identical to that of bits that have experienced severe torsional bit vibrations in the field” and that observed damage had a “different character than the chipping observed on bits that have whirled” in that they showed the loss of “single massive chip” rather than showing the smaller and more numerous chipping that is associated with whirl.

Stick-slip can be recognized by observing surface torque measurements and looking for the following specific characteristics (Fear et al. 1997) shown in **Fig. 1.4**:

- The frequency of surface torque oscillations will decrease below the fundamental frequency, reflecting the sticking time downhole
- Peak surface torque will increase to a value approximately equal to the static torque required to break the bit/BHA free, plus the torque required to rotate the drillstring
- The observed surface torque rise is usually accompanied by a drop in surface rotary speed, which creates an inertial force opposite the string rotation
- The surface torque will drop below the level required to rotate the drillstring as the bit and BHA break free downhole

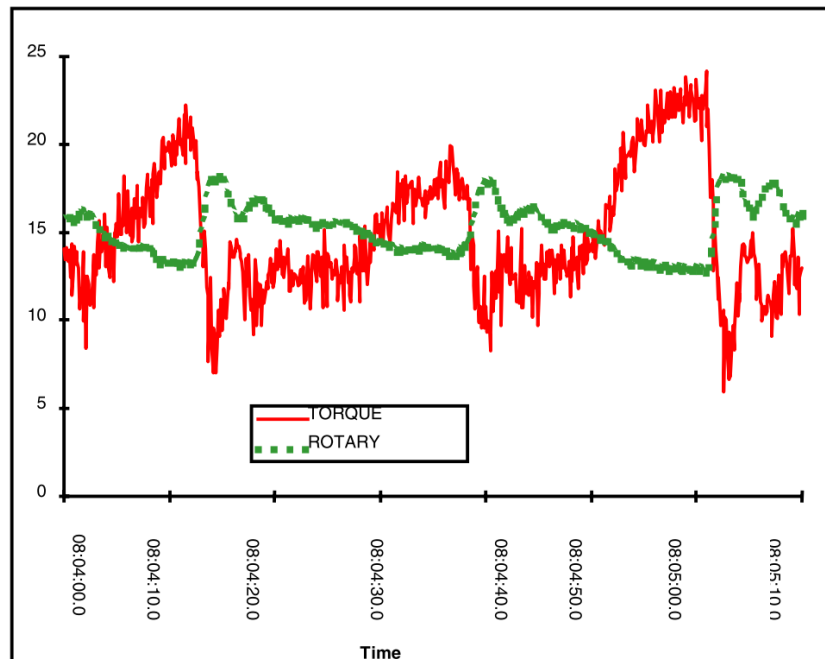


**Fig. 1.4 – Torque and rotary speed response to fully developed stick-slip (Fear et al. 1997)**

When fully developed stick-slip behavior is observed, there exists a linear rise in torque, associated with the deceleration of the BHA during the sticking phase to a maximum value, which is associated with the required torque to free the bit and BHA, followed by a drop in torque corresponding to a rapid acceleration of the BHA after it has broken free during the slip phase (Fear et al. 1997). When stick-slip is observed using real time surface data by its linear “ramping” pattern, followed by an abrupt drop-off in torque (Fear et al. 1997), it makes operational sense to both decrease the weight being applied to the bit, and to increase the surface rotary speed, because these two parameters are often closely linked and this will cause the bit behavior to become more normal (Dufeyte and Henneuse 1991). These practices were confirmed with laboratory testing, in which, in every case, torsional vibrations became worse in harder rock, at higher weight on bit, at lower rotary speeds, with PDC bits, and with duller or worn bits (Brett 1992).

Stick-slip is often studied as a torsional pendulum, coupling the axial and torsional vibrations in various modes and regimes based on the relationship between the rate of angular deviation, or rate of perturbation, and the driving rotational speed (Richard and Detournay 2000). The drill string resonance frequency is known as the first mode, or the stick-slip period (Efteland et al. 2014). Second and third modes of stick-slip can sometimes be visible using downhole dynamics recorders in wells that use thin, long, flexible drill strings (Efteland et al. 2014). Stick-slip vibrations can also be studied using fast Fourier Transforms (FFT) and other algorithms that convert time or space domains into the frequency domain to understand the drill string vibration

distribution and frequencies corresponding to each of the stick-slip modes (Efteland et al. 2014); however, a detailed review of the techniques and current practices will not be included. Conversely, a detailed discussion of the coupled nature of stick-slip to whirl will be discussed in a later section of this section.

Popular engineering redesign techniques to mitigate stick-slip can include managing bit depth of cut, increasing the drill string stiffness, and active-damping. Depth of cut management can be accomplished either operationally or with the use of depth of cut control bits containing rubbing elements that limit the indentation depth of the cutter and reduce the torque variation that sustains stick-slip, shown in **Fig. 1.5**.

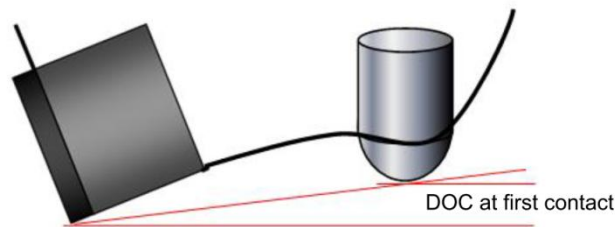


**Fig. 1.5 – Depth of cut element limits cutter indentation (Davis et al. 2012)**

Increasing the drillstring stiffness reduces the severity of the winding and unwinding and torsional deflection of the torsional spring system, and thus bit speed and torque oscillation (Davis et al. 2012). Active-damping of torsional vibrations with software that interfaces with the rig control system such as Soft-Torque™ and Soft-Speed™ can be fast and effective (Efteland et al. 2014). An example of the

effectiveness of active torque control can be seen in **Fig. 1.6**, where torsional oscillation was eliminated in two cycles.

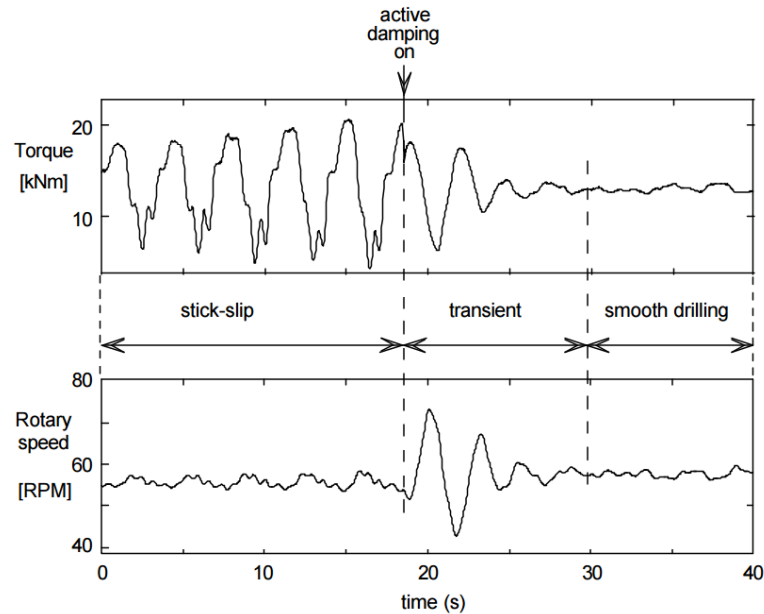


**Fig. 1.6 – Active damping eliminates stick-slip in two cycles (Kriesels et al. 1999)**

## **Buckling**

Buckling in the drillstring is likely present in the wells that Ultra Petroleum has drilled and will continue to drill, therefore it needs to be considered in this study. In the absence of weight on bit and assuming a perfectly straight vertical hole, the drill string will be straight also (Lubinski 1950). As weight is applied, the critical value of weight is reached for which the drill string fails to remain straight because it can no longer remain stable (Lubinski 1950). When this happens, the drill string contacts the borehole wall at a point of tangency with an associated contact force (Lubinski 1950). As even more

weight is applied, another critical value is reached in which the drill string makes contact with the borehole wall at a second location; this process repeats and an increasing number of contact points between the drill string and borehole wall emerge as the weight applied to the bit increases (Lubinski 1950). As higher orders of buckling are encountered there develops some reversing stresses, which increase with the diameter of the hole and can result in fatigue failure of the drill string (Lubinski 1950). Also, as higher orders of buckling are encountered the shape of the buckled string changes, the location points of tangency and maximum fatigue stress change, the magnitude of the force between the buckled pipe and the borehole wall increases, and the angle of inclination of the drill bit and subsequently the angle of force on the bit increases (Lubinski 1950). These changes can increase the likelihood of drillstring failure, promote the creation of inefficient borehole patterns, and increase wellbore deviation.

### **Whirl**

Polycrystalline Diamond Compact (PDC) bits can achieve rates of penetration (ROP) several times those of three-cone bits. However, due to accelerated bit wear, their drill rates can fall quickly to the three-cone baseline, resulting in performance that can actually be much worse than that of a three-cone bit (Brett et al. 1990). As PDC bits wear, they develop a wear-flat area in the matrix holding the diamond table, but as long as the diamond table lips are still present, and not worn away, the PDC bit can drill at rates almost as fast as a new bit (Brett et al. 1990). **Fig. 1.7** shows the wear-flats that can develop from whirl and stop drilling.

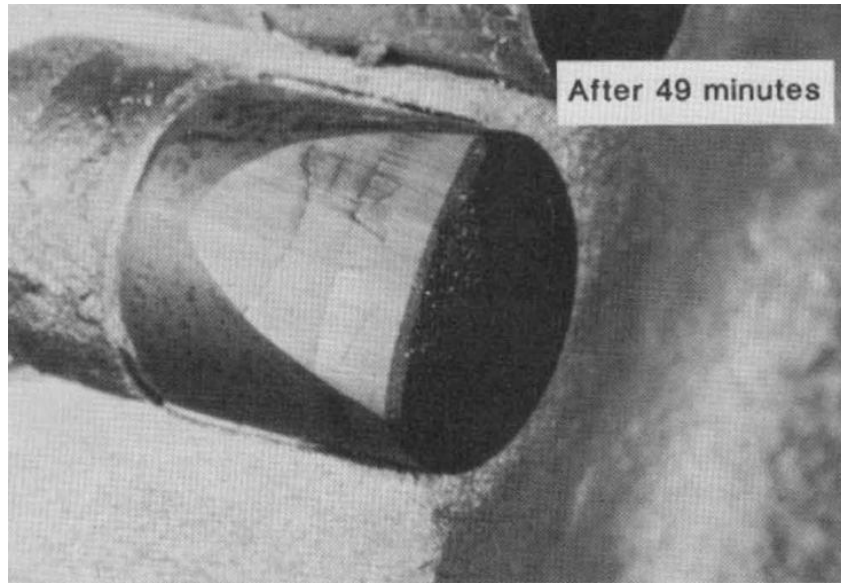


**Fig. 1.7 – PDC cutter wear on bit that stopped drilling (Warren et al. 1990)**

Rather than thermal degradation, which is typically easily managed by forced convection from mud flow, the primary mechanism of wear on PDC bits is a result of cutter chipping caused by impact force on the face of the diamond table and can prevent their application in harder formations (Brett et al. 1990). PDC application can also be limited when rocks are too “ratty” or too inhomogeneous for acceptable performance (Warren et al. 1990). In laboratory test, it is not uncommon to see chipping on PDC bits after two feet of drilling. The steady-state loads applied to cutters during most drilling situations are too low to cause cutter chipping but impact loading caused by bit vibrations would explain why chipping occurs (Brett et al. 1990). Bit whirl also causes these detrimental impact loads, by a phenomenon where the bit moves primarily laterally around the hole (Brett et al. 1990). A whirling bit can move sideways, backwards, and farther per revolution than a true rotating bit. The result of this motion



is that the bit is subjected to higher impact loads (Brett et al. 1990). Two factors cause whirl to regenerate while drilling, first, the centrifugal force that pushes the bit towards the borehole wall becomes exaggerated at high rotary speeds, as higher rotational speeds results in much larger side forces and displacement (Warren et al. 1990), and second, the center of rotation of the bit (Brett et al. 1990). The deviation of a bit from its center of rotation can cause non-axisymmetric loading of the bit, which in turn promotes whirl and its damaging effects. This can be combated with the use of smooth, long, non-active gauge profiles (shown in **Fig. 1.8**), and has been proven in laboratory and field experiments, resulting in smaller responses to side loads (Pastusek et al. 1992).



**Fig. 1.8 - PDC drill bits with smooth, non-active gauge profiles of increasing length  
(Pastusek et al. 2005)**

When a bit whirls, it can cut over-gauge holes, the cutters move faster, and forces are generated to reinforce the tendency to stay in a whirling state. The lateral vibrations and movements during bit whirl are associated with a borehole pattern, which can oftentimes include the creation of ledges and boreholes so large that the bit loses contact with the wellbore wall. The magnitude of bit acceleration associated with whirl can be over 100g (Brett et al. 1990).

A variety of ways to mitigate bit whirl have been proposed, including bit stability and balanced cutting structure design, drill string stabilization above the bit face, stabilization of the bit face with whirl-arresting features, the use of chamfers and other cutter-edge geometries, bit gauge profile, and operating procedures. Small displacements in the position of the bit require large amounts of restoring or realignment force to prevent whirl (Warren et al. 1990). Ensuring that the rotation is properly aligned, balanced, and properly confined by use of low-friction bearing or stabilizers is key to preventing whirl (Warren et al. 1990). This will simultaneously, prevent the creation of ledges caused by intermittent bit whirl in the borehole and thus will prevent stabilizers from becoming hung up (Warren et al. 1990). When attempting to stabilize the bit face for the purposes of reducing whirl the focus is on stopping whirl before it starts. If the bit is perturbed such that its alignment moves slightly off center, the center of rotation can change severely, causing the bit to “walk” around the hole. This walking is associated with very large sustained side forces that can promote the stability of the whirling condition over the non-whirling condition (Warren et al. 1990). One technique for stabilizing the bit and preventing whirl, is to reduce the bits aggressiveness. As the

cutting structure becomes more aggressive, the tendency for the bit to “grab” the borehole wall increases and thus increases the chance of initiating whirl; this is promoted by sharp, right angle edges from reduced back rake angles on the bit (Warren et al. 1990).

When designing or selecting an anti-whirl bit, some important design rules should be considered. These include the magnitude of the imbalance force and its direction with regards to the cutting structure, the size and location of the cutter devoid area, the gauge style, and the cutter back rake (Cooley et al. 1992). Typically, cutters are positioned on the bit face until the desired or required stability is achieved, which is a function of total force and force direction. The goal is to create a cutting structure in which the sum of the cutting forces equates to zero value in the center of the bit, however, this is near impossible and there exists on every anti-whirl bit, a sector or location where cutting elements are placed that decreases the bit stability (Cooley et al. 1992). In practice, the aim of these anti-whirl bits is to reduce the vibrations level and to reduce borehole patterns (Cooley et al. 1992).

Changing the bit profile is another technique for mitigating whirl, being a flat-profile bit is less prone to whirl than a more tapered-profile bit (Warren et al. 1990). Subsequent works after Warren, et al. further this work and notes that a bit’s gauge length, gauge profile, and gauge aggressiveness need to be considered when evaluating the steerability, while simultaneously trying to reduce whirl (Dupriest and Sowers 2010). Other methods to suppress whirl include lowering the frictional contact between the bit gauge and the borehole wall as well as designing a bit with cutters in a deep cone. Bits

with this design can also reduce the effects of whirl by resisting lateral movement, due to their nature of opposing the whirl generated from the cutters located outside the cone (Warren et al. 1990).

Major efforts have recently been made in the industry to eliminate drilling inefficiencies related to whirl, especially with the widespread practice of directional drilling. The major concern to directionally drilling, while attempting to eliminate whirl, is related to being able to achieve acceptable built rates. Subsequently, the effects of reduced side-cutting or non-active gauge and extended bit-gauge lengths have been studied to show their effects on steerability, and whirl-induced borehole patterns. Several major issues need to be considered when drilling directional wells: tool face control, dogleg severity (DLS), borehole quality (Pastusek and Brackin 2003), eliminating bit and BHA vibrations, and accurately predicting bit-BHA build rates (Pastusek et al. 2005). Of these consideration, the first two are constrained by the planned well geometry, and thus cannot be altered while attempting to meet the objective; however, borehole quality and bit-BHA vibrations are aspects that can be controlled, both by design and operational practices. Certain bit designs and system parameters can result in oscillating borehole patterns including hole spiraling, rippling, and hour-glassing that can be persistent (shown in **Fig 1.9**) and can affect torque and drag while drilling, log quality, and the ability to run casing (Pastusek and Brackin 2003).

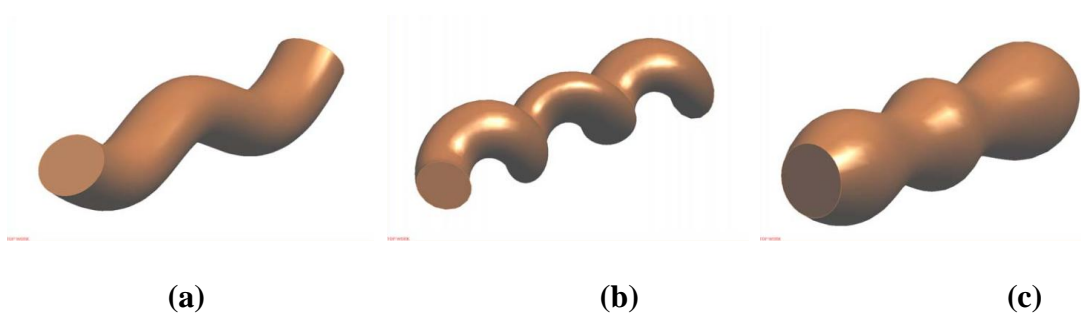


**Fig. 1.9 – Types of oscillating borehole patterns including the rippling 2D oscillation (a), spiraling 3D corkscrew (b), and hour-glassing cyclic hole enlargement (c) (Pastusek and Brackin 2003)**

As mentioned, these patterns are primarily a function of bit side cutting, which is a nonlinear function of side force, gauge design, rotary speed, rate of penetration, rock strength, and cutter dull state. The bit side cutting angle is equivalent to bit tilt, and has been confirmed in laboratory testing (Pastusek et al. 2005). Rotary speed has been shown to contribute to the dynamic whirl motion which is distinctly different than the motion from buckling or BHA “flexing.” In the case of “flex” or dynamic bending, a lateral side force at the bit is the excitation, while during “twirl, it is an equal offset distance of the center of mass of the drill string centerline that excites the vibration. This lateral bending mode can be excited at one, two, or higher multiple of the rotary speed. **Fig. 1.10** shows the differences characteristics between these motions and the vibration severity response of each motion type with increasing rotary speed (Bailey et al. 2010).

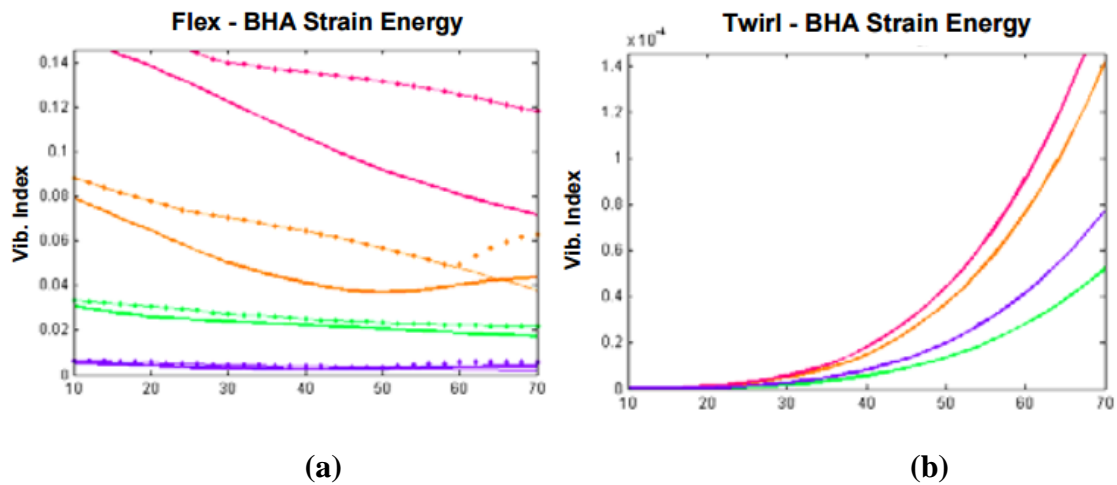


**Fig. 1.10 – Vibration index decreases with increasing rotary speed during BHA flexing or buckling (a), while it increases with increasing rotary speed during “twirl” or forward synchronous whirl (b) (Bailey et al. 2010)**

Reduced vibrations are associated with increased performance of the bit-BHA system, which allow for higher penetration rates, hole curvatures, and increased bit life (Santos et al. 1999) (Fear et al. 1997). Operationally, reducing the whirl vibration becomes a matter of applying enough WOB to prevent unintended side-cutting and borehole patterning as a result of insufficient DOC (Dupriest and Sowers 2010), but also a matter of being able to accurately predict hole curvature and build rates with steerable assemblies (Pastusek et al. 2005) given bit and BHA considerations. In 2005, extensive laboratory testing was completed in combination with finite element modeling to understand, model, and predict the amount of side-cutting that is attainable as function of bit tilt resulting from bit gauge length, side force, and rock strength. A variety of rocks with varying strengths and a variety of bits with varying gauge profiles were tested and

as a result a linear relationship between the side displacement of the bit as a function of drilling depth was discovered. A predictable and repeatable relationship was also discovered between bit tilt or side-cutting angle and bit side load and was determined to vary in severity depending on rock strength and bit gauge length (Pastusek et al. 2005). Further, this work recommends that a bit gauge length of four inches should be the starting point in bit selection to achieve the build angle requirements in the majority of directional drilling applications. This gauge length has whirl reducing characteristics, while maintaining the ability to achieve 5-7°/100ft at moderate steering forces (Pastusek et al. 2005), which is adequate for most directional drilling applications.

In 2010, Dupriest and Sowers documented a two-year world-wide campaign to reduce drilling inefficiencies related to whirl, through the use of drill bits with longer gauge areas to constrain side cutting and reduce the amplitude of whirl-induced patterns. These practices were shown to allow for desired steerability requirements to be achieved with four inch and longer gauge length bits, while also reducing vibrations, increasing ROP, improving borehole quality, and reducing tool damage (Dupriest and Sowers 2010). The bits studied were manufactured with gauge profiles that would not interfere with the lateral aggressiveness of the bit, and allowed for rotary steerable systems used to properly steer. The authors proposed and proved that bits with 4 in gauge lengths should be the industry standard instead of the current standard of a two inch gauge length, and further suggest that those involved in the well design process should continue to extend the bits gauge length until steering or other behaviors were affected negatively. It was also shown that acceptable build rates were achievable with the use of

passive or semiactive gauge profiles, which results in constrained side cutting and more efficient drilling from lower levels of whirl while still giving the bit steerability (Dupriest and Sowers 2010).

Finally, operational practices are a widely-used technique for mitigating whirl. Whirl is worse at higher rotary speeds, due to fact that the centrifugal regenerative force increases in a square relationship with rotary speed (Brett et al. 1990). Simultaneously, as weight on the bit increases the bit becomes more stable (Warren et al. 1990), due to depth of cut constraining the lateral motion. Further, because the damage associated with whirl is due primarily to impacts on the cutter face over a very short period, and thus may occur while the driller is seating the bit on bottom, the weight transfer to the bit should be rapid to reduce damage (Warren et al. 1990), since the linear torque/weight-on-bit relationship is a function of depth of cut.

### **Coupled stick-slip and whirl**

Stick-slip and whirl have been known to exist in rotary drilling for years, but it was only until recently that industry research focused on the interaction between these two phenomena and their co-existence. The work by Leine and van Campen (2002) gave insight into the transition between stick-slip and whirl, by the observation of discontinuous bifurcations, where the stick-slip vibration disappears when the whirl vibration appears. In this work, Leine and van Campen describe the adverse effects of insufficient torsional rigidity in the drillstring, the physical nature of the lateral deflections due to compressive force in the BHA, and the experiments performed in this study involving both direct full-scale dynamics measurement at the bit as well as the



theoretical modelling to prove the bifurcation theory (2002). During whirl, it was observed that the mean bending moment is considerably higher than during stick-slip; also, the friction torque was observed to be higher during whirl than during stick-slip, due to the increase in lateral deflection during whirl (Leine and van Campen 2002). Whirl has been found to be characterized by higher levels of friction, and a positive slope of the friction curve as a result of the viscous friction forces induced by fluid forces, which eliminate the Stribeck effect and constant rotation becomes stable (Leine and van Campen 2002). **Fig. 1.11**, **Fig. 1.12**, and **Fig. 1.13** show the transition between stick-slip and whirl and the observed trends in downhole rotation speed, mean bending moment, and downhole friction torque, as a function of time, angular velocity, and downhole rotation speed, respectively.

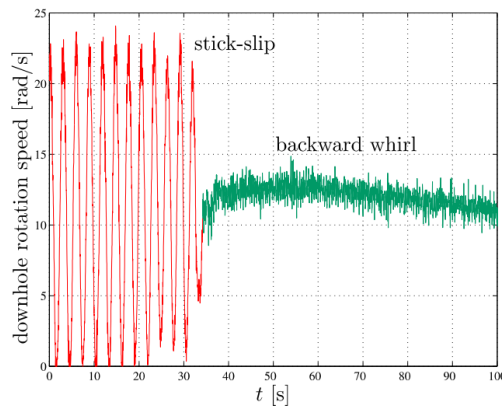


**Fig. 1.11 – Measured downhole angular velocity versus time shows the dysfunction type as a function of downhole rotational speed (Leine and van Campen 2002)**

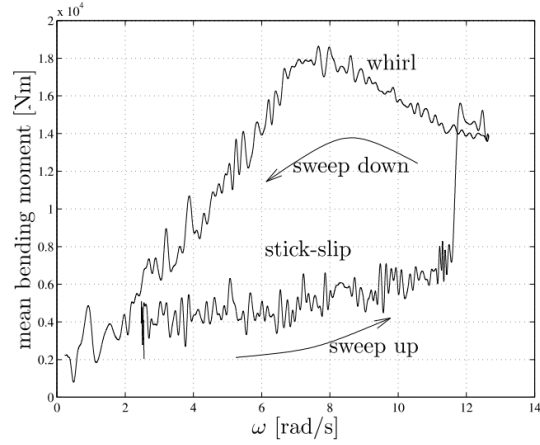


**Fig. 1.12 – Measured downhole bending moment versus surface angular velocity showing the sweep-up trend of stick-slip followed by sweep down trend of whirl (Leine and van Campen 2002)**

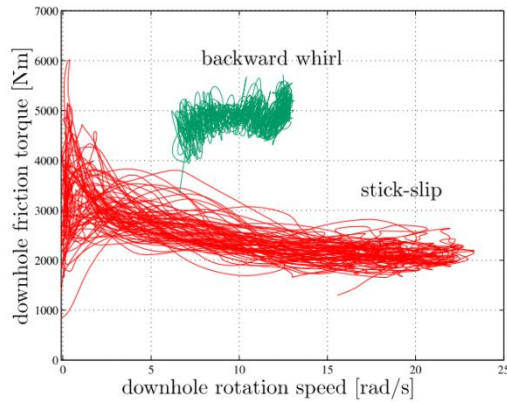


**Fig. 1.13 – Measured downhole friction curve showing the torque losses associated with both sick-slip and whirl (Leine and van Campen 2002)**

A major conclusion of this work is that the whirl vibration excludes the stick-slip motion, such that there is either lateral whirl or torsional stick-slip; however, according to Leine and van Campen, there exists a hysteresis phenomenon in between the transition between vibration modes, in which the two vibrations are co-existing stable attractors (2002).

With the advent of high-frequency vibrations measurement capabilities, new research, drilling measurements, and modelling have allowed insights to be gained regarding the physical nature of the vibrations experienced in rotary drilling. Some of these findings have included investigations into tool failure rates as a function of vibrations, better understanding of the coupled nature between stick-slip and whirl, the discovery and understanding of new vibrational modes such as high frequency torsional oscillation (HFTO) and synchronous torsional oscillation (STO), and advanced understandings of bit damage and designs for the purposed of mitigating each vibration type.

The use of downhole dynamics measurements have been used to analyze dysfunction at the bit to promote more efficient drilling, but such measurements have also been used to provide an explanation for measurement while drilling (MWD) failure as well as to model and predict the failure rates of MWD tools (Reckmann et al. 2010). In 2010, a statistical study was conducted in which vibrations data recorded at 5-second intervals from more than 12,000 drilling and reaming hours, over a total of 425,000 feet was collected and analyzed to predict MWD failure rates. It was shown that cumulative energy loss in the form of lateral motion was the most common and significant vibration

related to tool failure, while variance in the tool rotational speed as a result of backwards whirl was shown to be the most severe (Reckmann et al. 2010). It was shown that cumulative stick-slip is also significant, but energy lost in its inefficiency was more related to drilling performance than tool failure (Reckmann et al. 2010). **Fig. 1.14** below shows the predicted failure time as a function of root mean square (RMS) lateral acceleration threshold.

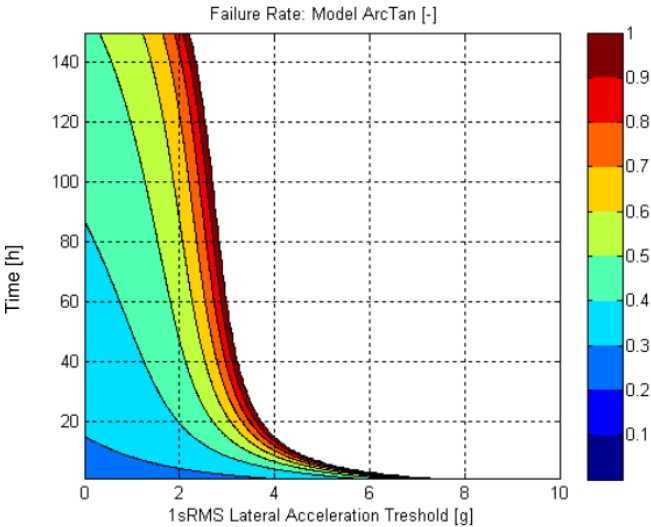


**Fig. 1.14 – MWD failure rate versus 1sRMS acceleration and time, fitted with a parametrical model (Reckmann et al. 2010)**

By displaying the color-coded probabilities of failure, these results show that minimal time at sustained high levels of vibration can cause MWD tool failure and provide a means of predicting the remaining lifetime before failure.

In addition to predicting failure rates, performance was analyzed in the study using the downhole MWD data, which showed some unique relationships between vibration modes. For example, high lateral vibration tend to occur at low values of stick-slip; thus a non-zero value of the stick-slip index is healthy while drilling (Reckmann et al. 2010). **Fig. 1.15** below shows density of lateral vibrations observed as a function of the stick-slip index.

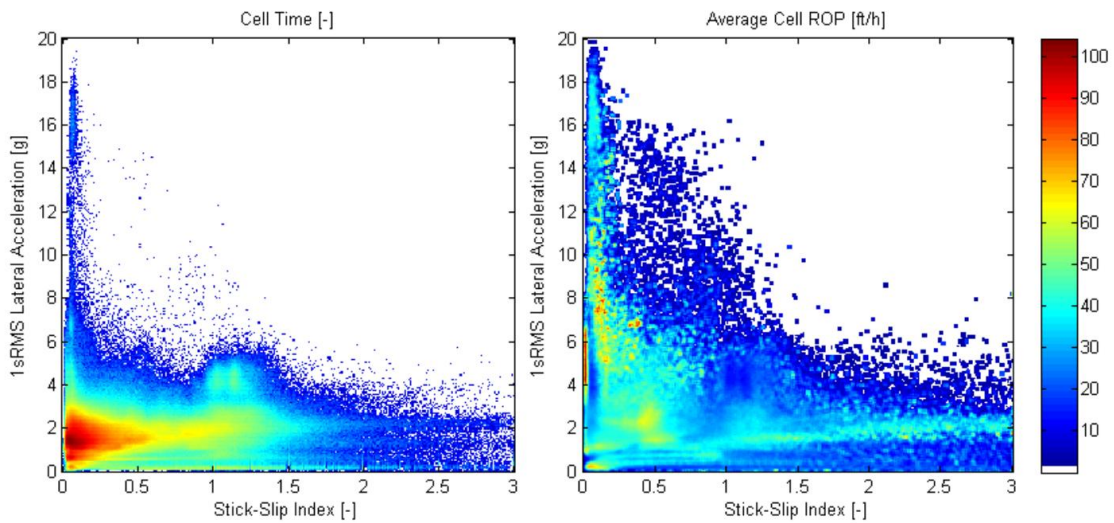


**Fig. 1.15 – Data distribution and ROP versus Stick-Slip Index and 1sRMS Lateral Acceleration (Reckmann et al. 2010)**

From these results it was determined that a stick-slip index value of about 0.5 promotes optimal performance, increased ROP, and significantly lower lateral vibrations (Reckmann et al. 2010).

Conventionally, bits have been thought to experience only one type of vibration, either whirl or stick-slip at any given time, and thus the forensic information about the

wear mechanism observed from the bit damage could be used to diagnose the dysfunction. However in 2013, a group of scientists at Baker Hughes proposed a new model for bit damage during stick-slip, involving acute lateral vibration during the slip phase that correlated well with observed bit damage (Ledgerwood et al. 2013). This work was a continuation of previous work (Ledgerwood et al. 2010) where it was proposed that stick-slip, not whirl, was the most common vibration in vertical wells containing hard-rock, as well as being responsible for the majority of PDC bit damage in today's conventional wells. According to Ledgerwood et al. (2013), advancements in cutter-technology from when PDC bits were first introduced have allowed drillers to apply more WOB to increase drilling efficiency, but have also made PDC bits more susceptible to stick-slip. During experimentation, high-frequency vibrations sensors were used, which fit into the shank of the bit, capable of storing 5-second burst data, while measuring axial, lateral, and torsional vibrations using accelerometers (Pastusek et al. 2007). These bits were deployed in situations where drilling parameters were intentionally set to promote dynamic dysfunction, in an effort to create stability maps showing the realms of stick-slip, smooth drilling, and backwards whirl to help observe the characteristics of each dynamic state (Ledgerwood et al. 2013). Backwards whirl was detected from the accelerometer's measurements by way of proprietary processing and was found to occur at high frequency as shown by **Fig. 1.16**:

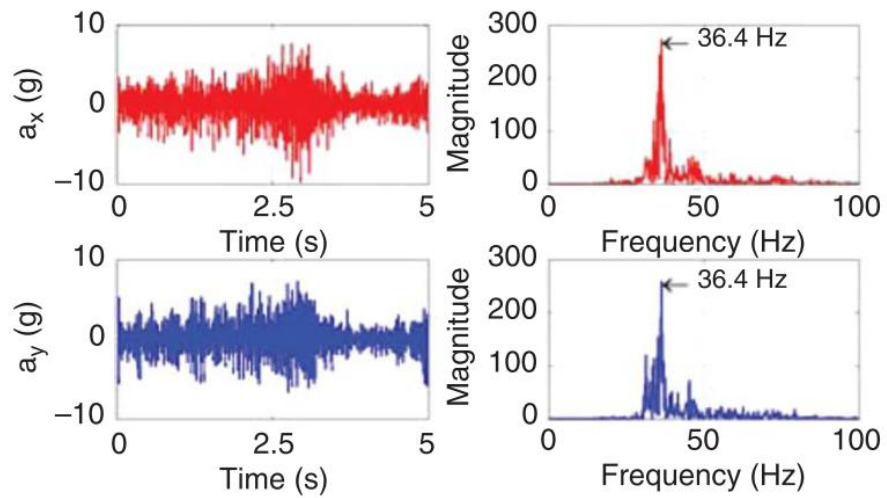


**Fig. 1.16 – In-bit device measurement of accelerations during backward whirl (Ledgerwood et al. 2013)**

The burst data used to capture this whirl, shows that this vibration type occurs at high frequency and is comprised of micro events throughout its propagation. The whirl also was found to show lower amplitudes (not shown) in the BHA than at the bit through these downhole measurements (Ledgerwood et al. 2013).

Stick-slip and torsional resonance of the drill collars were also observed in the measured data from this experimentation, and were found to exist at much lower frequencies than whirl (Ledgerwood et al. 2013). **Fig. 1.17** below shows an instance of well-developed stick-slip occurring at a low frequency.

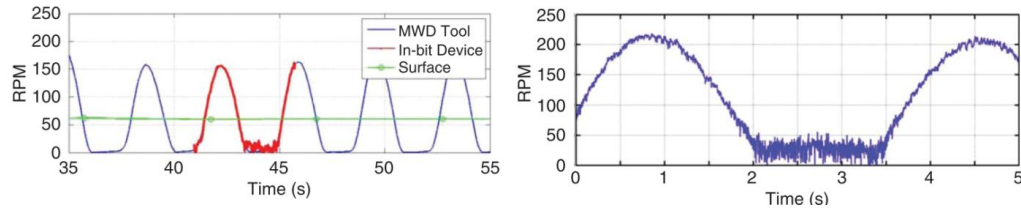


**Fig. 1.17 – Downhole measurement of rotational speed during stick-slip  
(Ledgerwood et al. 2013)**

The stick-slip shown contains a distinct “sticking” phase, where the bit comes to a near-zero rotational speed or full stop for about 1.5 seconds, which is followed by a rapid acceleration during the “slip” phase to speeds up to and exceeding 200 RPM.

The torsional resonance of the drill collars that was observed during the study behaved differently than stick-slip because while the bit showed brief negative rotation, it never exhibited a distinct “sticking” phase, and none of the data collected suggests that the torsional resonance was damaging the PDC bits (Ledgerwood et al. 2013). **Fig. 1.18** below shows an instance of torsional resonance and the observed bit speed response.



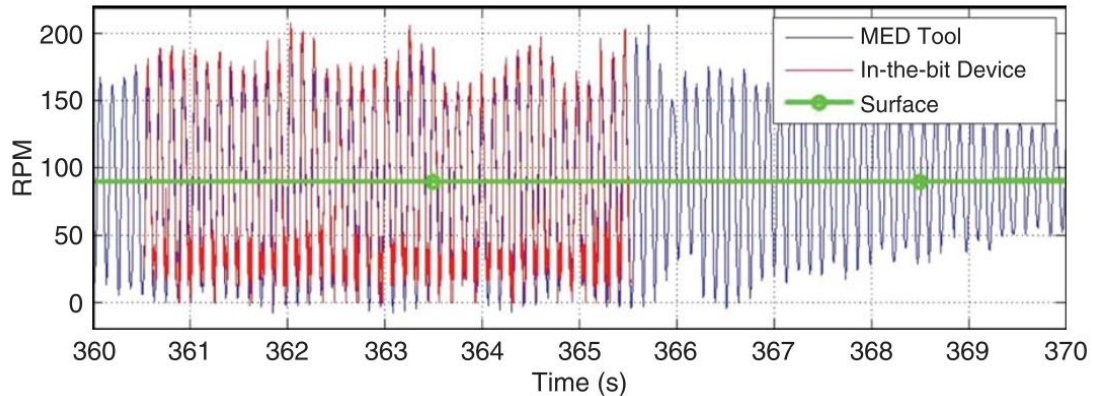


**Fig. 1.18 – Bit rpm measured in-bit-device and commercial MWD tool during drill-collar torsional resonance (Ledgerwood et al. 2013)**

Torsional resonance of the drill collars was first identified in 1998 during BHA modeling to show natural frequencies at which these torsional oscillations occur (Warren and Oster 1998). The characteristics of torsional resonance of the drill collars proposed by Warren and Oster (1998) were observed during this field study and torsional resonances of their BHA were shown to coincide with discrete frequencies of 4, 8, and 9 Hz for the system under study (Ledgerwood et al. 2013).

The most notable discovery of this work is that significant lateral vibrations can occur during the slip phase or the high-rpm portion of the stick-slip cycle and was observed to do so with field downhole dynamics measurements (Ledgerwood et al. 2013). During the field trials, five of the wells tested were analyzed and showed no indication of drill-collar resonance or whirl, however the bits dull condition when pulled from the well showed wear consistent with lateral vibrations, which upon further analysis was shown to be occurring during the high-rpm portion of stick-slip

(Ledgerwood et al. 2013). **Fig. 1.19** below shows whirl-like lateral vibrations occurring in the slip-phase of stick-slip.

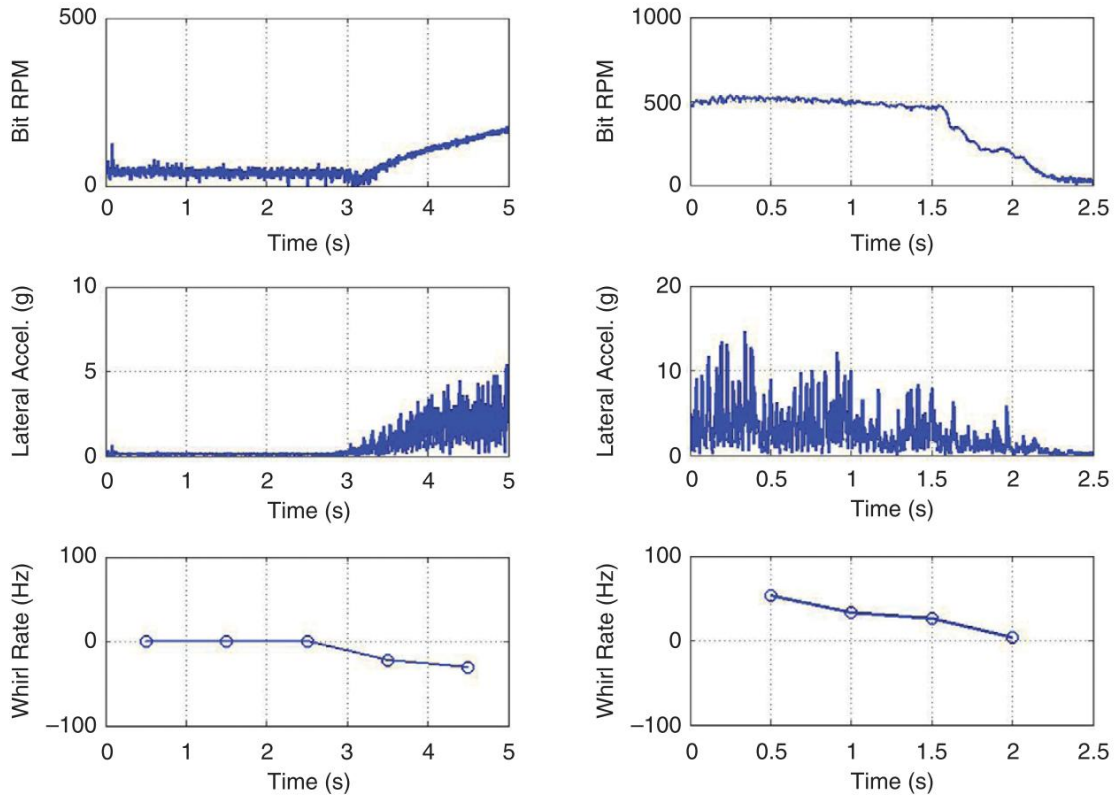


**Fig. 1.19 – Downhole measurements showing the coupling of whirl with stick-slip (Ledgerwood et al. 2013)**

During the time period shown, the bit experiences high lateral vibrations, which occurs at the end of the stick phase and a result of backwards whirl, and occurs at a frequency proportional to rotary speed (Ledgerwood et al. 2013). It is important to note that during analysis, elevated lateral accelerations were also observed during the slip phase that were not observed to be well-defined motions such as forward or backwards whirl

(Ledgerwood et al. 2013). A major conclusion is that high lateral vibrations were more likely to occur with more severe stick-slip (Ledgerwood et al. 2013). This suggests that the results presented in Leine and van Campen (2002) which assumed that coupled stick-slip and whirl motion is rare or nonexistent, may be inaccurate due to non-inclusion of effects such as mass imbalance, interaction with the nonperfect wall, and rock-bit interaction (Ledgerwood et al. 2013).

In situations where stick-slip and whirl vibrations become coupled and are performance limiting, it has been shown that the use of roller reamers can help to reduce lateral side forces, while simultaneously reducing frictional drag that can be generated by integral blade stabilizers (IBS) (Sowers et al. 2009). This allows more torque to become available to the bit, due to it not being lost in the BHA during transmission, while simultaneously promoting lower lateral and tangential vibrations (Sowers et al. 2009).

Another design change that can address both stick-slip and whirl is related to the geometry and cutting structure of the PDC bit. In 2011, Baker Hughes designed, manufactured, and tested a variety of PDC bits in an attempt to test the five leading theories for preventing the stick-slip vibration. This work was done both in the laboratory and in full-scale well testing (Jain et al. 2011). The tests included the testing of anti-whirl and reduced exposure designs, as well as bits with bit-rock interaction numbers larger than one (Detournay and Defourny 1992), which are all supposed to be less prone to stick-slip, and testing of highly aggressive or worn bits, which are thought

to be more prone to stick-slip (Jain et al. 2011). As a result of the extensive testing, the following conclusions were drawn (Jain et al. 2011):

- Bit design has a significant effect on the stick-slip behavior
- Traditional anti-whirl designs did not appear to reduce the incidence of stick-slip
- The concept of a bit with bit-rock interaction number larger than 1 could not be conclusively tested; however, an exceedingly long profile bit was tested and showed to exhibit severe stick-slip
- Aggressive bits are more prone to stick-slip than non-aggressive bits
- Reduced exposure bits, with depth of cut controlling features resist stick-slip
- Worn bits have a stronger tendency to stick-slip than non-worn bits
- Measured stick-slip behavior did not show consistent correlation with aggressiveness or lateral stability of the bits
- Bit designs that inhibit falling friction characteristics successfully resist stick-slip

Keeping these guidelines in mind when selecting a bit for application in wells prone to whirl and stick-slip can greatly reduce the amount and severity of each vibration mode observed.

With dynamic dysfunction research becoming the focus of the industry in recent years with mitigation, effects on bit damage, and the prospect of reduced drilling costs at its core, a variety of new vibration modes have been observed with the advent of high-frequency downhole data. Among these are high frequency torsional oscillation (HFTO) and synchronous torsional oscillation (STO).

High frequency torsional oscillation has been observed in rotary drilling only with the use of high frequency measurement tools, and exhibits an oscillating behavior at frequencies ranging from 40 to 90 Hz and beyond that resembles a fast chatter (Pastusek et al. 2007). It is believed that episodic failure of the formation being drilled is responsible for driving this resonance within the BHA, due to variances in loading on the cutter faces (Warren and Oster 1998). However, it is believed that bit/hole/BHA resonance is independent of bit speed during this vibration and that there exist two possible explanations for moderate changes in the frequency of this vibration. First, a reduction in DOC as the bit speeds up and second, a brief elevation of the driving frequency as the bit interacts with the existing borehole pattern (Pastusek et al. 2007). Regardless of the explanation, HFTO has been shown through frequency domain analysis to exhibit excited frequencies which are in close agreement with the natural torsional frequencies of the drilling system (Oueslati et al. 2013). Strong correlations have also been developed between the occurrence of HFTO and low gamma ray count and high bulk density, regardless of PDC bit design or manufacturer (Oueslati et al. 2013).

HFTO, while exhibiting variations in tangential acceleration, has not yet been proven to show any component of lateral acceleration and in fact, has been shown to be mutually exclusive from severe lateral vibrations such as backwards whirl (Jain et al. 2014). Conversely, it has been shown to be strongly coupled with axial vibrations (Jain et al. 2014), shown to occur simultaneously with stick-slip (Oueslati et al. 2013), and has also been associated with rotary steerable component failure (Chen et al. 2006). The

region over which HFTO occurs can be visualized by the stability diagram shown in **Fig. 1.20**.

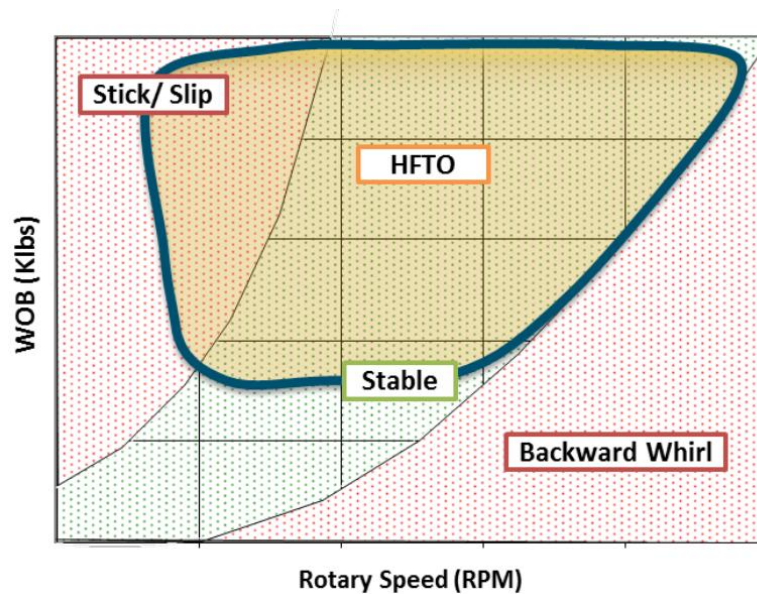


**Fig. 1.20 – Stability diagram including the regime of HFTO (Jain et al. 2014)**

HFTO has not currently been associated with bit damage, and theories related to the possibility of PDC bit damage occurring with HFTO are related to the presence of hard or abrasive formations or significant backwards rotation (Jain et al. 2014). The range of tangential accelerations that have been observed during HFTO can exceed 20 g RMS (Jain et al. 2014; Oueslati et al. 2013; Pastusek et al. 2007).

Synchronous torsional oscillation has only been documented in rotary drilling by a team from ExxonMobil during the development of a “Drilling Mechanics Model for Surveillance, Root Cause Analysis, and Mitigation of Torsional and Axial Vibrations” (Ertas et al. 2013). The vibration was observed to be self-existing but could also

coincide with unstable stick-slip, where sustainable periods of small variations in bit torque occurred. This typically ended with a single severe stick-slip cycle towards the end of the interval, that was not periodic, involved prolonged stalling of the drill bit and an associated buildup of torque, with the additional bit torque transmitting to surface (Ertas et al. 2013). STO was found to occur when the frequency of a periodic excitation coincides with one of the higher-frequency torsional resonances. It was found to be a stable vibration, showing significant variation in bit RPM when in combination with large excitation amplitude and large torsional compliance of the drilling system (Ertas et al. 2013). During analysis, it was observed that STO was primarily excited by the rotary speed of the bit and that there was potential resonance with measure depth or drillstring length, where resonances move towards lower rotary speeds with increasing depth (Ertas et al. 2013). This vibration was not considered critical from a tool damage perspective but was found to cause sub-optimal drilling performance. It was also undetectable by most surface data acquisition systems, as a minimum of 10 Hz data is required (Ertas et al. 2013). An example of unstable stick-slip and first-harmonic resonance (STO) is shown in **Fig. 1.21** along with the results of a Fourier Transform showing the two dominant frequencies in the signal, which shows the primary or fundamental stick-slip mode and the synchronously excited resonance.

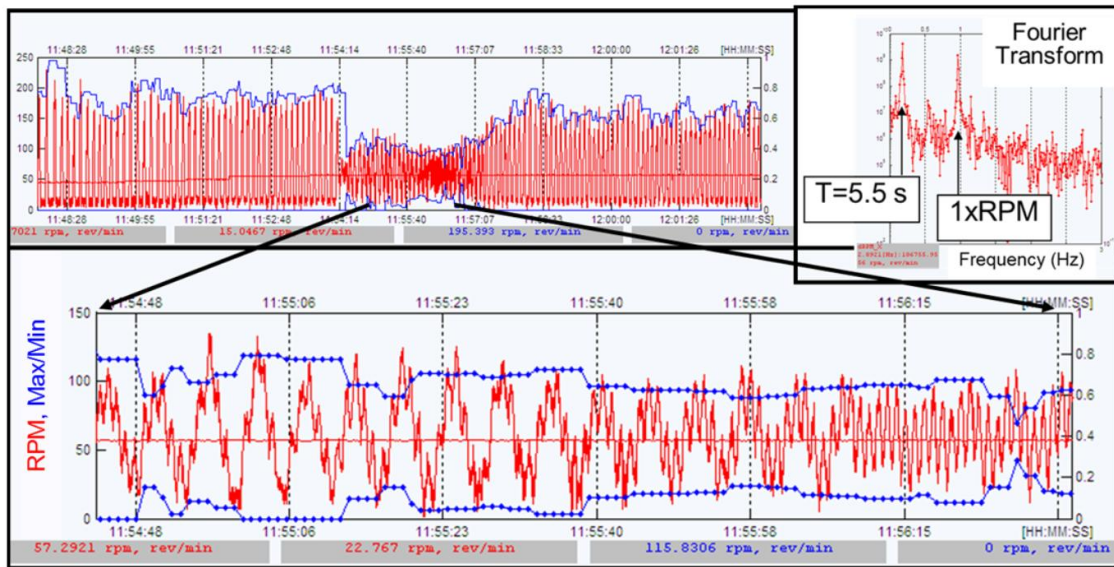


**Fig. 1.21 – An instance where both unstable stick-slip and first-harmonic resonance is observed in the downhole RPM and Fourier Transform (Ertas et al. 2013)**

### **Mechanical specific energy**

Ever since the widespread application of rotary drilling for petroleum, engineers have attempted to quantify the efficiency of drilling and create meaningful correlations to the formations and subsurface environments, in which they are drilling. This has included everything from correlations between penetration rates and pore pressures (Jordan and Shirley 1966), to measures of specific energy in rock drilling (Teale 1964), to real-time correlations between bit torque and lithologies (Falconer et al. 1988), to concepts of the “Drilling Response” and “Drilling Alerts” (Jogi and Zoeller 1992), to using the concept of coefficient of sliding friction (Pessier and Fear 1992), to using high frequency drilling dynamics to detect lithologies and model drilling dynamics



(Reckmann et al. 2007), and even the use of unique ROP predictor models based on bit-specific coefficient of sliding friction and mechanical specific energy as a function of confined rock compressive strength (Caicedo et al. 2005) and (Guerrero and Kull 2007). However, the oil and gas industry has seemed to adopt the concepts presented in “Maximizing Drill Rates with Real-Time Surveillance of Mechanical Specific Energy” by Dupriest and Koederitz (2005) and this thesis will discuss Ultra Petroleum’s applications and results from using this concept.

“The Concept of Specific Energy in Rock Drilling” was first proposed by Teale (1964) and is defined as the energy required to excavate a unit volume of rock. In the context of rotary drilling, it can be thought to be proportional to the mechanical energy required to force a tool into a rock surface (Teale 1964). According to Teale, rotary drilling may be described as a combination of two distinct actions: ‘indentation’, where the cutting edges of the bit are continuously pushed into the rock, and ‘cutting’ where the bit is given a lateral movement to remove fragments of rock from the cutting surface (Teale 1964). The minimum amount of energy required to excavate a given volume of rock will be dependent entirely on the nature of the rock, and the difference between the actual and theoretical specific energy is a measure of the energy lost in mechanical motion wasted outside the rock system. This can include energy lost in breaking excavated rock into smaller fragments than necessary or in frictional losses between tools and rock (Teale 1964). Work is done both by the thrust, or indentation pressure, and by the torque component energy, whereby the specific energy is dimensionally identical with the pressure or stress (Teale 1964). Therefore, the ideal or

minimum specific energy required for a given rock, in all cases, is numerically equivalent to compressive strength of the material being drilled in units of pressure or stress (Teale 1964).

Dupriest and Koederitz (2005) took this concept of rotary specific energy and applied it at the rig-site, as a real-time tool for rig-site personnel to maximize penetration rates. By plotting Mechanical Specific Energy (MSE) in real-time, six rigs that were selected for the three-month pilot increased their penetration rates by 133% and field records were re-established on 10 of the 11 wells (Dupriest and Koederitz 2005). According to Dupriest and Koederitz (2005), “the manner in which a bit is run is often more important than which bit is run,” and the technique proposed to determine these efficient operating parameters is the “drill rate” test, which consists of experimentation with WOB and RPM settings followed by observation of the impact on ROP. By plotting ROP versus WOB, three operating regimes of the bit can be observed, and the point at which ROP stops responding linearly to increases in WOB or the “founder” point can also be observed (Dupriest and Koederitz 2005). **Fig. 1.22** shows example ROP versus WOB plots, and displays the three regions of bit operation, as well as detailing some common potential limitations that may affect the amount of efficient performance that is possible, shown by the non-linear trend between ROP and WOB at higher WOB than the founder point.

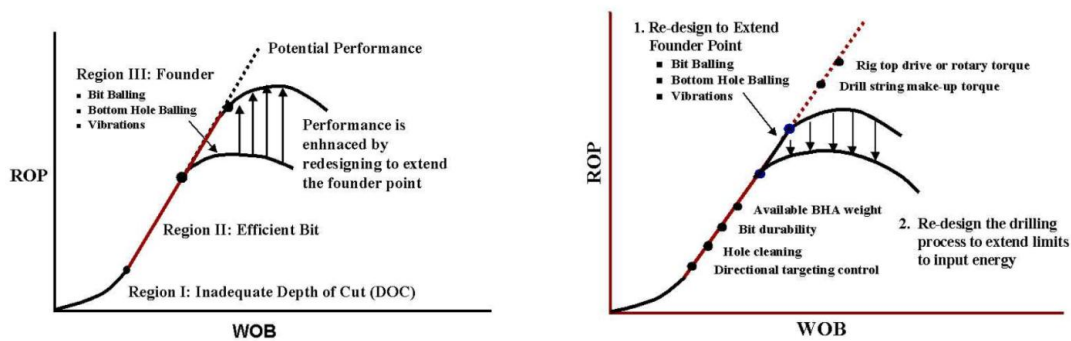


**Fig. 1.22 – ROP versus WOB plots showing bit operating regions and bit founder (Dupriest and Koederitz 2005)**

Region I corresponds to a lack of performance due to inadequate or inefficient depth of cut (DOC); Region II corresponds to efficient drilling, where ROP increases linearly with WOB, above Region I and below Region III; and Region III corresponds to bit founder or bit dysfunction and inefficient drilling (Dupriest and Koederitz 2005). Also shown in this **Fig. 1.22** are two categories of factors that can determine ROP. First, factors that create dysfunction or founder, such as bit balling, bottomhole balling, and vibrations and second, factors that limit the amount of energy input such as make up torque, hole cleaning efficiency, hole integrity, top drive torque rating, solids handling capacity, etc. (Dupriest and Koederitz 2005).

Surveillance of MSE can be used in real-time to find the founder point, and can even be used to determine the cause of the limiting dysfunction or founder in some cases (Dupriest and Koederitz 2005). Mechanical specific energy is defined by the following equation shown in **Fig. 1.23**:

$$\text{MSE} = \frac{480 \times \text{Tor} \times \text{RPM}}{\text{Dia}^2 \times \text{ROP}} + \frac{4 \times \text{WOB}}{\text{Dia}^2 \times \pi}$$

**Fig. 1.23 – Mechanical specific energy equation (Dupriest and Koederitz 2005)**

When a bit is operating in Region II, MSE equals the ratio of ROP to WOB, and remains a constant value for a given formation because it is operating in the linear portion of the ROP versus WOB curve. However, if the bit is operating in Regions I or III, MSE will reflect the disproportionate amount of energy that is being sacrificed or wasted for the given ROP (Dupriest and Koederitz 2005). It should be noted that MSE, as it reflects the confined compressive strength of the rock being drilled, will change as the lithology changes (Dupriest and Koederitz 2005). However, as bits are only about 30-40% efficient at maximum performance (Pessier and Fear 1992), that it is often beneficial when plotting this in real-time on the driller's display to show an adjusted MSE ( $\text{MSE}_{\text{adj}}$ ) to better reflect the actual confined compressive strength of the formation being drilled, which can typically be accomplished by multiplying the MSE value by a factor between 0.30 to 0.40 (Dupriest and Koederitz 2005). The largest source of discrepancy between MSE and the  $\text{MSE}_{\text{adj}}$  value can be attributed to drillstring frictional losses, which is consistent with ideas proposed by Teale (1964). This discrepancy may falsely make the bit appear to be consuming more energy than it actually is, and is the reason that the  $\text{MSE}_{\text{adj}}$  value should primarily be used as a trending tool, rather than a direct measure of rock compressive strength (Dupriest and Koederitz 2005).

Dupriest (2006) later published recommendations for improved performance in “Comprehensive Drill-Rate Management Process To Maximize Rate of Penetration,” and discussed associated techniques and world-wide practices that showed impressive instantaneous ROP improvements in excess of 100-200%. This work is more concerned with the application of the mechanical specific workflow rather than the concept of MSE, and includes an explanation of the “linear response model” and concept of the “economic limit of redesign,” because according to his theory, having the knowledge of using MSE to identify bit dysfunction, does not ensure that drill teams knows why the inefficiency is occurring, or how to correct it (Dupriest 2006). Dupriest proposed that “success in maximizing the ROP in every foot of hole derives as much from management of the workflow as the development of drilling technology” and further, “MSE is a technology, while the ROP management process is a broad workflow designed to ensure MSE and numerous other sources of data are used effectively to maximize ROP” (Dupriest 2006). Of the numerous ROP-limiters that have been identified, only four are directly related to the drill bit, which are designated “bit limiters,” and include bit balling, bottomhole balling, and two types of vibrations: whirl and stick-slip (Dupriest 2006). With the (near) elimination of bit balling in non-aqueous fluids (NAF), the most common forms of bit dysfunction are now vibrational in nature, corresponding to higher (stick-slip) or lower (whirl) WOB; and the ranges where whirl and stick-slip occur often overlap (Dupriest 2006).

Dupriest proposed two fundamental concepts, first, the “economic limit of redesign,” which relates to the level of achievable performance through operational

practices and engineering redesign before the next improvement or redesign opportunity would cost more to implement than it would save cost, thus become uneconomic, and second, the “linear response model,” which relates to operation in Region II of the ROP versus WOB curve (previously discussed) and is used to communicate the relationships of bit performance and ROP management process from a scientific point of view. The linear response model was used to create the following workflow procedure (Dupriest 2006):

1. Raise the WOB. If the ROP response is linear (as determined through MSE surveillance), the bit is efficient.
2. Continue raising WOB until non-linear response is observed, or the ROP becomes non-bit limited
3. In the first case, make operational adjustments to the extent possible to minimize MSE then operate at just below the founder. For both bit and non-bit limiters, identify and document the nature of the founder and communicate it to engineering.
4. Redesign the system appropriately to extend the identified limiter and repeat step 1-4.

When using this workflow, there can inherently be only one ROP limiter, at any point in time or in any given hole interval, to be identified for redesign, because the various limiters reside at different locations on the linear response (ROP as a function of WOB, Region II) line; allowing the limiters to be prioritized (Dupriest 2006). Thereby, if the digital data displayed at the rig-site showed in real-time a decline in WOB with a

simultaneous increase in MSE, the driller could document the occurrence of whirl, and conversely if a decline in WOB with a simultaneous decrease in MSE, the driller could document the occurrence and mitigation of stick-slip (Dupriest 2006). This process allows rig-site personnel to document bit dysfunctions in real-time, and relay these occurrences to designated experts or highly trained engineers for vibrations analysis (Dupriest 2006). In addition to the large improvements in ROP, secondary benefits including improved tool life, bit life, and borehole quality were experienced through the implementation of these workflows and control drilling practices (Dupriest 2006).

During the beginning of this study, Ultra Petroleum engineers and rig personnel were trained on the practices discussed in this section by Fred Dupriest. Ultra Petroleum subsequently incorporated these practices and workflows into their wellsite operations to reduce dysfunction and improve performance.

### **Pinedale Anticline lithology and drilling considerations**

The Pinedale Anticline is the largest commercial gas accumulation in the Northwestern Green River Basin (Freeman 1999) and has produced significant volumes of gas from tight sandstone reservoirs, since adopting stimulation techniques developed in the neighboring Jonah field (Gray et al. 2002). Tight gas reservoirs typically have porosity ranges of less than 10% and permeability's of less than 0.1 millidarcy or 100 microdarcy (Han et al. 2013b). However, reservoirs with enhanced permeability due to possessing natural fractures can result in higher production rates (Gray, David et al. 2003), especially when combined with hydraulic fracturing to connect the wellbore drilled near a swarm of fractures to a larger area of the reservoir (Gray et al. 2002). The

Lance and Mesaverde formations have porosities less than 12% and average 7.7% and 7.6% respectively, while having permeability's less than 44 microdarcy and averaging 15.8 and 6.4 microdarcy respectively (Nelson et al. 2009). **Fig. 1.24** details the location of the Pinedale Anticline in the Greater Green River Basin.

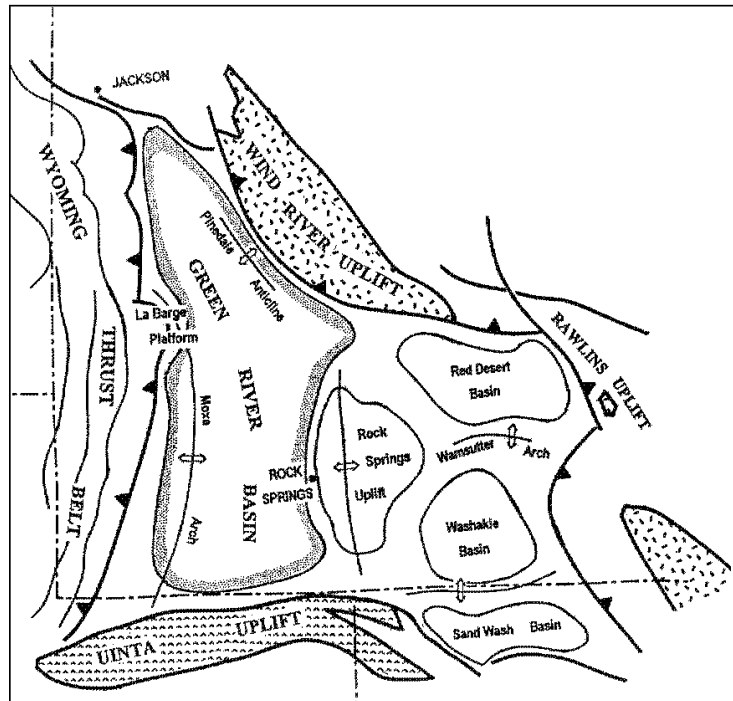


**Fig. 1.24 – The Greater Green River Basin Geologic Structure (Gibson 1997)**

The Pinedale Anticline stretches approximately 35 miles long, is about 6 miles wide, and is estimated to have 159 TCF of sweet gas in-place (Law and Spencer 1989), contained primarily in the tight sands of the Lance and Mesaverde Formations. The reservoir sediments contained in the 5,500-ft thick “Lance Pool,” consisting of the Lance Formation, the Upper Mesaverde, and an “unnamed” Paleocene unit, which overlies the Ericson Sandstone Formation (Han et al. 2013b), were deposited rapidly in the late



Cretaceous, and then were eroded off the western upland, where they were then carried by fluvial systems flowing east, and were redeposited as fluvial channel sandstones and siltstones, floodplain shales, and minor coals (Gray et al. 2002). The Lance and Mesaverde were then buried by up to 8,000 feet of Tertiary rocks, which compressed these sands into low-permeability, tight sandstones (Gray et al. 2002). The individual sandstone units only average about 25 feet in thickness (Bowker and Robinson 1997) (Robinson 2000), and as a result, when these small reservoirs are isolated, they are oftentimes non-commercial (Gray, D. et al. 2003). However, when a few of the sand units are stacked vertically, they can be 100 feet thick, and allow for commercial drilling (Gibson 1997). Horizontal drilling is impractical on the anticline, due to the lenticular sand bodies and the stratigraphic nature of the area, thus deviated S-shaped wells (the figure on p. 50) drilled from a single pad are prevalent (Han et al. 2013b), and the vertical, production sections of these wells can encounter as many as 100 individual sandstone units (Gray et al. 2002). **Fig. 1.25, Fig. 1.26, and Fig. 1.27** show the location and geologic cross-sections of the Pinedale Anticline and of the Lance and Mesaverde formations.

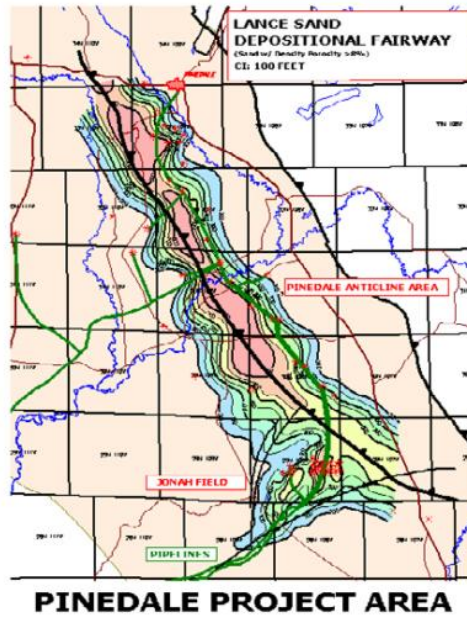


Fig. 1.25 – Pinedale Anticline Map (Gray et al. 2002)

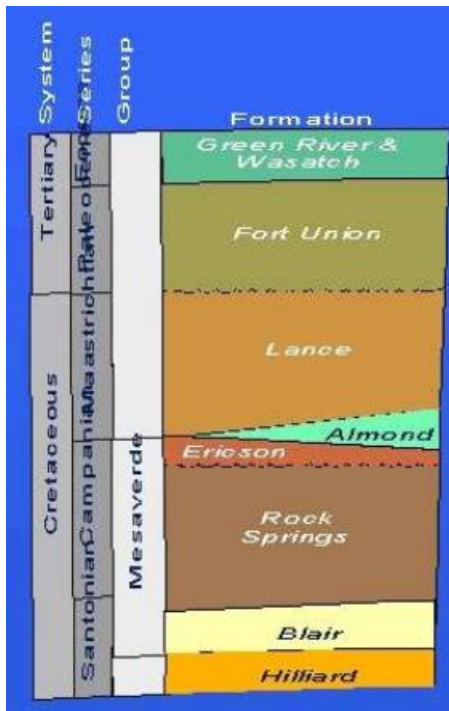
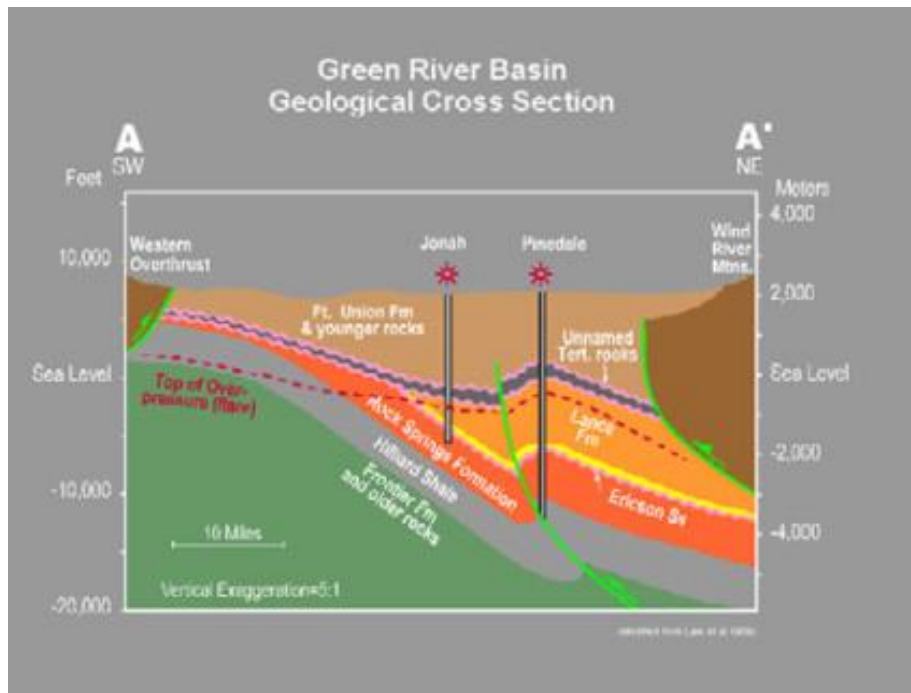


Fig. 1.26 – Pinedale Anticline Formations (Bowker and Robinson 1997)



**Fig. 1.27 – Pinedale Anticline Geological Cross Section (Gray et al. 2002)**

By observing rock mediums that are horizontally transverse isotropic (HTI), meaning that there exists one open set of near-vertical, fluid filled fractures, while performing AVAZ analysis on the seismic data, it was discovered that there was a correlation to zones of high intensity fracturing at the top of the anticline (Gray, David et al. 2003). These fractures are the result of increased stress near the top of the anticline, and are cut at the fault, west of the crest (Gray, David et al. 2003). **Fig. 1.28, Fig. 1.29, Fig. 1.30, and Fig. 1.** show the relevancy of the AVAZ analysis and confirm the existence of natural fractures, where the color white (**Fig. 1.28**) and the color red (**Fig. 1.29, Fig. 1.30, and Fig. 1.**) show a high intensity of natural fracturing on each plot. These natural fractures are the result of overpressures in

the Lance Pool, which are common in many of the deeper Rocky Mountain basins (Han et al. 2013b). The Lance Pool is a freshwater formation that has a reservoir pressure gradient that increases from near-hydrostatic (0.43 – 0.5 psi/ft) at 7,000-ft to a value of 0.9 psi/ft at 13,500-ft (Nelson et al. 2009), due to the active or recent generation of hydrocarbons at a rate exceeding the rate of hydrocarbon migration (Spencer 1989).

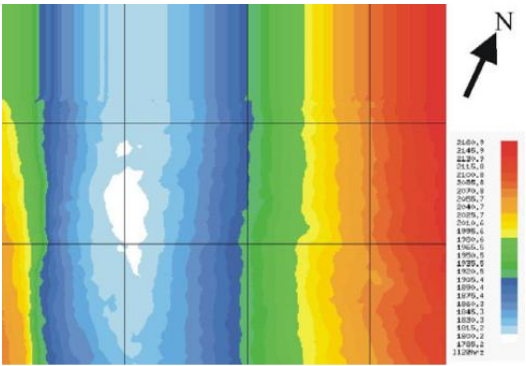


**Fig. 1.28 – Structural Time-Interpretation of the Lower Lance (Gray et al. 2002)**

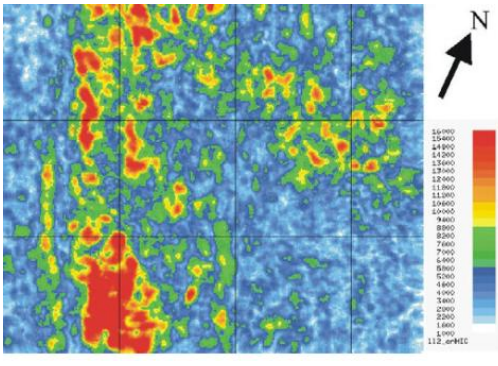


**Fig. 1.29 – Map-view of the migrated fracture intensity Lower Lance horizon (Gray et al. 2002)**

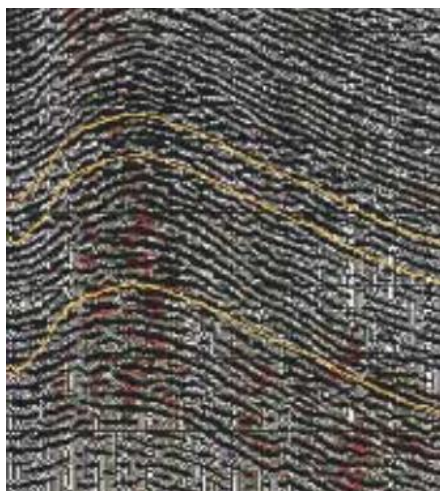


**Fig. 1.30 – P-waves show high intensity fracturing in zones of high stress (on west side and on crest of anticline) (Gray et al. 2002)**



**Fig. 1.31 – S-waves confirm high intensity fracturing using amplitude versus offset (AVO) methods (Gray, David et al. 2003)**

These practices were applied across the field and confirmed that the anticline showed prevalence of high stress zones across the crest, and also allowed the visualization of fracture swarms around good wells, as shown in **Fig. 1.32** and **Fig. 1.33**.

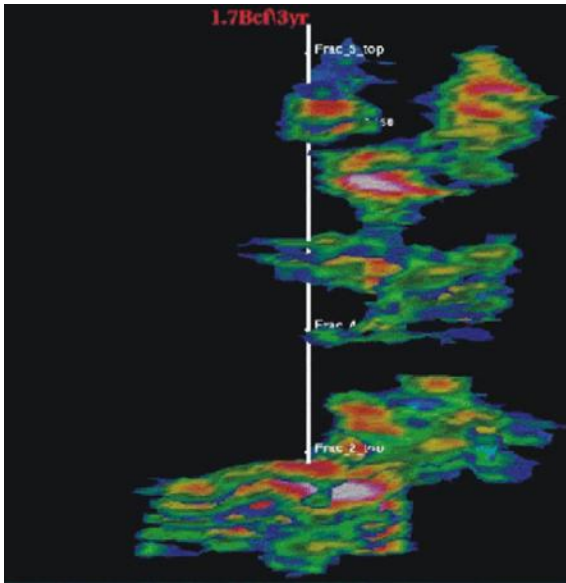


**Fig. 1.32 – Multiple reservoirs with high density natural fractures around a good gas well in the Pinedale Anticline (Gray, David et al. 2003)**

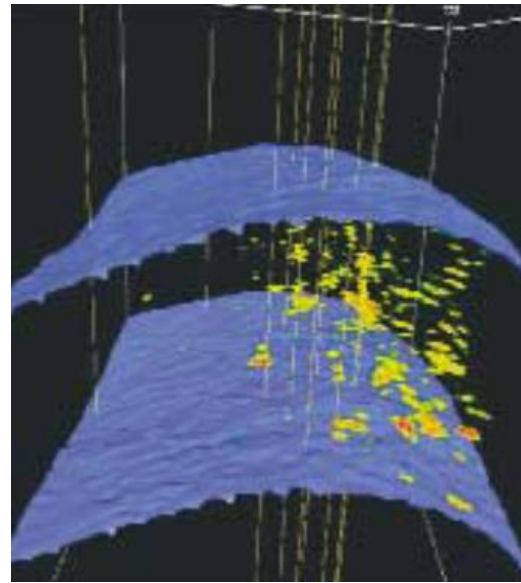


**Fig. 1.33 – Visualization of geobodies with high natural fracture density between Upper Lance and Mesaverde formations (Gray, David et al. 2003)**

These trends influence companies developing the Pinedale Anticline, and provide a good baseline for higher probabilities of geologic success.

Typical modern wells drilled in the Pinedale Anticline are S-shaped, with 5 to 25 degrees of inclination in the upper sections, followed by a tangent section that holds its inclination for anywhere from 1,000 to 5,000 feet, before returning to vertical for the production section and finishing at around 15,000 feet measured depth (MD) (Han et al. 2013b). The surface hole is typically drilled with water-based mud (WBM) to

approximately 1,200 to 1,500 ft MD, then 9-5/8-in casing is run and cemented to surface (Han et al. 2013b). Following, the 8-1/2-in intermediate hole is drilled using WBM to the Tertiary boundary (TK boundary), building to a maximum inclination of around 25 degrees, with as much as a 2°/100 ft dogleg severity (DLS), and then dropping to vertical with as much as a 1.5°/100 ft DLS (Han et al. 2013b), and following a 7-in string of casing is run and cemented (Han et al. 2013b). For the 6-in vertical production sections, the interval is drilled with oil-based mud (OBM) or non-aqueous fluid (NAF) and typically has a target depth (TD) at the top of the Ericson Sandstone Formation (Han et al. 2013b). The open hole and casing sizes used in the typical Pinedale Anticline well design, are referred to as a “slim-hole” drilling design, which are used to access fields that have high reserve potential but low production rates, and allow these areas to be economically developed by reducing the well cost (Medley et al. 1997). **Fig. 1.34** shows a typical “slim-hole” well plan for the Pinedale Anticline.

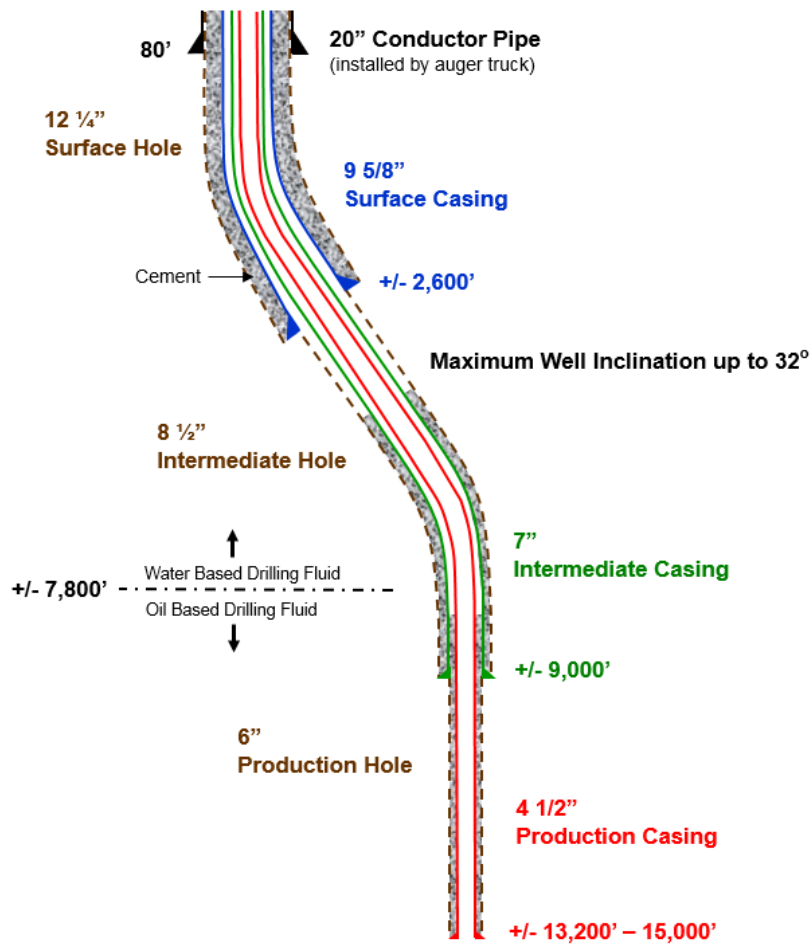


**Fig. 1.34 – Slim-hole well plan for Pinedale Anticline (courtesy of Ultra Petroleum)**

There are two strategies for drilling directional drilling the S-shaped wells in Pinedale; first, the use of conventional adjustable kick-off sub (AKO) positive displacement motors (PDM) during the shallow directional drilling, followed by the use of a vertical-seeking tool to complete the remainder of the well (Han et al. 2013b). The second strategy involves the use of an AKO PDM throughout the entire well, from



beginning to TD (Han et al. 2013b). Although it has been observed in some studies (Han et al. 2013b) that the use of the second strategy can be cost saving, Ultra Petroleum chooses to use the first strategy, for two reasons. First, to have assurance about the exact placement of each wellbore in their 10-acre well spacing development strategy. This is so that infill drilling can occur effectively if a decision is made at a later date to develop the field at 5-acre spacing. And second, to reduce the likelihood and severity of borehole patterns, that can be detrimental in running production casing in these deep wells. The 10-acre spacing allows for recovery of 60% of recoverable reserves (Kneller et al. 2006).

The drilling considerations as a result of the geology present in the Pinedale Anticline center around the changing rock strength as a function of depth and the affects these vibrations experienced at the bit has on its dysfunction. The sand-shale sequences found in the upper, middle, and lower Lance have unconfined compressive strengths (UCS) ranging between 10 and 20 ksi, with confined compressive strengths (CCS) averaging between 20 and 30 ksi, and as high as 100 ksi (Barton et al. 2008) (Gent et al. 2009). There has been a multitude of research involving bit performance improvements due to changing lithology and durability while drilling these laminations between hard and soft rock. Tripping to replace a bit, as a results of slow penetration rates and short bit runs, is both costly and unproductive, and exposes rig crews to potentially dangerous operations (Gent et al. 2009), thus there have been multiple efforts by various bit vendors to improve the cutting efficiency of their bits while transitioning between the tight, hard sands of the Lance and Mesaverde formations and the soft shales that are

experienced in this field. They have focused on cutter edge geometry (Barton et al. 2008) (Gent et al. 2009), blade profiles (Gent et al. 2009), hybrid bits (Pessier and Damschen 2010), and non-planar PDC cutters (DiGiovanni et al. 2014) among others as proposed solutions to mitigate these issues. The severity of rapid bit wear and degradation has been so significant, that it has been observed that it not uncommon to plan for a three bit strategy while drilling the 6,000-ft production interval in the Pinedale Anticline: the first, second, and third bits drilling approximately 3,500 ft, 1,500 ft, and 1000 ft respectively (Han et al. 2013a).

In addition, to bit redesign, there has been significant positive displacement motor (PDM) research regarding durability of these tools given the rigorous environment, in which they have been selected to be the preferred method of targeting these resources (Azizov et al. 2011). Finally, BHA analysis (Han et al. 2013a) and improvements in directional drilling techniques and practices (Han et al. 2013b) have shown improvements in ROP and bit life.

The work by Barton et al. (2008) proposed a new PDC cutter edge geometry, which both reduced torque by 30% and increases ROP by 100% compared to conventional cutter geometries. The bit tested in this work used a 15 degree chamfer angle, compared to the conventional 45 degrees, reducing the backrake seen by the formation, and employed thermostable cutters, which reduce the preferential wear of non-leached, non-thermally stable PDC due to thermal breakdown above 700°C (Barton et al. 2008). In evaluating the performance of this new cutter design, Barton et al. (2008) compared the resultant torque and penetration rate of the new altered edge

geometry (AEG) against the standard enhanced cutter geometry, using the same bit design, with mathematical modeling, laboratory testing, field trials, and full-scale rig testing. The results in Pinedale included both a 23% increase in average ROP and a 42% increase in average interval length drilled in the production hole and a 49% increase in average ROP and a 12% increase in average interval length drilled in the 8-1/2-in intermediate hole, where WOB produced lower reactive torques (Barton et al. 2008). The key performance differentiator in the bit design was the ability of the thermostable cutters to prevent or significantly slow down the initial wear of the PDC, after which the bit would behave less efficiently like any other bit (Barton et al. 2008). The AEG design also showed significant reductions in the lateral accelerations and shocks experienced at the bit.

Gent et al. (2009) proposed a new PDC design that involved updated blade profiles, enhanced stability design features and processes, and next-generation PDC cutters to mitigate the negative effects of drilling the harsh conditions in the Pinedale Anticline. The blade shape geometry of the new PDC bit design incorporated a shortened cone length and a reduced cone angle (shown in **Fig. 1.35**), which influenced the inherent stability, cutting efficiency, hydraulic efficiency, durability, and bit steerability (Gent et al. 2009).

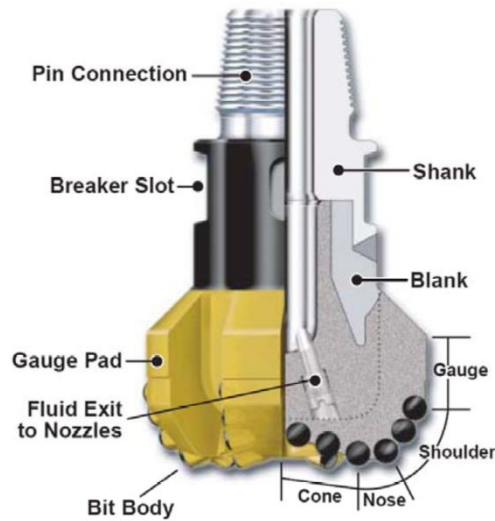


**Fig. 1.35 – Diagram of a PDC drill bit (Gent et al. 2009)**

These changes also allowed additional cutters to be placed on the outer nose and shoulder to improve the durability of the entire cutting structure and create a smoother geometric transition between cone and nose, making the work done each of the individual cutters in this area more evenly distributed and prevents overloading of individual cutters (Gent et al. 2009). Enhanced stability was incorporated in the form of built-up blade matrix behind and around the upper shoulder cutters and gauge cutters, to reduce lateral movement, absorb lateral impact loads, and protect these cutters from impact damage during unstable bit operation (Gent et al. 2009). The next-generation PDC cutters used in conjunction with the new bit design (shown in **Fig. 1.36**), incorporate improved leached diamond tables and interfaces, where the interstitial cobalt has been removed from the diamond surface, and optimized particle size and sintering conditions (Gent et al. 2009).

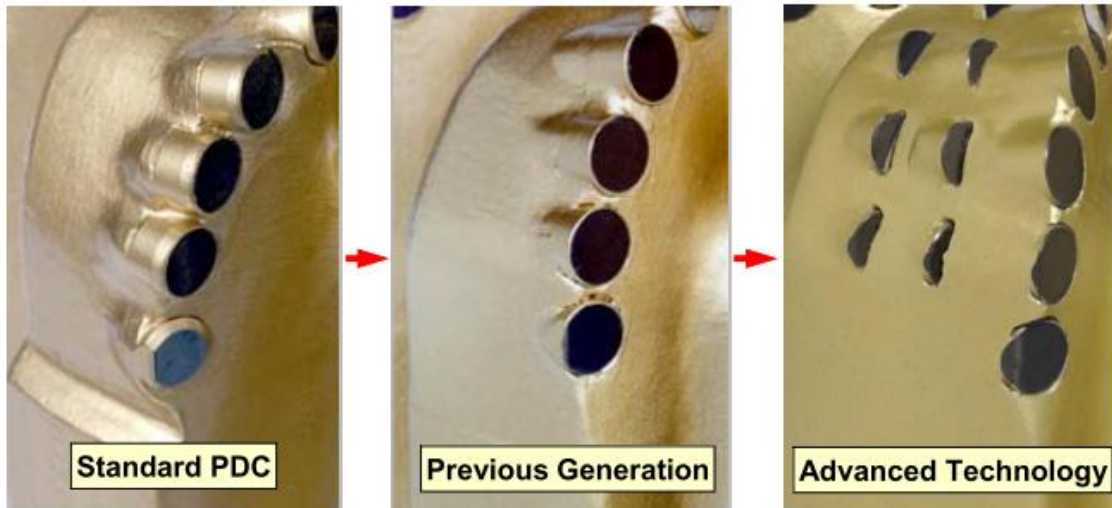


**Fig. 1.36 – Enhanced lateral stability feature development (Gent et al. 2009)**

These differences improve the abrasive wear resistance, and allow the use of a thinner diamond table to improve drilling efficiency and require less WOB to drill even after the bit is in the worn state (Gent et al. 2009). Finite element analysis and modelling showed that these new cutters have lower hoop stress, which improve the diamond durability, and was confirmed with drilling simulator testing in a laboratory setting, followed by field validation. In Pinedale, after 316 bits runs, the new-technology PDC bits drilled 14% further and 15% faster on average in the upper Lance, or during the first bit run of the production interval, and 20% further and 26% faster on average in the middle and lower Lance formations, while also showing noticeable improvements in the bit dull conditions (Gent et al. 2009).

In 2010, Baker Hughes, in an effort to address applications in which traditional roller cone bits are rate-of-penetration limited, PDC and roller cone bits are torque or

weight-on-bit limited, highly interbedded formations with high torque fluctuations cause premature failures and limit the mean operating torque, and motor applications where higher ROP, DLS, and toolface control are desired, developed and tested a series of hybrid bits, that combined the benefits of both designs (Pessier and Damschen 2010). With significant advances in PDC cutter technology, PDC bits have all but completely replaced roller cone bits, except in specific applications, where the torque requirements of a conventional PDC bit exceed the capabilities of the drilling system, such as hard, abrasive, or interbedded formations (Pessier and Damschen 2010). The basic design for hybrid bits fitting the smaller hole application, are two cone, two-bladed bits based on proven four- and six-bladed PDC bit design, creating a new aggressiveness that falls between that of roller cone and PDC bits (Pessier and Damschen 2010). **Fig. 1.37** shows an example of an advanced modern hybrid bit design.

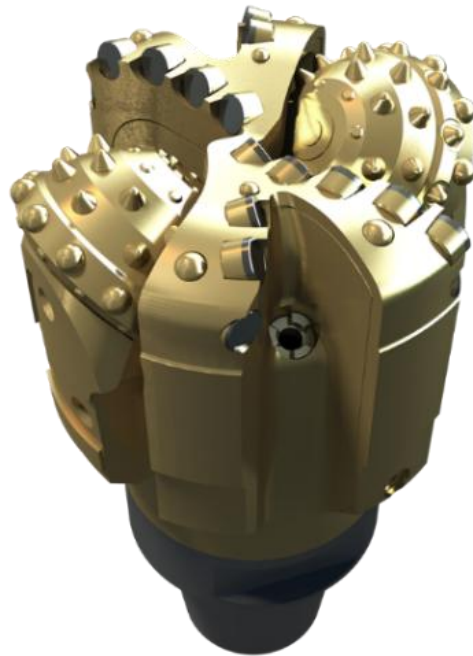


**Fig. 1.37 – Baker Hughes 2-cone/4-blade Kymera FSR Hybrid Drill Bit showing depth-of-cut (DOC) control features on each PDC blade (Hughes 2014)**

The hybrid bit takes advantage of the intermittent crushing action of a roller cone bit and combines it with the continuous shearing action of a fixed blade PDC bit, allowing the roller cone elements to create a deep damage zone in the rock being drilled, possibly fracturing hard rock, and alleviating the stresses experienced by the PDC elements while penetrating and shearing the rock; this synergy results in less wear and damage than is experienced with conventional PDC bits, due to less torque oscillation and lower vibrations (Pessier and Damschen 2010). The hybrid bits were tested against PDC and roller cone bit to benchmark their performance in soft rocks such as shale, medium strength carbonates, hard rocks such as quartzite and gabbro, and also in

interbedded formations (Pessier and Damschen 2010). For pure shale drilling, it is clear that PDC bits are the best tool; however, for hard and abrasive rocks and interbedded formations, the hybrid bits were shown to outperform both roller cone and PDC bits, by achieving higher penetration rates, with lower weight-on-bit, and with lower mechanical specific energy (Pessier and Damschen 2010). In the performance testing of these bits at the interfaces, it was shown that the PDC bit torque could change as much as 60%, while the hybrid bit torque only changed by 18%, during transitions between hard quartzite and medium strength Carthage marble (Pessier and Damschen 2010). The hybrid bits showed to they can provide less severe responses to changes in the drilling condition, such as interfacial transitions between soft and hard rocks, that cause phenomenon such as negative drilling breaks (Pessier and Damschen 2010).

The most recent bit advancement that has been trialed in Pinedale is the use of non-planar PDC cutters, shown to improve cutting efficiency, developed by Baker Hughes (DiGiovanni et al. 2014). Diamond is the hardest man-made material that is available in large quantities; however it has one significant weakness, which is temperature (DiGiovanni et al. 2014). Diamond oxidizes in an oxygen-rich environment at temperatures nearly 650°C, and becomes more rapid at temperatures nearing 750°C, which is attainable while drilling abrasive rock (DiGiovanni et al. 2014). Drilling hard formations at low depth of cut can generate massive amounts of localized heat, which can affect bit performance as it depends on the thermal stability of the PDC cutters (DiGiovanni et al. 2014). When these cutters become overheated, they experience abrasive wear at much higher rates, which leads to lower penetration rates and higher



MSE (Vaughman et al. 2003). The multidimensional non-planar cutter design proposed by DiGiovanni et al. (2014) shown below in **Fig. 1.38**, employs a recessed feature and unique regional geometry, that facilitates mechanical and thermal work dissipation while cutting rock and changes as wear progresses through the various structures.



**Fig. 1.38 – Multidimensional non-planar cutter (DiGiovanni et al. 2014)**

Complex modeling followed by a rigorous series of laboratory tests, that included single cutter tests, lathe testing, visual single point cutter (VSPC) tests, thermal load measurements, and full bit testing in a bottom hole simulator were completed before trialing the bit in Pinedale, Wyoming (DiGiovanni et al. 2014). The 50 well field trails in the production interval resulted in an average of 12% increase in distance drilled, with an increase of 15% in ROP, where the operators longest and fastest intervals to date were completed using these cutters (DiGiovanni et al. 2014).

Besides non-productive time (NPT) as a result of tripping to replace a worn bit, there has been significant time lost due to PDM failure, primarily due to the elastomer

elements in the stator failing because they lacked the required material tensile strength to maintain sealability and resist wear between the rotor and stator in high torque applications (Azizov et al. 2011). There existed a need for new elastomers to increase motor reliability and performance to match the PDC bit performance; thus a “high-performance,” proprietary elastomer was developed to attempt to better meet those needs and was shown to be able to increase motor torque output by 50% in some applications, while simultaneously decreasing the relative wear rate of the elastomer (Azizov et al. 2011). This technology was tested in Pinedale in a 4-3/4-in motor used in the production interval, and showed a 26% improvement in the average distance drilled, along with ROP increases as high as 95% (Azizov et al. 2011).

## *1.2 Provided information*

Appendix A contains information provided by Ultra Petroleum.

## 2. PROBLEM STATEMENT

The primary objective of this study is to determine the in-situ dynamics state of the bottom hole assembly and drill bit, and how this excited vibrational state contributes to the bit damage seen from the drill bits pulled out of the well. Proving the existence of stick-slip, whirl, other vibrations such as synchronous torsional oscillation (STO), and the coupled nature of these phenomena will be key in describing the exact nature of the bit damage seen from these wells. While drilling in the area of interest, changes from soft to hard laminations provides instantaneous loss of depth of cut and promotes bit damage from chipping due to whirl. While attempting to maintain high penetration rates in the harder laminations can initiate stick-slip and other torsional vibrations. This can result in two types of bit damage; first, cutters can be torn off the matrix from reverse rotation, and second, in the excited forward rotation, whirl-like damage can occur due to loss of depth of cut. These concepts will need to be proved in this study and the physical nature of the bit dysfunction will be discussed.

The implementation of operational practices and engineering redesign can mitigate or suppress the detrimental effects of the bit's excited vibrational state. However, these dysfunctions in the drilling process must first be identified, both in real-time and in post-drilling analysis for improvements to be made. The implementation and evaluation of the practices and techniques used to mitigate the experienced dysfunction will be fundamental to proving performance improvements.

### 3. METHODS

#### 3.1 *Mechanical specific energy*

Mechanical specific energy can be used in real-time when displayed on the drilling rig to rigsite personnel as a surveillance tool for observing and correcting inefficiencies in the drilling process and during post-drilling analysis as a means to study specific bit dysfunctions that are a function of other drilling parameters such as weight-on-bit, rotary speed, and rotary torque. In this manner, instances of stick-slip and whirl can be observed when comparing changes in these parameters. Stick-slip can be observed with an increase in MSE following a subsequent increase in the weight being applied to the bit. Whirl can be observed with a decrease in MSE following a subsequent increase in the weight being applied to the bit. Also, changes in formation strength and type can be identified with changes in MSE and torque when observed over a depth interval or period of time, given constant rotary speed and weight applied to the bit. If MSE increases while keeping WOB and RPM constant, then the new formation is of greater confined compressive strength, while if MSE decreases, the new formation is of lesser confined compressive strength. Proving that MSE can appropriately identify each type of drilling dysfunction and can detect changes in lithology is fundamental in determining its ability to be used as a performance improvement tool.

#### 3.2 *Drill bit forensics analysis*

Post-drilling analysis, in the form of drill bit forensics analysis can give scientists insight into the vibrational state that the drill bit experienced while it was beneath the

earth's surface. Since those involved in the drilling process cannot directly observe the bit and damage mechanisms visually or via remote video surveillance while it is drilling deep into the subsurface, one of the longest and most effective tools in determining how damage occurs to the bit is to grade the bit and its observed damage in efforts to correlate it with dysfunction and severity. The International Association of Drilling Contractors (IADC) created a dull bit grading standard for describing and recording bit damage, which is used in the overwhelming majority of operations around the world. However, while these standards provide a means for recording damage to the cutting structure, bearing seals, gauge, and why the bit was pulled, it is limited in that does not record the shape of the cutter face damage in relation to the characteristic damage mode. The standard recording process is subjective and does not fully describe the damage to the bit.

By associating the shape of the cutter damage and its location to the type of dysfunction experienced downhole, instances of whirl, stick-slip, and axial bit bounce can be observed and recorded to enhance the understanding of how the bit became dull. **Fig. 3.1** below shows the characteristic location of wear for each given bit dysfunction.

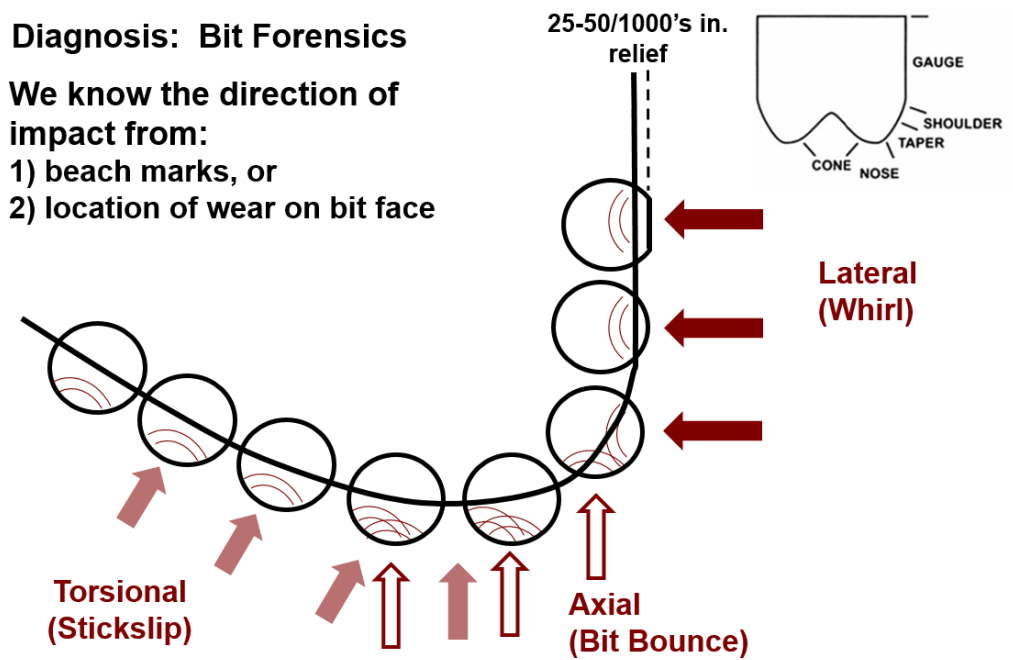


**Fig. 3.1 - Bit forensics diagram (courtesy of Halliburton)**

Keeping record of bits that showed wear, specifically in the form of beachmarks, or other wear patterns, previously described in the introduction, allow engineers to make design changes for subsequent wells and change operating practices to mitigate these vibrations.

### 3.3 *Memory-based vibration recording subs*

Memory-based vibrations and downhole dynamics recording subs (from here on called “memory subs”) can help to diagnosis the downhole in-situ vibrational state of the bit and bottom hole assembly, by recording continuous high-frequency measurements of



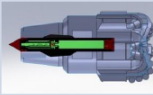

temperature, pressure, rotational speed, weight-on-bit, torque, lateral or radial acceleration, tangential or torsional acceleration, axial acceleration, bending moment, and hole inclination. These measurements can sample measurements at rates greater than 1000 Hz with high accuracy and then record to memory at a lower frequency to then be accessed when the memory sub is retrieved from the subsurface. These measurements can be paired with surface data recorded at the rigsite to show correlation and trends between the surface and subsurface. This information promotes a higher level of understanding of the exact nature of the bit and bottom hole assembly dynamics, and allows new technology or other designs to be selected and implemented for subsequent wells based on more accurate information. It also allows rigsite personnel and drill teams to better understand optimal drill parameters for specific sections of subsequent wells, while also shining a light on major limitations of the drilling system or well design if they are present.

The memory tools used in this study, depending on the specific tool, measure all of the parameters previously described, and do so at a sampling rate of 1000 Hz, while writing to memory at 1 to 2 Hz. In the case of every well included in this study, a high frequency memory tool was placed at the bit and near the highest integral blade stabilizer or roller reamer included in the bottom hole assembly. Each of these high frequency memory tools recorded temperature, rotational speed, weight-on-bit, lateral acceleration, tangential acceleration, axial acceleration, and inclination. In only one well case was a specific memory tool, the Lower Mechanical Sub (LMS), run in combinations with the standard drilling dynamics tools to capture pressure, bending,

weight-on-bit, and torque in addition to rotational speed, downhole accelerations, and temperature. **Fig. 3.2** below shows a breakdown of the capabilities of each tool and **Table 5.1** shows which tools were deployed on each well.

## Memory-Based Dynamics Measurements Tools



	Brief Description	Vibration Axes	WOB	TOB	Bending Axes	Annular pressure	Internal pressure	Precise RPM	RPM Estimate	Temp	
<b>BlackBox™</b> 400Hz / 2.56s statistics	Single axis vibration in a puck, for drilling optimization	1	✗	✗	0	✗	✗	✗	✓	✓	
<b>BlackBox RPM</b> 400 / 2Hz	Multi-axis vibration in a puck, for drilling optimization	3	✗	✗	0	✗	✗	✓	✗	✓	
<b>BlackBox HD</b> 800Hz / 2.56s statistics	Multi-axis vibration and rpm for use in a bit	3	✗	✗	0	✗	✗	✓	✗	✓	
<b>BlackBox LMS</b> 256Hz / 2Hz	5" non-mag collar based tool (Load Measurement Sub)	0	✓	✓	1	✓	✓	✓	✗	✓	

**Fig. 3.2 - Capabilities of NOV downhole dynamics tools (courtesy of NOV)**

The “Data Loggers” shown later in **Table 5.1** that were used to record the downhole data on the wells included in this study are prototype research and development downhole dynamics tools being trialed by NOV and are similar to, but more capable than the BlackBox Subs shown in **Fig. 3.2**. The data loggers operations and characteristics are most similar to the BlackBox RPM model because the data logger records the same parameters and writes data to memory at the same frequency, but is capable of sampling data at over 1000 Hz. The data loggers also do not calculate



downhole RPM as a function of acceleration as many dynamics tools do, but instead measure the rotational speed directly with a gyroscope, making them different than the tools shown above. Five to ten second bursts of high-frequency data is also capable of being recorded with the data logger tool, making it different than the tools shown; however, none of the tools used in this study were set up to record bursts of data.

### *3.4 Measurement while drilling (MWD) and open hole well logging*

Measurement while drilling (MWD) subs and open hole well logging can be used to gather information about the formation as well as wellbore shape and direction. These measurements include but are not limited to caliper logs, porosity and density logs, resistivity logs, gamma ray logs, as well as inclination and azimuth measurements. While a variety of these measurements were taken on the wells included in this study, only gamma ray logging will be discussed.

Gamma ray measurements record the existence of naturally occurring radioactive materials including uranium, thorium, and potassium in the formation. These measurements are recorded in API units, and are typically assumed to correspond to the volumetric clay content in the pore space of a particular rock or material. Higher gamma ray values correspond to higher clay content, while lower gamma ray values correspond to lower clay content. While clay contents can vary from field to field, clean sand and clay abundant shale baseline values can be designated for a particular formation allowing differing rock types to be easily identified based on their inferred volumetric clay content. **Fig. 3.3** on the next page shows a spectral gamma ray log and correlates

high gamma ray and uranium measurements with increased total organic carbon, or shale, which contains organic rich clay materials.

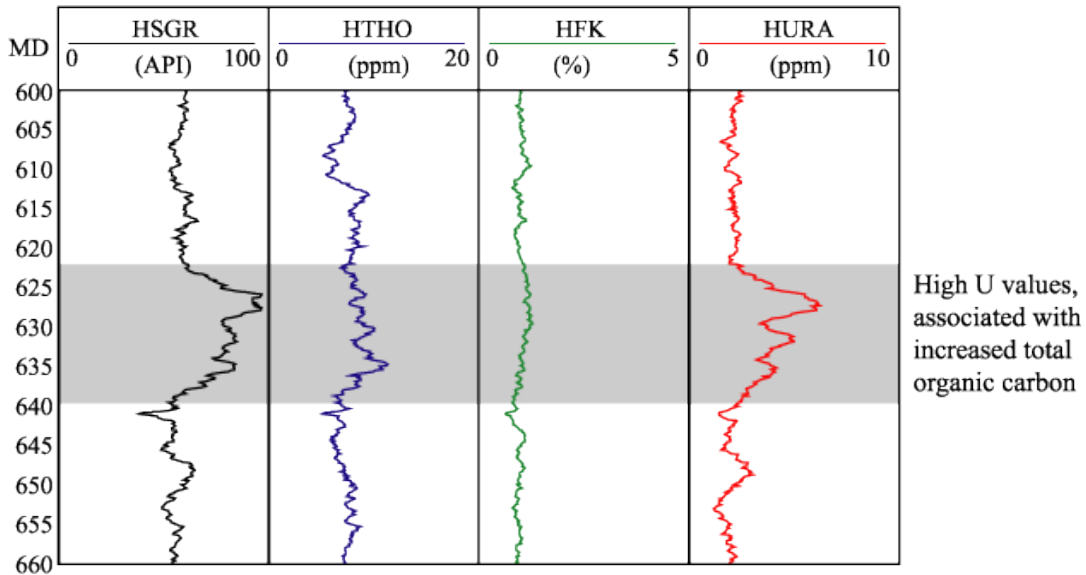


**Fig. 3.3 – Spectral gamma ray logging shows increased total organic carbon**  
**(Courtesy of Texas A&M University)**

In drilling, gamma ray logs are used to determine changes in rock type and subsequently rock strength. In a given formation, gamma ray values allow for various interbedded rock types to be differentiated based on their value in API units. In this way, sand, silt, and shale laminations can be identified in post drilling analysis and differing confined compressive strengths can be assumed.

#### 4. OBJECTIVES AND PROCEDURES

The primary objective of this study is to determine the in-situ dynamics state of the bottom hole assembly and drill bit, and how this excited vibrational state contributes to the bit damage seen from the drill bits pulled out of the well. Proving the existence of stick-slip, whirl, other vibrations such as synchronous torsional oscillation (STO), and the coupled nature of these phenomena is important, but more important, is understanding how these dysfunctions can be mitigated to improve drilling performance through experimentation, analysis, and redesign.

In an effort to mitigate the vibrations, that were believed to have been seen during early wells and as a results of service company analysis, a variety of practices, techniques, and design changes were tried and tested to improve performance. Among these are the use of physics-based continuous improvement practices, the use of roller reamers instead of integral blade stabilizers, the use of extended gauge bits, and the use of depth of cut control features on drill bits. System improvements including active torque control and increased diameter drillpipe were proposed during the analysis involved in this study and active torque control was installed on one of the rigs in the fleet, but no results were obtained from its implementation prior to the completion of this work.

#### 4.1. *Physics-based continuous improvement practices*

Physics-based continuous improvement practices were taught to engineers and rigsite personnel in September 2014 and involved subjects including the following:

- performance management workflows
- bit mechanics
- mechanical specific energy
- rock mechanics
- bit balling
- general vibrations
- whirl
- stick-slip
- axial vibrations
- interfacial severity
- bottom hole balling
- borehole stability
- filter cake morphology
- hole cleaning
- integrity testing
- wellbore integrity management.

Fig. 4.1 shows an example ROP versus WOB plot, that highlight some potential redesign opportunities that the operator could explore in attempting to improve performance.

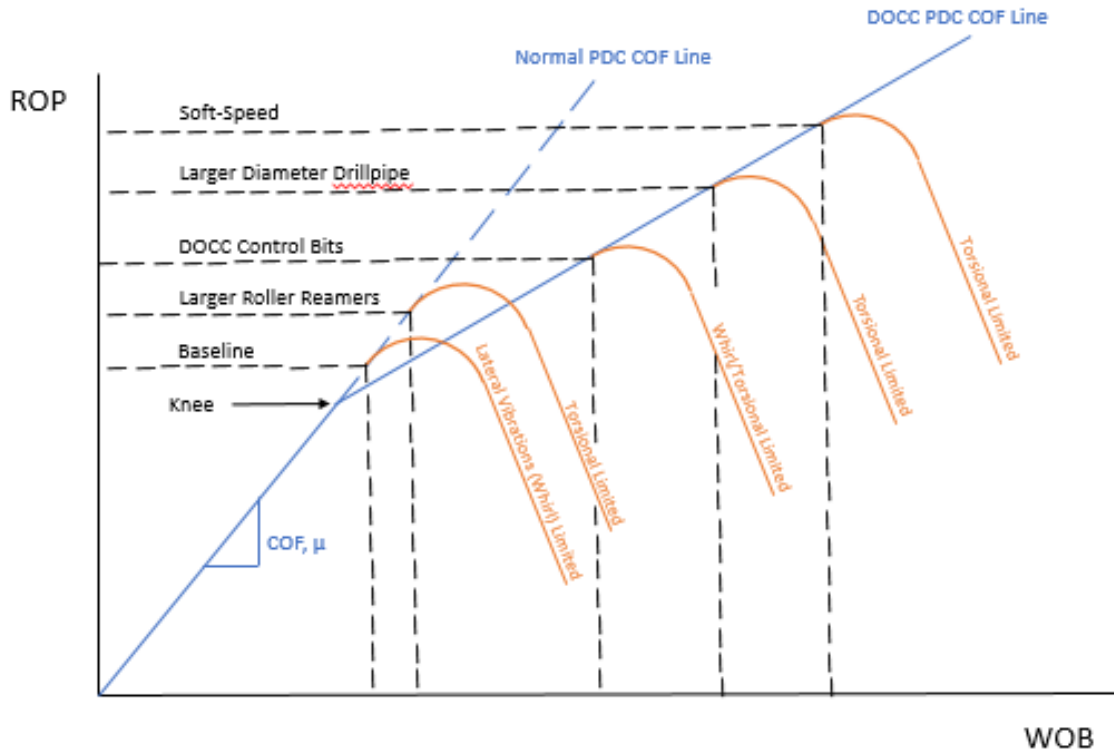


**Fig. 4.1 - Example ROP versus WOB plot showing bit founder and redesign opportunities for the operator**

Accompanying the physics being taught was a list of operational procedures and tests that could be used to identify and address observed dysfunction. These tests and procedures included WOB step tests to identify the onset of torsional oscillation and stick-slip, RPM step tests to determine non-resonant rotational speeds, and step by step

detailed instruction for drillers related to real-time dysfunction reduction using surface operating parameters.

#### *4.2. Roller reamers*

The use of roller reamers instead of integral blade stabilizers (IBS) helps to promote reduced wellbore friction that is created as a consequence of the components in the bottom hole assembly rubbing against the borehole wall. Because of their construction which includes free-spinning rolling cylinders which rotate about bearings, roller reamers reduce sliding friction by transferring some of the energy, otherwise lost or generated into potential energy as the drill string winds up due to sliding friction, into rotational energy.

Prior to the physics-based training the operator exclusively used 5-7/8" integral blade stabilizers in their bottom hole assembly design. The conventional BHA design involved using an IBS in both the second and third positions spaced on average about seventy feet apart, while the Schlumberger PowerV vertical seeking rotary steerable tool occupied the first or near bit stabilizer position. The operator also practices using a thread-on bearing housing stabilizer in conjunction with the straight downhole motor incorporated in their bottom hole assembly design. During the experiments involved in this study a combination of BHA designs were used. The first design incorporated the use of 5-7/8" integral blade stabilizers, the second used 5-7/8" roller reamers, and the third used 6" roller reamers. An example BHA sheet can be seen in the figure on p. 93. The idea to use 6" roller reamers was predicated on the idea that a full gauge stabilizing

element would perform better in a hole that was drilled slightly over gauge, due to large amounts of side-cutting as a result of high lateral near bit side force and accelerations. The full gauge roller reamer would accomplish this by reducing the clearance between the rolling elements of the roller reamer and the borehole wall, thereby reducing the amplitude of lateral motion in the bottom hole assembly and ultimately the severity of the maximum angle of bit tilt.

#### 4.3. *Extended gauge length bits*

When trying to reduce the side-cutting of the drill bit as a function of the higher amplitude lateral motion above the bit in the BHA, there are a number of techniques that can be employed to accomplish these vibrations reductions. Among these techniques are reducing the gauge cutting activity and increasing the bit's gauge length. We can reduce the gauge cutter activity by removing or reducing the number of cutters that are present on the bit gauge. This promotes less side cutting and a reduced tendency for creating borehole patterns, while simultaneously promoting more efficient drilling by decreasing the amount of energy used to drill in directions offset from the target location.

Increasing the gauge length of the drill bit, provided that there is not simultaneously an increase in the severity of the bit's taper profile or an increase in the amount of undercut on the gauge profile, can reduce the amount of side-cutting that the bit naturally wants to exhibit by reducing the amount of allowable bit tilt the bit can achieve. Bit tilt is a function of contact angle between two points on a rigid beam, the bit acting as the beam. Therefore, if the length of the beam is increased, given the same

containment or hole size, the amount of bit tilt or achievable build rate angle is reduced proportionally to that increase in length. This can be visualized in **Fig. 4.2** below:

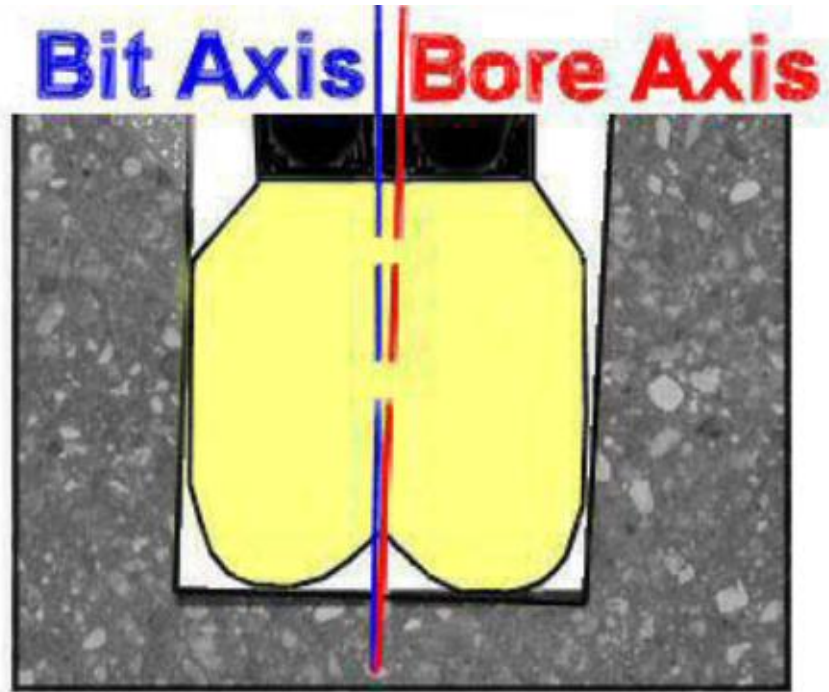


**Fig. 4.2 – Bit tilt, which is the angle measured between the bit axis and bore axis, can be reduced with extended gauge bits by reducing the amount of distance a bit can rotate or tilt off center before making contact with the borehole wall (Pastusek et al. 2005)**

For the straight, vertical hole section that is being studied, both reduced gauge cutter activity (shown in **Fig. 4.3**) and increased bit gauge length were proposed during the physics-based training. However, due to these practices being implemented prior to this vibrations study and the operator adopting these practices on every well, the effect



of extended bit gauge length cannot be directly compared with prior performance from a physics-based analysis.

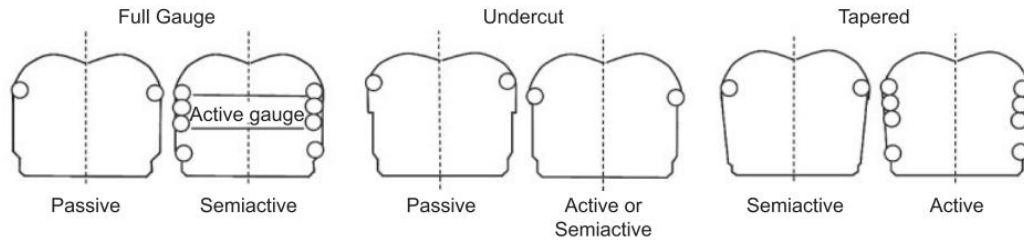


**Fig. 4.3 – Reduced gauge activity reduces side cutting, severity of lateral vibrations, and borehole patterns (Dupriest and Sowers 2010)**

#### 4.4. *Depth of cut control bits*

To manage stick-slip and other torsional vibrations, a depth of cut control bit was tested during this study. Depth of cut control bits accomplish mitigating torsional vibrations by limiting the amplitude of depth of cut oscillation. During periods of torsional oscillation and full stick-slip, the depth of cut can oscillate between high values during periods of high bit torque, low bit rotational speeds, and over-engagement of the cutter face to low or even zero values during periods of low bit torque, high rotational speeds, and under-engagement of the cutter faces. Depth of cut control bits contain rubbing elements that are placed behind the cutting elements on the nose of PDC bit blade, which limit the cutter engagement, thus preventing cutter over-engagement. This prevention of over-engagement limits the excitation force and torque responsible for sustained periods of torsional oscillation and limits the range of oscillation by reducing

one boundary. Operational practices can address the other boundary, which is related to loss of depth of cut, by preventing the disengagement of the cutter face. Specifically, when high WOB is applied to a depth of cut control bit, depth of cut loss can be reduced or eliminated, which reduces the amplitude of torsional oscillation and eliminating the dysfunction. In this way, depth of cut control bits can constrain lateral and torsional motion, which ultimately leads to higher penetration rates and longer bit life.

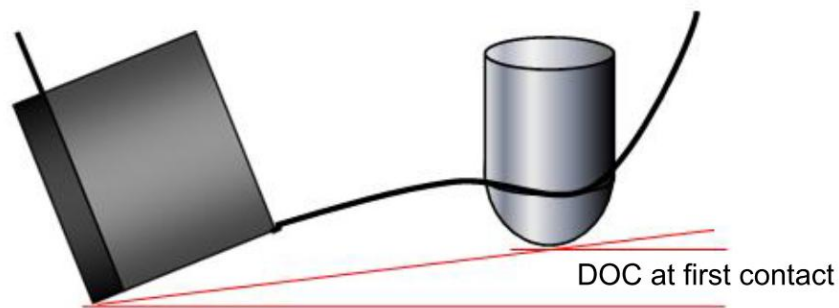


**Fig. 4.4 – When the rubbing surfaces make contact with the bottom of the hole they prevent over-engagement of the cutters into the formation being drilled by carrying some of the applied axial load (Davis et al. 2012)**

When weight is applied to a depth of cut control bit, the bit initially responds with its normal aggressiveness, until the rubbing elements make contact with the formation (shown in **Fig. 4.4**) and start rubbing, at which point they start to carry some of the applied axial load or weight on bit. This causes a shift in aggressiveness as increases in WOB correspond to lower incremental increases in ROP, while

simultaneously extending the bit founder for severe torsional oscillation. In this way higher penetration rates can be achieved with depth of cut control bits.

#### *4.5. Active torque control*

After the completion of this study, active torque control was installed and tested on one of the rigs in the operator's fleet. Because no downhole dynamics data was recorded from bit runs using this technology, its performance cannot be compared at this time. Active torque control works through active damping of either the topdrive torque or rotational speed, such that additional power is not added into the rotational system, which would promote torsional oscillation. Instead these systems allow for excess energy absorption to take place in the drill string, keeping the energy fluctuation away from the bit. New technologies in these systems have allowed them to become self-tuning and ultimately more effective in reducing torsional oscillations.

#### *4.6. Larger diameter drill pipe*

Drill pipe is the primary tubular that allow the transmission of forces from surface to the bit in the subsurface. Conventionally the size of drill pipe used is selected based on the hole size and equivalent circulating densities required by the formation being drilled. Sometimes the drill pipe and other components of the drillstring can limit the achievable drilling performance for a well due to insufficient torsional rigidity or stiffness to allow efficient transfer of torque from surface to the bit. This limitation can be compounded when drilling hard, deep, highly laminated formation. In this study, no

changes were made to the drillstring between trials; however the potential benefits of increasing the torsional rigidity of the drillstring by increasing the diameter of the drill pipe will be discussed later.

During this study it was determined by the author that the torsional compliance of the drillstring was too great to effectively mitigate torsional oscillation at the bit, while providing an acceptable drill rate and subsequently efforts were made throughout the study to persuade the company to increase the diameter of its drillpipe.

#### *4.7. Procedure*

Understanding the unique location and mechanism of bit damage that occurs while drilling the highly laminated and deep production intervals is fundamental to the study. Due to this priority, the first testing and measurement procedure developed during the study involved being able to track and record the unique features of the bit damage and to also track progress from well to well. Taking photographs of each bit after each bit run allowed this objective to be accomplished. These photographs were added to the standard procedure of completing an IADC bit dull grading worksheet, and included high resolution images of the bit viewed from below, as well as, close up images of each PDC blade and cutters. This procedure not only builds a database of bit images, but also allows engineers and analysts to observe the bit wear mechanism from miles away electronically as each bit is pulled from the well. **Fig. 4.5** below shows representative pictures of the bits used in the first bit run of the production interval from the wells included in this study.



**Fig. 4.5 - Bit forensic pictures from Wells 1, 2, and 3 respectively**

A detailed analysis of the wear mechanisms and features seen on the outside cutter rows will be discussed later in this work, describing how a combination of vibrations contributed to the rapid damage observed.

In order to determine the effectiveness of the changes in operational practices and each of the design changes, a standardized test procedure was developed. This procedure incorporated specifications for measurement tool placement to ensure repeatability, while also remaining economically viable within the operator's budget. With these concerns in mind, two vibrations measurement tools were run in each bottom hole assembly, one near the bit just below the vertical seeking rotary steerable assembly and the other roughly 120 ft above that just below the third position roller reamer or

integral blade stabilizer. Also, in one of the wells a downhole measurement tool was incorporated to record the downhole WOB, torque, and bending moment for the given directional well profile. This tool was only used on one well due to its high cost and limited availability, however, the measurements obtained from its use can be assumed to be similar to offset wells included in this study due to the similarity in well profiles and designs.

Upon receiving the data from the operator and service companies, which included well names and API numbers, well schematics and directional plans, final well surveys, bit records and post-run pictures, bit datasheets, downhole vibrations measurements, third party vibrations analysis, one-second surface rig data, open hole well logs, mud logs and mud reports, daily drilling reports, and geologists formation picks, the author became familiarized with the plethora of data and designed an analysis procedure. This procedure included looking at entire bit runs for locations of dysfunction as a function of both mechanical specific energy, lateral and tangential bit vibrations, and lateral and tangential bottom hole assembly vibrations, as well as, designing specific tests to prove vibrations reductions during periods of dysfunction. Plots were created to show:

- reduction in lateral BHA and bit vibrations as a result of using larger roller reamers
- potential resonant rotational speeds
- the onset of synchronous torsional oscillation and stick-slip,

- the WOB and bit founder relationship for regular and depth of cut controlling PDC bits
- the relationship between gamma ray (rock strength) and vibrations levels
- the coupled nature of bit lateral and tangential accelerations during periods of STO and stick-slip
- a fast Fourier Transform on a period of synchronous torsional oscillation.

In order to create these plots and present these findings a number of steps were taken to ensure data accuracy and reliability. The first of these steps was to appropriately synchronize the high frequency data between the various downhole dynamics and memory based tools with the high frequency surface data. In this way important calculations and parameters could be derived using a combination of the data. Some of these calculations included depth of cut, mechanical specific energy, bit coefficient of friction, and downhole bit rotation speed derived from pump rate. Their equations are shown below:

Downhole bit RPM from pump rate:

$$RPM_{bit,pump} = RPM_{rotary} + (Q_{pump} * \mu_{motor}) \dots \dots \dots \text{Eqn. 1}$$

where:

- $RPM_{bit,pump}$  = estimated downhole bit rotational speed (rev/min)
- $RPM_{rotary}$  = rotational speed of topdrive or Kelly (rev/min)
- $Q_{pump}$  = the total flow rate through the mud pumps and standpipe (gpm)
- $\mu_{motor}$  = the motor specific ratio of revolutions to flow volume (rev/gal)

Depth of cut:

$$DOC = \frac{ROP}{RPM_{bit}} * \frac{12}{60} \dots \dots \dots \text{Eqn. 2}$$

where:  $DOC$  = depth of cut (in/rev)  
 $ROP$  = penetration rate (ft/hr)  
 $RPM_{bit}$  = instantaneous bit rotational speed (rev/min)

Bit coefficient of friction:

$$COF = \frac{36 * T}{D * WOB} \dots \dots \dots \text{Eqn. 3}$$

where:  $COF$  = bit coefficient of friction (dimensionless) [Tangential force]/[Normal force]  
 $T$  = rotary or downhole torque (ft-lbs)  
 $D$  = bit diameter (in)  
 $WOB$  = surface or downhole weight-on-bit (lbs)

Mechanical specific energy:

$$MSE_{psi} = \frac{480 * T * RPM}{D^2 * ROP} * \frac{4 * WOB}{\pi * D^2} \dots \dots \dots \text{Eqn. 4}$$

where:  $MSE$  = mechanical specific energy (psi)  
 $T$  = rotary or downhole torque (ft-lbs)  
 $RPM$  = rotary speed or downhole bit rotational speed (rev/min)  
 $D$  = bit diameter (in)  
 $ROP$  = penetration rate (ft/hr)  
 $WOB$  = surface or downhole weight-on-bit (lbs)

After datasets were created using these equations, the data was plotted to observe trends. Simultaneously, the author conducted an extensive literature review, based on subjects that he believed he was seeing in the data. This process was repeated over several iterations until an understanding of the physical nature of the drill string dynamics and bit damage and location was perceived to be well understood.



## 5. RESULTS

### 5.1 High level vibrations overview

In order to adequately represent and understand the changes in drilling dysfunction present in the wells in this study, it was important to plot significant operational parameters as a function of either time or depth. This included both surface operating parameters and downhole measured parameters being plotted in Microsoft Excel. The **Fig 5.1** represents this type of plot showing key measured parameters as a function of time listed below:



**Fig. 5.1 – Surface and downhole measurements versus time Well 1 Bit Run 2**

The parameters shown in **Fig 5.1** include the following by track number:

1. Surface (red) and Downhole (blue) Mechanical Specific Energy
2. Lateral Accelerations in the BHA (red) and Instantaneous Depth of Cut (blue)
3. Lateral (red) and Tangential (blue) Bit Accelerations
4. Bit (red), BHA (blue), and Rotary (green) RPM
5. Bit (red) and Rotary (blue) Torque
6. Bit (red) and Rotary (blue) Weight on Bit
7. Rate of Penetration (blue) and Gamma Ray (red)

The combination of tracks show a few distinct types of dysfunction during the time period displayed in **Fig. 5.1**. Well-developed, full stick-slip is shown during the following time intervals, 350,000 to 350,200 seconds and 351,050 to 352,000 seconds shown in yellow, while unstable stick-slip and synchronous torsional oscillation (STO) are shown during the intervals 350,200 to 350,500 seconds, 350,550 to 351,050 seconds, and 352,000 to 353,700 seconds shown in red.

Stick-slip events are associated with high instantaneous gains in DOC that oscillates with a regular periods. These events tend to show much lower levels of both lateral and tangential bit and BHA accelerations than STO. The periods of stick-slip show a well-defined “sticking” phase in the RPM track, presented in **Fig. 1.2**, as well as, clear signs of the motor stalling, as it is observed to show periods of negative rotation and RPM ramping while transitioning between cycles. Stick-slip is observed to have large swings in WOB and torque both at surface and downhole during each oscillation or cycle.

Periods of unstable stick-slip and synchronous torsional oscillation are associated with sustained periods of low DOC, that allow the bit to vibrate around the bottom of the hole, unconstrained by the indentation action of the cutter faces. These periods are shown to have the highest levels of bit and BHA accelerations during each of the bit runs, both laterally and tangentially. Unstable stick-slip and STO vibrations are also associated with less severe changes in RPM due to not storing excess amounts of torsional energy in the drill string during a prolonged sticking phase. However these vibrations have been shown to exhibit zero and even backwards bit rotational speeds as well as very fast forward rotations. Limited change in WOB and torque values measured both at surface and downhole have been observed with the occurrence unstable stick-slip and STO, which can be attributed to the lack of DOC and limited oscillation in DOC.

The results of this study show that unstable stick-slip and STO are virtually impossible to detect at the surface when looking at WOB, RPM, and torque measurements, while full stick-slip is easily observed with oscillations in surface WOB and torque, and with asymmetric torque signatures with time, as shown in **Fig. 5.2**.

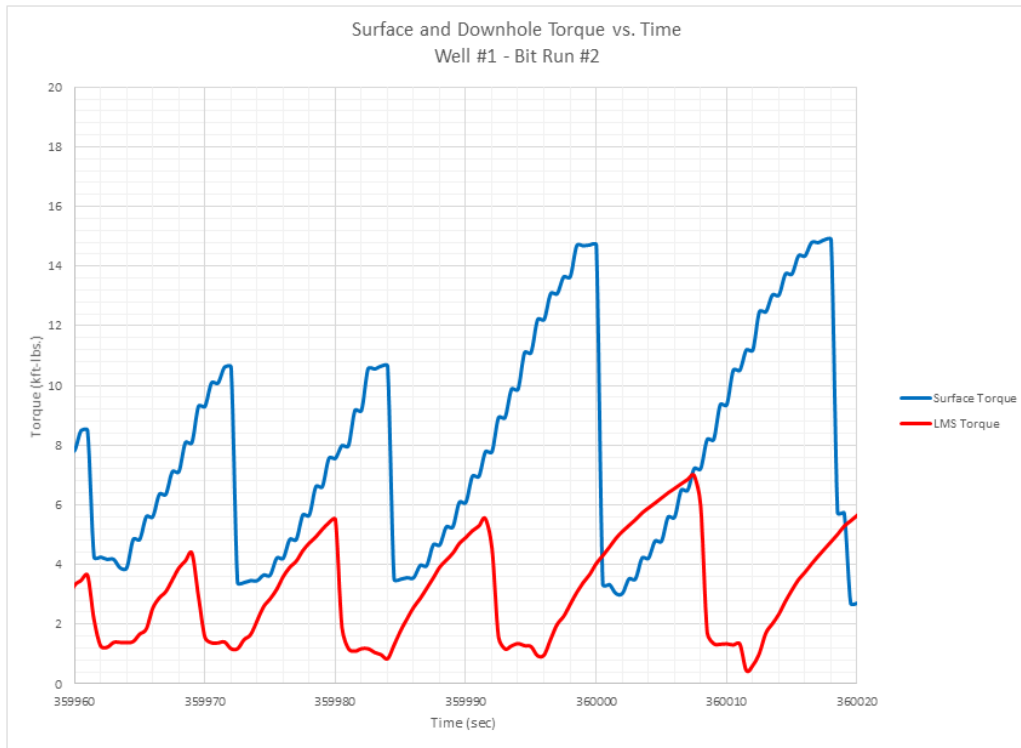


**Fig. 5.2 – Asymmetric torque signature during full stick-slip**

Mechanical specific energy, when estimated using surface measurements, is capable of capturing these vibrations and could even be used to capture the difference between STO and other vibrations. During periods of full stick-slip, unstable stick-slip, and STO, MSE shows elevated readings of approximately the same value. This value corresponds to the presence of some form of inefficient dynamic dysfunction. However, using the one-second data capabilities of the rigs recording the measurements during the study, the MSE values during full stick-slip show that it tends to oscillate with changes in WOB and torque, showing a noisy asymmetric signal at the same frequency as the first torsional mode of stick-slip. These trends can be observed in **Fig. 5.3**.

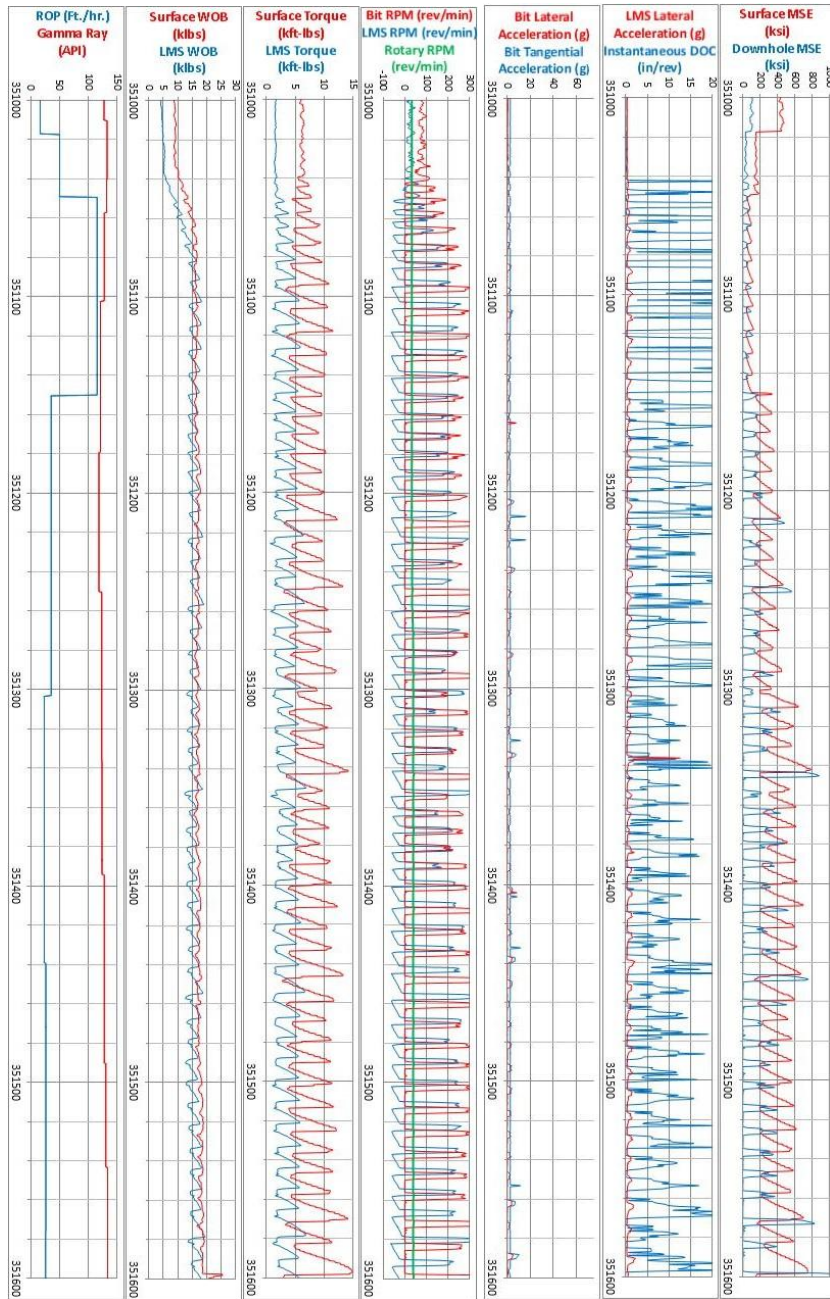


**Fig. 5.3 – Stick-slip observed by MSE**

STO and unstable stick-slip, on the other hand, tend to show little oscillation in MSE value due to the small variations in WOB, torque, and DOC during its excitation.

STO and unstable stick-slip also show higher mean MSE values than stick-slip due to their greater dynamic inefficiencies. These trends can be observed in **Fig. 5.4**.

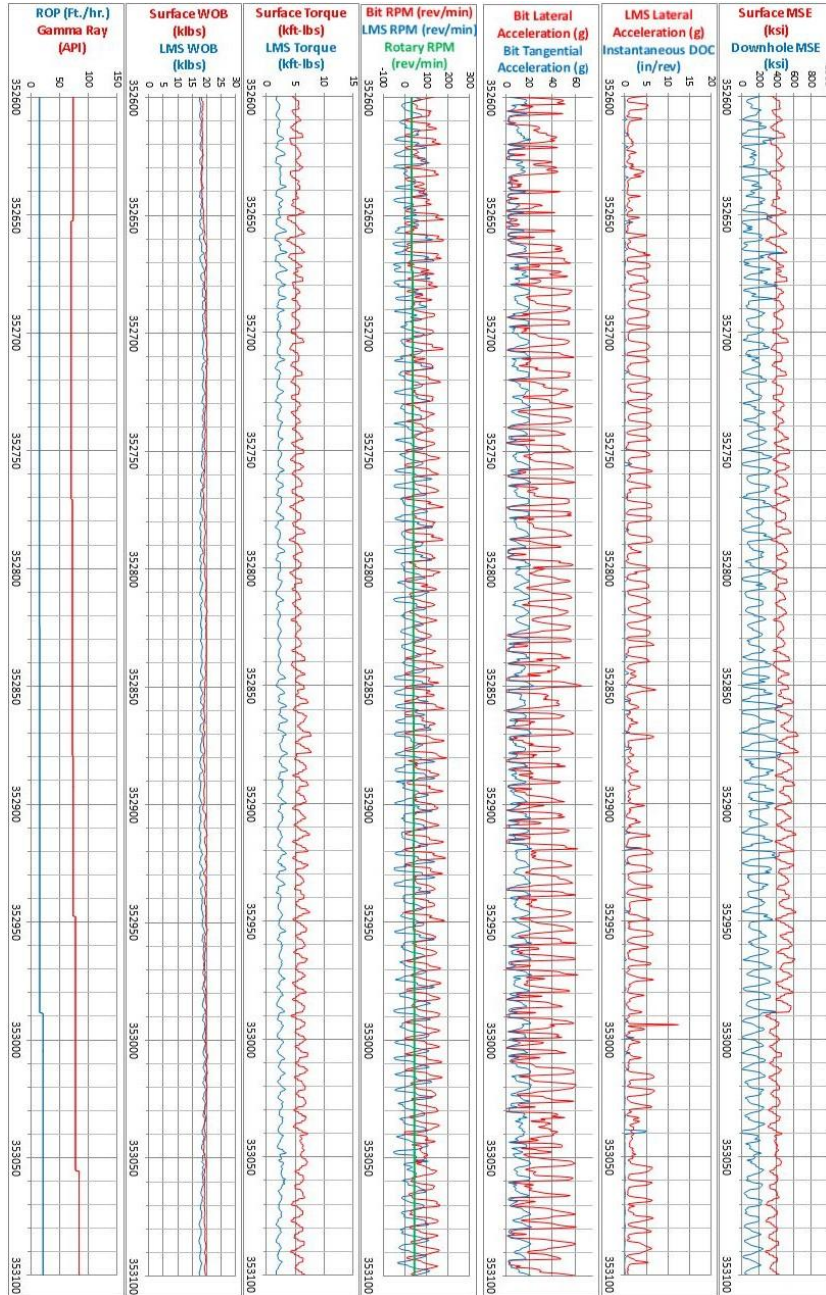


**Fig. 5.4 – Synchronous Torsional Oscillation observed by MSE**

## 5.2 *Equipment involved in each well*

Different equipment was utilized throughout the study, allowing for conclusions to be drawn from comparisons about the effectiveness of specific tools in reducing vibrations. However, due to data quality and availability, none of the bit runs from the wells included would be considered a true base case representing the BHA design that was standard practice for the company prior to physics-based training. This is because in each of the bit runs containing a complete set of data, a new piece of technology was tested. In fact, there were other wells to choose from which included downhole dynamics measurements, however, it was determined that the three wells included in this work would be most effective and representative in the determination of dysfunction reduction and performance improvement, due to the completeness of the datasets from the wells included, as well as the specific technologies that each tested. **Table 5.1** details the equipment and design differences between the three case wells.

**Table 5.1 – Differences between BHA designs in each well**

<b>Well Equipment</b>	<b>Well #1</b>	<b>Well #2</b>	<b>Well #3</b>
First Run Bit Gauge Length Type/Depth In/Out	HC DP406FX 3 inches (9,765 – 12,905)	HC DP406FX 3 inches (10,630 – 13,487)	REED SK613M- M1D – 3 inches (8,435-11,926)
Second Run Bit Gauge Length Type/Depth In/Out	HC DP406FX 3 inches (12,905 – 13,932)	N/A - HC DP406FX 3 inches (13,487 – 14,700)	N/A - HC DP406FX 3 inches (11,926 – 12,922)
Third Run Bit Type/ Gauge Length Depth In/Out	N/A	N/A	N/A - HC DP406FX 3 inches (12,922 – 13,513)
Near Bit Tool	NOV Data Logger	NOV Data Logger	NOV Data Logger
String Tool	NOV Data Logger	NOV Data Logger	NOV Data Logger
Lower Mechanical Sub	Yes	No	No
Stabilizer Type	5-7/8” Roller Reamer	6” FG Roller Reamer	5-7/8” IBS

In **Table 5.1**, the differences in bit type, bottom hole assembly stabilization elements, and measurement devices are highlighted. Only the third well ran a bit that included designed depth of cut controlling features. The table also shows bit runs that were either not required to achieve the target depth or that did not incorporate downhole dynamics measurement by showing “N/A”, thus these bit runs are not included in the study. **Table 5.1** also shows the differences in downhole measurement devices that were incorporated, primarily the use of an NOV Lower Mechanical Sub (LMS) tool on only the first well. Without this tool, downhole WOB, torque, and bending moment are not measured. The NOV Data Logger tool, which measures downhole dynamics information such as



accelerations can be used to infer vibrational state, was used on every well in the study and was in part a reason why these wells were selected. The Data Logger tool has superior measurement accuracy and higher frequency capabilities to standard NOV Blackboxes. Finally, **Table 5.1** shows the differences in bottom hole assembly stabilization equipment incorporated in each of the case wells.

The BHA designs deployed in the three wells are very similar, excluding the stabilization equipment incorporated and the addition of a ten foot LMS tool in the first well. For the purposes of this study, the differences in the BHA design excluding the stabilization equipment is considered negligible in terms of vibrations. This means that it is not expected that the other equipment in the BHA will behave significantly different from case to case from the perspective of adding amplitude or severity to the vibrational state of the BHA and bit. **Fig. 5.5** shows the BHA used in the first bit run from Well 1. The **Fig. 5.5** gives both the size and position of the stabilization elements incorporated in the BHA as well as the relative sizes of the rest of the components included. From this geometry, properties such as torsional stiffness can be inferred.

BHA #1					
No.	Item	ID (in)	OD (in)	Length (ft)	Sum (ft)
1	HC DP406FX		6	1	1
2	BlackBox Sub	1.25	5	1.17	2.17
3	PowerV		4.75	14.38	16.55
4	Filter Sub	2.25	4.75	3.09	19.64
5	Hunting Motor		5	30.87	50.51
6	5 7/8" Roller Reamer	1.5	4.75	5.92	56.43
7	HOS #1	3	4.75	1.94	58.37
8	NMDC w/ MWD	2.69	4.8	31.09	89.46
9	HOS #2	3	4.75	2.02	91.48
10	Gap Sub	2.25	4.75	4.63	96.11
11	NMPC	2.69	4.81	10.14	106.25
12	LMS	1.13	5	10.84	117.09
13	BlackBox Sub	1.25	5	3.01	120.1
14	5 7/8" Roller Reamer	1.5	4.75	5.93	126.03
15	X/O Sub	2.5	5.25	3.02	129.05
16	24 Jts HWDP	3	5	740.44	869.49
17	Jars	2.25	5.25	29.68	899.17
18	5 Jts HWDP	3	5	153.95	1053.12



**Fig. 5.5 – Standard BHA design (Courtesy of NOV)**

It is important to note that **Fig. 5.5** does not detail the size, weights, and grades of the drill pipe and heavy weight drill pipe (HWDP) used on these wells, which were 4-in 14.0 ppf S-135 and 4-in 27.2 ppf S 135, respectively.

### 5.3 *Early observations*

Initial examination of the downhole data identified of the root limiter of the drilling system and provided a basis for comparison. Through examination of the downhole rotational speed oscillation and torque fluctuations on surface showed

torsional oscillation and full stick-slip were observed to be present throughout the majority of every bit run included in the study. It was observed that elevated lateral and tangential bit accelerations accompanied this speed oscillation, instigating an investigation of the relative instantaneous depth of cut range that the bit exhibited and of the vibrations levels with depth. The high frequency downhole data collected allows for this type of analysis, resulting in a better understanding of the loads and confining forces experienced by the bit during periods of torsional oscillation and stick-slip. **Fig. 5.6** shows a representation of the DOC range and associated lateral accelerations during a period preceding tool failure, in which high lateral accelerations were observed at the bit.

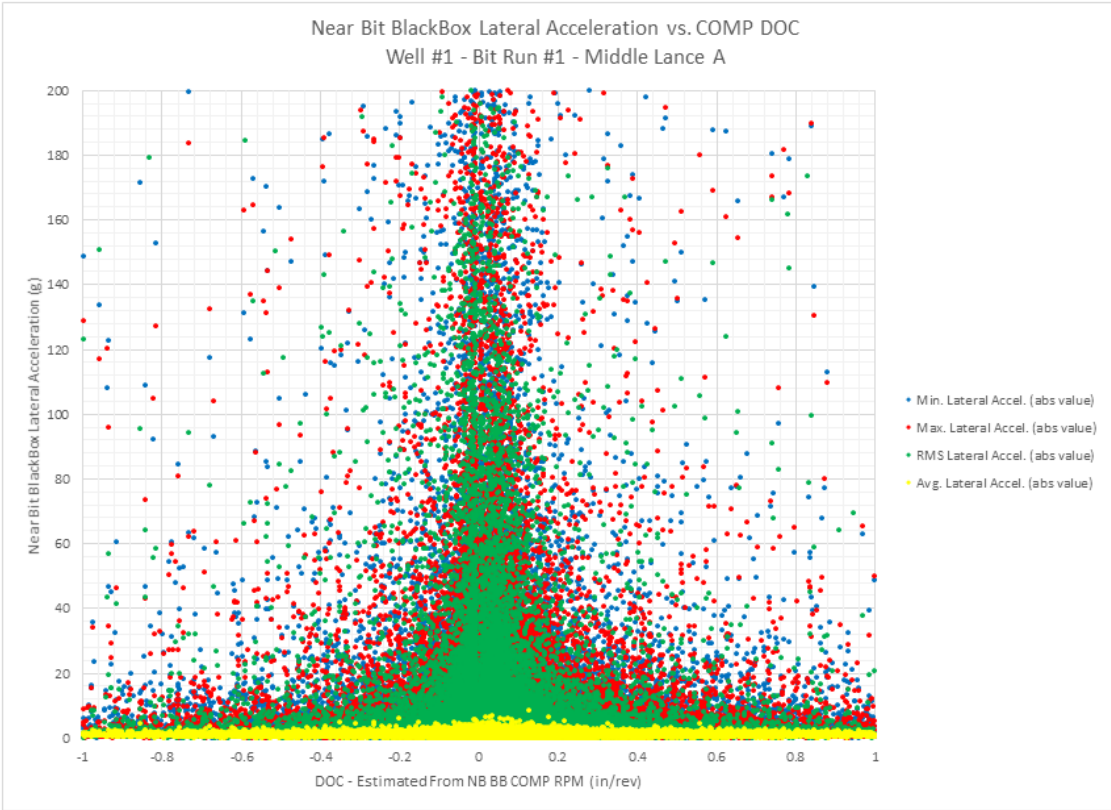


**Fig. 5.6 – Lateral bit acceleration versus DOC in the upper production interval**

Negative rotation and high lateral bit accelerations are observed, while showing the majority of instantaneous DOC oscillation between -0.2 and 0.3 inches per revolution. It is important to note that negative DOC does not correspond to the bit failing to remain in contact with the formation or drill in the opposite direction, instead it signifies negative instantaneous bit rotation which translates into negative DOC as calculated by equation 2. This type of plot also allows for observation and possible identification of various torsionally induced dysfunctions. Specifically, the unique characteristics of stick-slip and synchronous torsional oscillation can be differentiated using this type of plot, when examining the shape. The high lateral accelerations that occur at low DOC are associated with the occurrence of unstable stick-slip and STO, while the low lateral accelerations that occur over the entire DOC range signify full stick-slip.

It was interesting to observe that the severity of the elevated lateral bit accelerations associated with the occurrence of unstable stick-slip and STO decreased with increasing depth. **Fig. 5.6** shows a period of drilling in which STO and full stick-slip were observed in an upper part of the production interval with peak lateral accelerations higher than 200g at the bit, while **Fig. 5.7** below, on the other hand, shows a period of drilling in which STO and full stick-slip was observed which exhibits high lateral bit accelerations which peak around 100g.

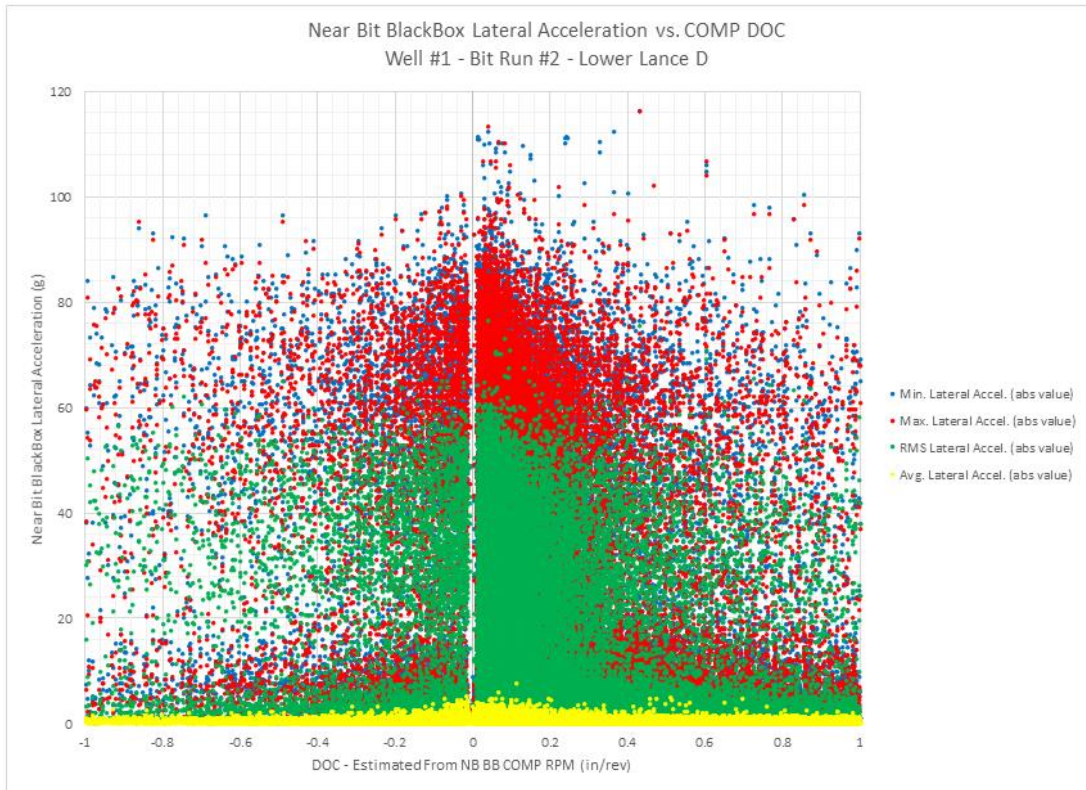


**Fig. 5.7 - Lateral bit acceleration versus DOC in the lower production interval**

It is believed that this reduction in peak acceleration level with depth is related to well geometry, and buckling mode severity, which is function of a number of factors including drill string constraint, applied weight, eccentricity, and location of the neutral point.

During the early stages of this study, it was first believed that alternating stick-slip and whirl events were dependent on the strength of the rock being drilled and weight being applied to the bit. However as the study progressed it was determined that torsional oscillation or stick-slip was present throughout the majority of every bit run, this bit speed oscillation was coupled with high lateral bit accelerations in the slip phase,

and it was responsible for the coupled and elevated lateral bit vibrations, rather than conventional whirl. As a results of the assumptions during the early phases of the study, design changes were made to address both types of dysfunction that included the following:

- the use roller reamers to ensure that friction in the BHA was not contributing the onset of stickslip
- the use of full gauge roller reamers to determine if the lateral vibrations could be reduced by reducing lateral BHA displacement because it was believed that an overgauge hole was often being drilled as a result of increased side cutting from whirl
- the use of extended gauge bits to reduce bit tilt and side cutting from whirl

#### *5.4 Effectiveness of lateral stability*

With the exception of extended gauge bits, the design changes promoting lateral stability that differ between the wells in this study could be compared and evaluated by examining the lateral bit vibrations in each case. This is because downhole dynamics measurement tools were run during the first bit run of each of the wells. Well 1 incorporated 5-7/8-in roller reamers with a 3-in gauge length bit that did not contain depth of cut controlling features, Well 2 incorporated 6-in roller reamers with a 3-in gauge length bit that did not contain depth of cut controlling features, and Well 3 incorporated 5-7/8-in integral blade stabilizers with a 3-in gauge length depth of cut controlling bit. By plotting the lateral bit vibrations as a function of depth of cut it was

possible to show not only the range over which high lateral accelerations were experienced at the bit, but also the relative magnitudes of lateral acceleration during each bit run. It was found to be more effective to display the lateral accelerations data over the entire bit run rather than by formation due to variances in operating parameters such as WOB and RPM, and locations of stick-slip, unstable stick-slip, and STO from well to well. Also, the first bit run from Well 1 has an incomplete dataset for DOC due to gyroscopic tool failure during the bit run, which prevented calculation of DOC.

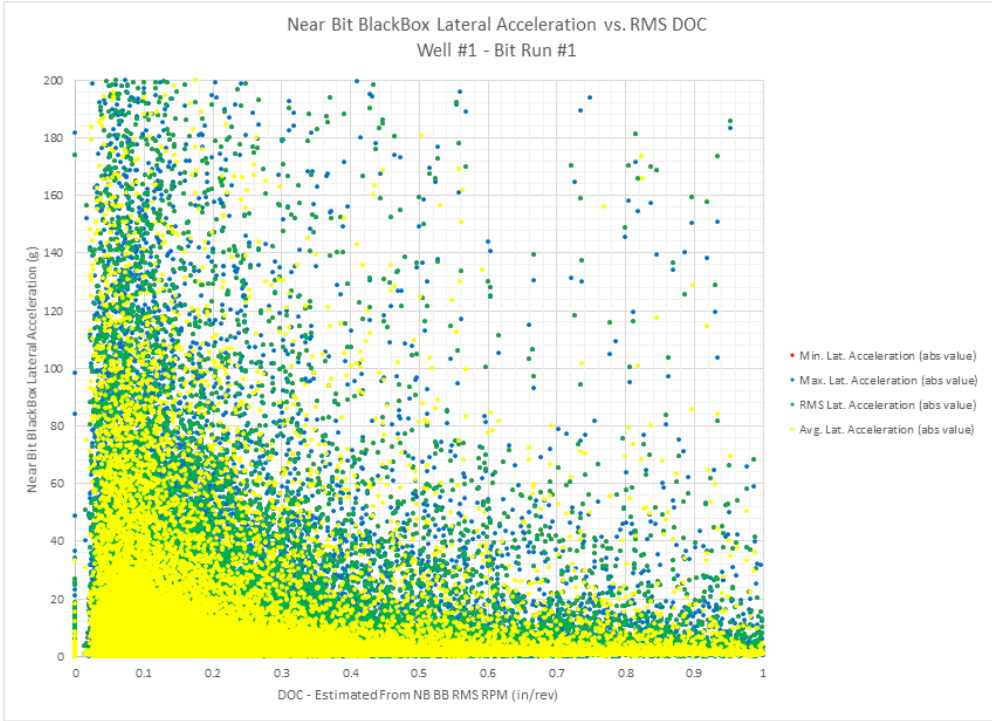


**Fig. 5.8 – Lateral bit acceleration versus DOC Well 1 Bit Run 1**

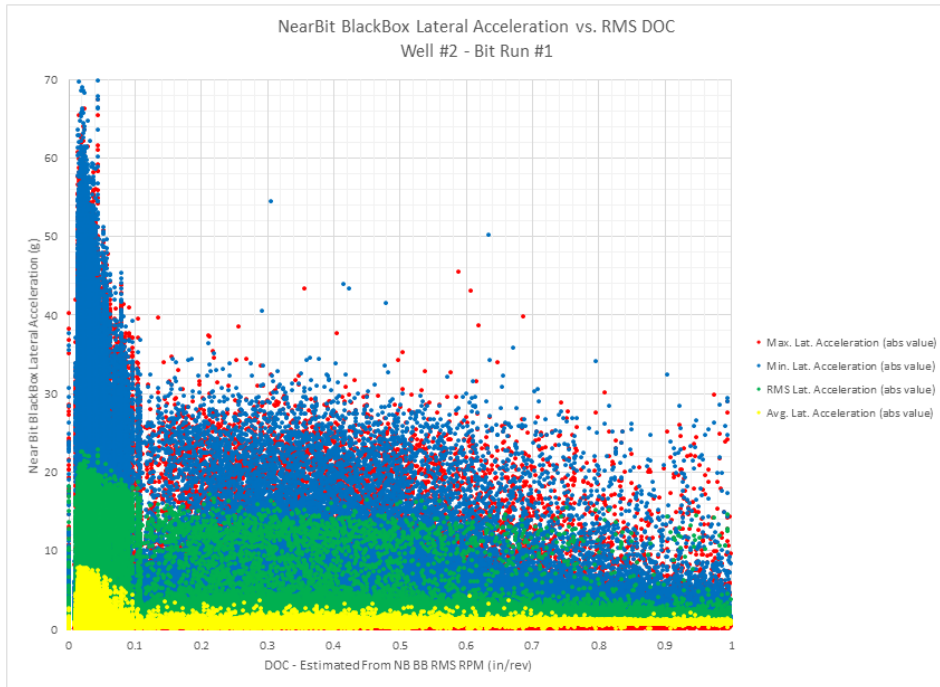


**Fig. 5.9 – Lateral bit acceleration versus DOC Well 2 Bit Run 1**

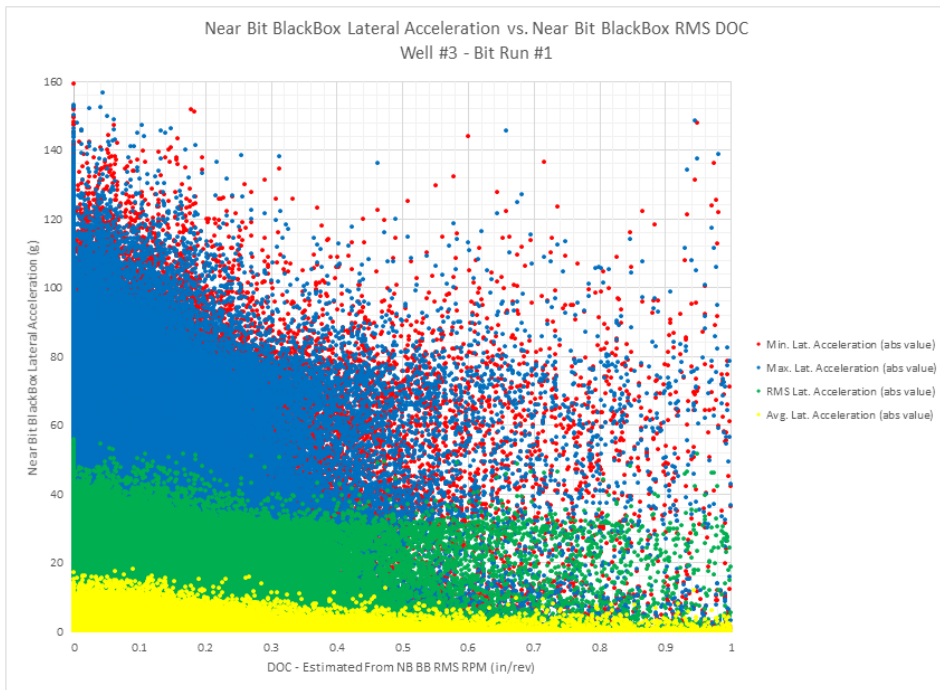


**Fig. 5.10 – Lateral bit acceleration versus DOC Well 3 Bit Run 1**



The plots show that high lateral accelerations were experienced at low DOC values, where limited containment forces were experienced due to a lack of indentation and allowed for lateral instability at the end of the bit. This reinforces the idea that STO and unstable stick-slip show sustained levels of high acceleration due to sustained periods of low DOC.

**Fig. 5.8, Fig. 5.9, and Fig. 5.10** show that Well 2 had the lowest levels of lateral bit accelerations over the entire DOC range, which can be attributed to its BHA design containing full gauge 6-in roller reamers to limit lateral movement and reduce bit side cutting. **Fig. 5.9** also shows that the use of the full gauge roller reamers promoted two distinct regimes of lateral acceleration; at DOC less than 0.1 in/rev Well 2 shows excited lateral acceleration which increases with diminishing DOC, while at DOC greater than 0.1 in/rev Well 2 shows an acceleration maximum value ceiling, which the author attributes to bit and string containment and low lateral displacement of the BHA, where peak and rms lateral bit accelerations do not exist over 30g and 15g respectively. Wells 1 and 3 show significantly higher levels of lateral bit accelerations than Well 2, showing peak accelerations greater than 200g and 140g respectively due enhanced side cutting from increased bit tilt and side force, similar to whirl, during periods of instability during STO.

The tangential accelerations as a function of DOC were also plotted to capture the coupled torsional response and severity with changes in depth of cut and with associated levels of lateral acceleration at the bit. It was expected that high tangential bit accelerations would be experienced with moderate levels of DOC as the bit begins its

sticking phase, which would diminish as DOC increased momentarily before the slip allowed a release of energy. These trends were observed as is seen in **Fig. 5.11**, **Fig. 5.12**, and **Fig. 5.13**; however, it was unexpected and interesting to notice that the highest levels of tangential accelerations were experienced during periods with low DOC, which were later observed to be associated with unstable stick-slip and STO.

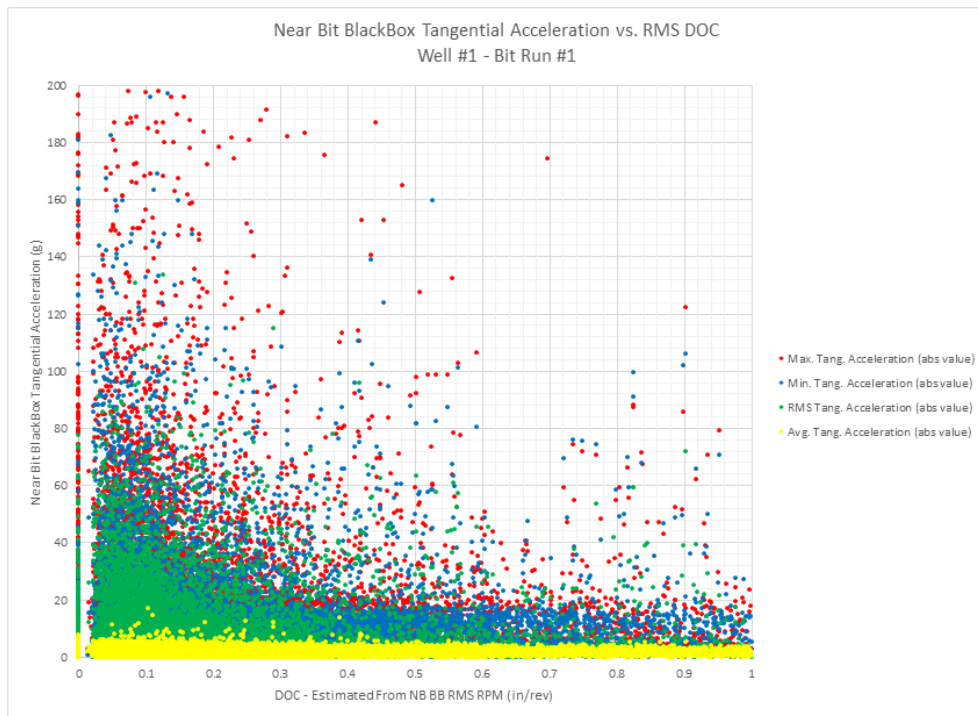


**Fig. 5.11 – Tangential bit acceleration versus DOC for Well 1 Bit Run 1**

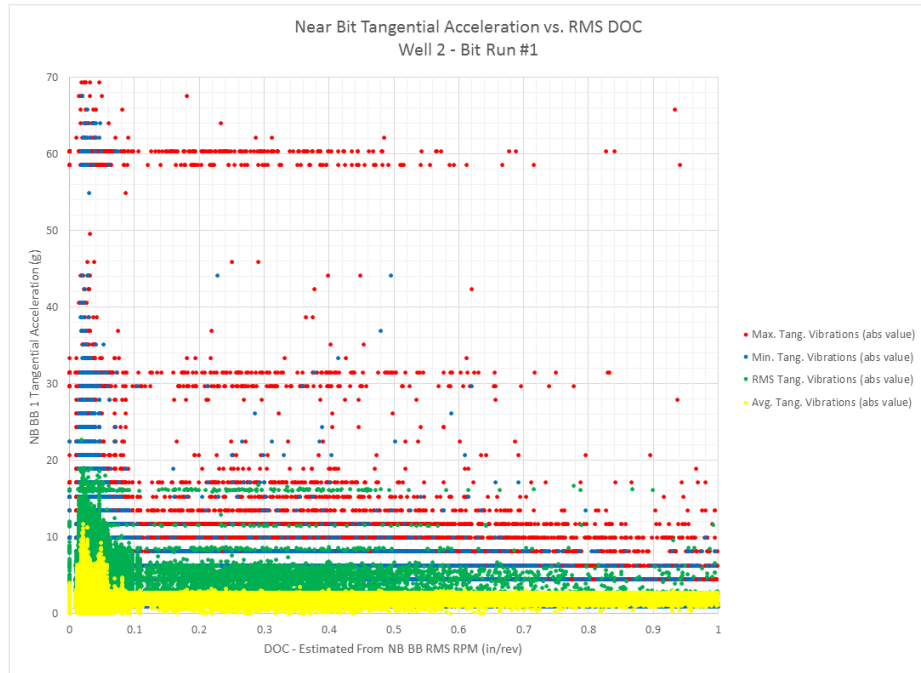


**Fig. 5.12 – Tangential bit acceleration versus DOC for Well 2 Bit Run 1**

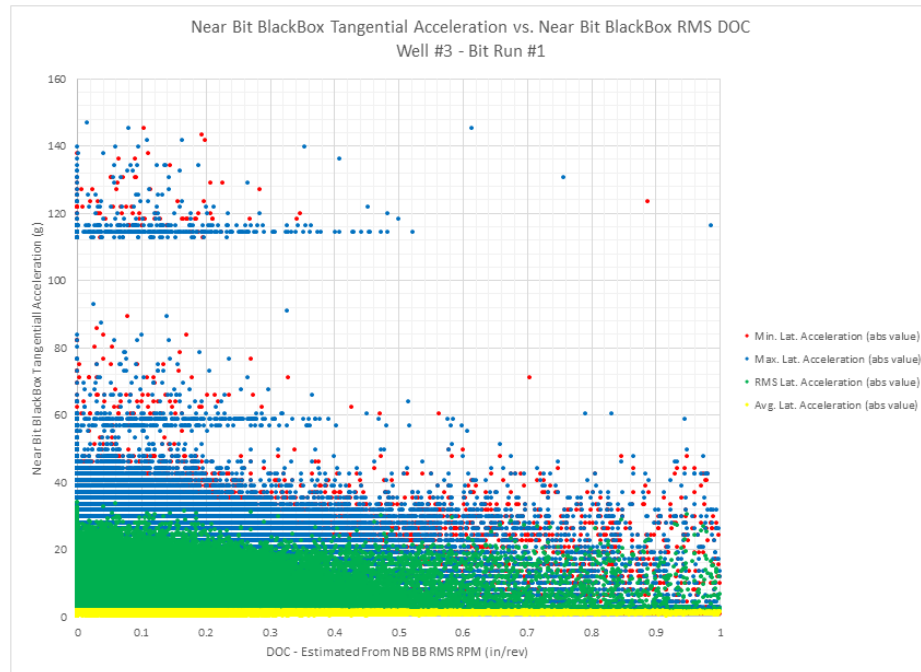


**Fig. 5.13 – Tangential bit acceleration versus DOC for Well 3 Bit Run 1**

The high tangential acceleration levels at low DOC were found to exist due to the coupled nature of the lateral and tangential accelerations during unstable stick-slip and STO experienced in these wells. While experiencing high levels of lateral accelerations, the bit simultaneously experiences high levels of tangential accelerations, with both occurring during the slip phase of these vibrations. These plots capture this nature and prove its persistence from well to well. **Fig. 5.12** shows that Well 2 had the lowest tangential bit accelerations throughout the bit run in addition to having the lowest lateral bit accelerations. Peak rms tangential bit accelerations in Well 2 occurred around 16g. This result is due to the coupled nature and relative magnitudes of the lateral and tangential bit accelerations in these wells, and later examination of the vibrational wave forms will prove this. Wells 1 and 3 show slightly higher levels of tangential bit accelerations than Well 2, showing peak rms acceleration values around 60g and 30g respectively. This discrepancy between the vibration levels between the wells can be attributed to the use of full gauge roller reamers on Well 2.

After observing the comparative levels of accelerations and dysfunction at the bit, it was important to examine the vibrations occurring at the NOV Data Logger in the BHA in order to measure its lateral stability and investigate possible resonance frequencies of the drilling system, as well as further understand the vibrations reduction as a function of the stabilization elements including the integral blade stabilizers, roller reamers, thread-on bearing housing stabilizer, and PowerV RSS. The lateral vibrations that occur in the BHA propagate down to the bit in a pattern that is similar to a sine wave

with amplitude variation as a function of stabilizer size and position and period variance as a function of length between stabilizers and other properties of the BHA.

First, an examination of the lateral BHA vibrations as a function of WOB applied was performed to identify potential performance limiters such as excessive whirl or other severe vibrations. This process included plotting lateral BHA vibrations as a function of applied WOB from both the surface and downhole measurements. In addition, lateral BHA vibrations were plotted as a function of rotary speed. Because all of the wells in the study do not incorporate the LMS tool and because future wells that will be drilled by the operator will not incorporate the LMS tool, it was important to be able to find confidence in the observation of similar trends between plots using either surface or downhole WOB and torque, such that the behavior of wells not including measurements of downhole WOB and torque could be predicted or visualized accurately. **Fig. 5.14** below shows an example of the lateral BHA vibrations experienced as a function of downhole WOB.

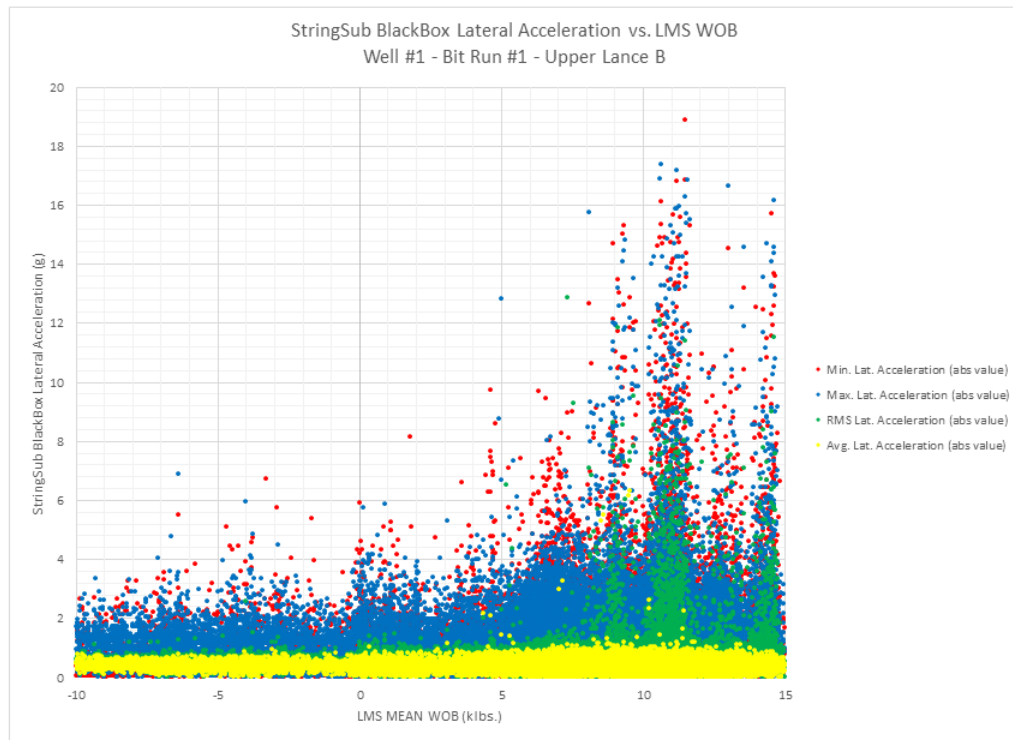


**Fig. 5.14 – Lateral BHA acceleration versus downhole WOB showing whirl pattern**

The BHA lateral vibrations follow a typical characteristic whirl pattern that shows an increase in lateral accelerations with an increase in WOB. This characteristic trend occurs until approximately 10,000 lbs WOB, at which point the lateral accelerations become excited to a higher state due to the transition between full stick-slip, which is naturally damping to lateral vibrations, into the occurrence of unstable stick-slip and STO. As mentioned previously, STO promotes higher coupled lateral vibrations in its slip phase than stick-slip, which can be observed both at the bit and in the BHA, as shown in this plot.

Oftentimes, due to excess torque and drag created from buckling or wellbore friction in deviated wells, the surface measurement of any given drilling parameter does

not always reflect the downhole in-situ state of that parameter. While this can be seen in some applications, generally wells with highly deviated or horizontal well paths, it is not observed in this case with WOB. For the majority of both bit runs on Well 1, which incorporated the LMS downhole measurement tool, the surface and downhole WOB measurements were in agreement within a few thousand pounds. An example of this can be seen in **Fig. 5.1** where deviation between the surface and downhole tracks is minimal. In some instances, such as when examining **Fig. 5.15** below, this could seem confusing. On surface, while drilling this particular formation, the surface measurements seem to not correlate with the downhole measurements in value due to a loss of applied weight as a result of part of that perceived applied weight being lost in wellbore friction from contact with the borehole wall. WOB values from surface showing a range from 0 to nearly 18 thousand pounds of applied weight can seem to correspond to downhole WOB values ranging from -10 to 20 thousand pounds of applied load. This however, is incorrect and the low and high values recorded by the downhole tool are related to instances where WOB was significantly reduced or applied quickly, such as making connections or during tripping, as those have been observed to be the sources of the largest discrepancies.

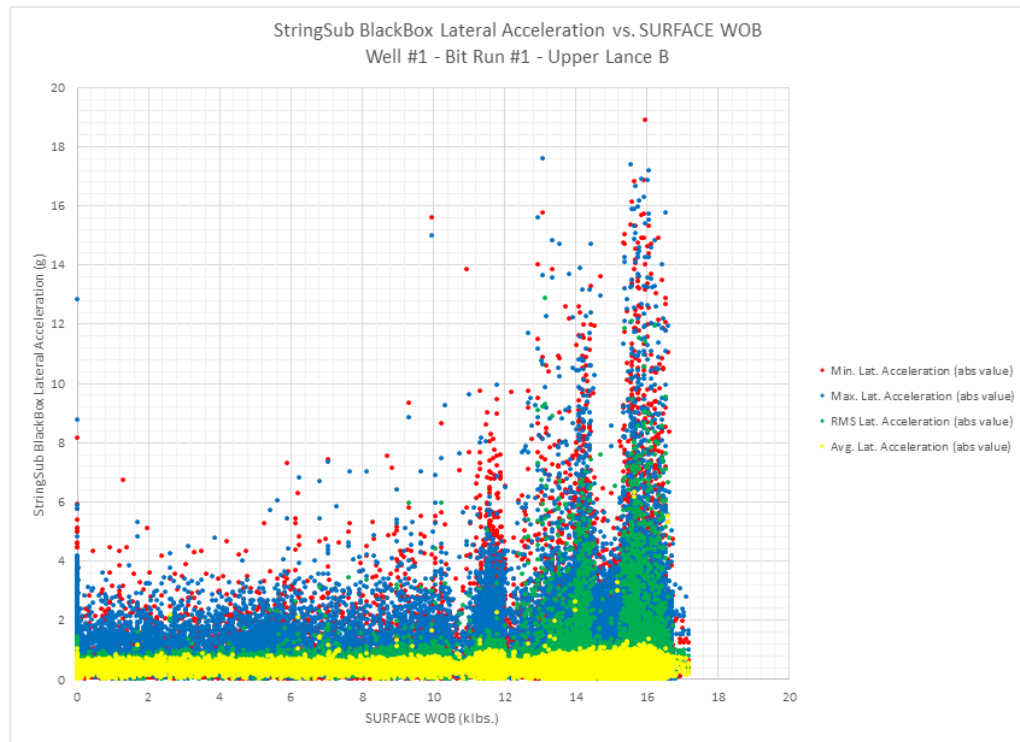


**Fig. 5.15 – Lateral BHA acceleration versus surface WOB showing whirl pattern**

The slight difference in shape between the surface and downhole plots can be attributed to loss of weight transmission noise during periods of low and high WOB, but the amount of this noise is a function of the load direction shape, nature of buckling, and frictional profile of the well. These losses are typically not well known or predictable without sophisticated BHA modelling, which was not performed during this study.

Given the variance in operation practices and parameter set values used between the three wells, the nature of and factors influencing some of the observed dysfunction, such as drillstring length and dependence on rotational speed resonance for example for STO, and given the potential sources of error that could be present in short interval analysis, it was determined that examination of the entire bit runs between wells, drilling



the same formations, would prove a more effective measure of dysfunction and vibrations reduction when evaluating equipment and new technologies, rather than the examination of individual formations. This methodology lends itself to observation of peak dysfunction and vibration levels, rather than short interval analysis, and is uniquely suited to this application as the most frequent dysfunctions occur over the majority of each bit run.

**Fig. 5.16, Fig. 5.17, Fig. 5.18, and Fig. 5.19** show the lateral string accelerations in the BHA as a function of WOB applied from each of the case wells and can be used to evaluate the severity of whirl given the applied load. These plots can also be used to evaluate the effectiveness of the stabilization elements in suppressing vibrations as the NOV Data Loggers were placed just below the stabilization device.

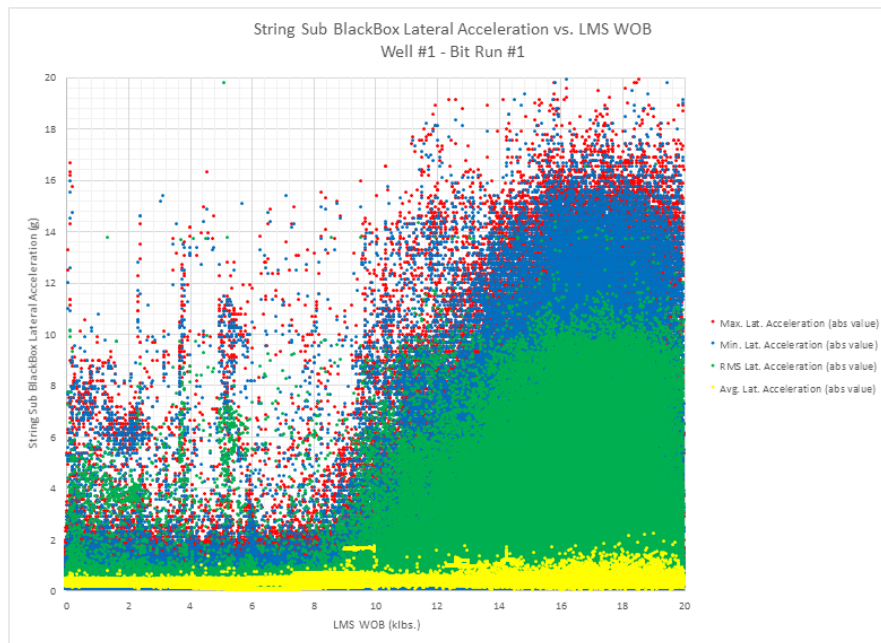


**Fig. 5.16 – Lateral BHA acceleration versus downhole WOB Well 1 Bit Run 1**

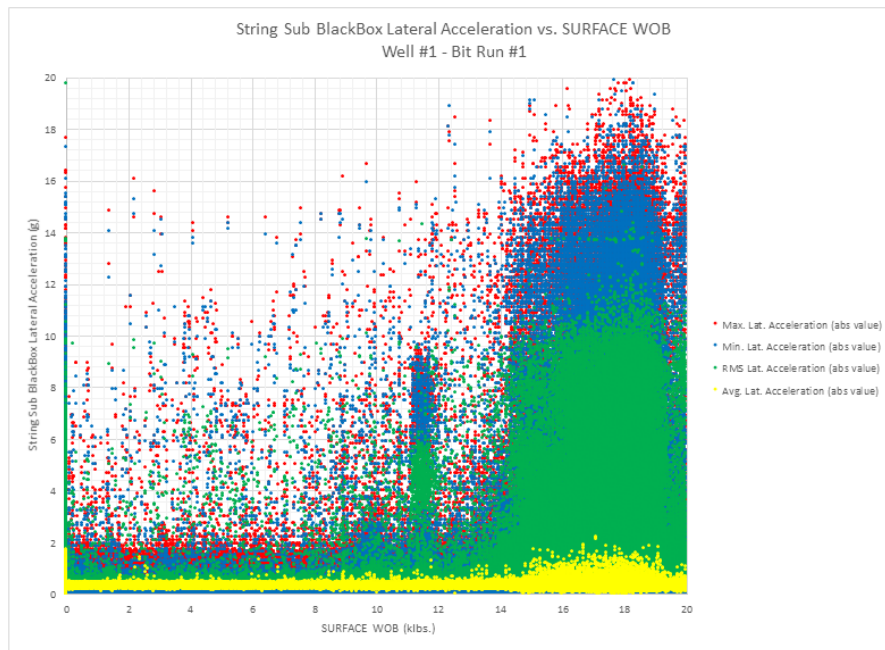


**Fig. 5.17 – Lateral BHA acceleration versus surface WOB Well 1 Bit Run 1**

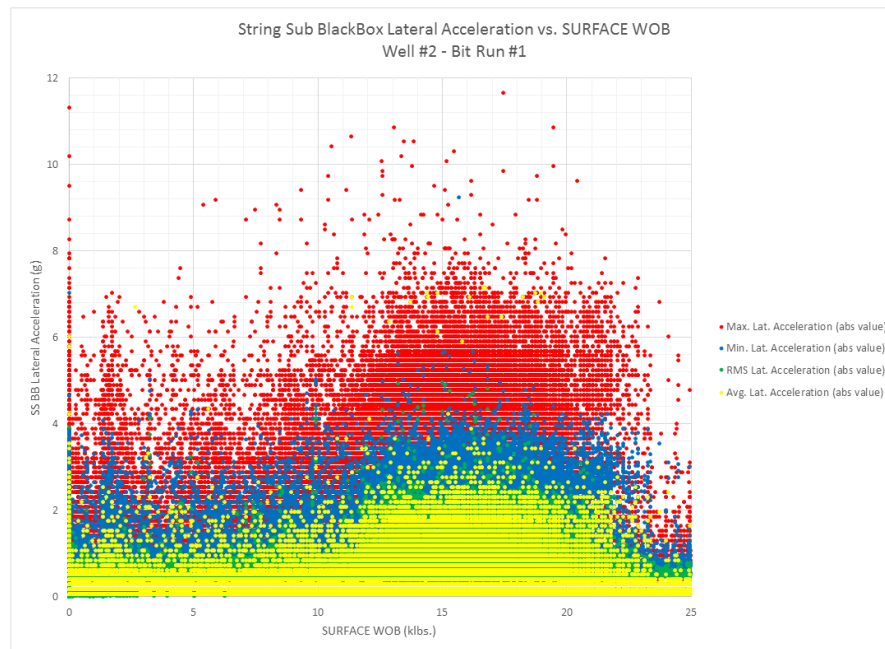


**Fig. 5.18 – Lateral BHA acceleration versus surface WOB Well 2 Bit Run 1**

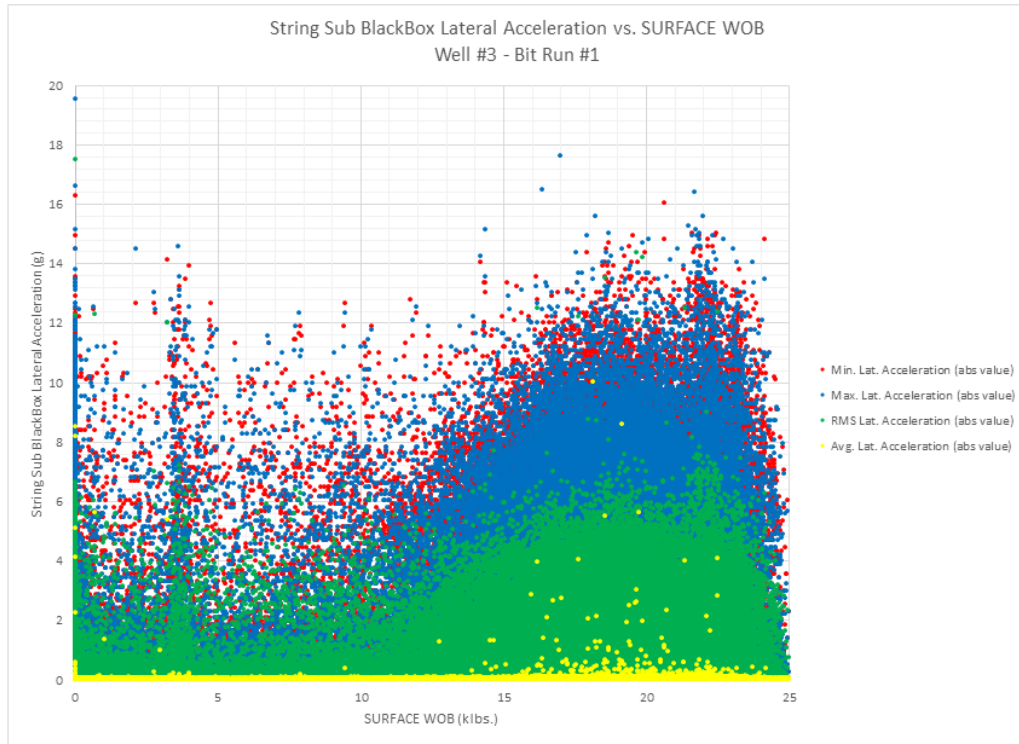


**Fig. 5.19 – Lateral BHA acceleration versus surface WOB Well 3 Bit Run 1**

**Fig. 5.16, Fig. 5.17, Fig. 5.18, and Fig. 5.19** again show that the increased lateral support of the full gauge 6-in roller reamers used in Well 2 provides for the most effective device at reducing string vibrations in this study, which can be attributed to having lower lateral clearance with the borehole, thus preventing lateral movement in a likely overgauge hole. Well 2 showed the lowest levels of lateral acceleration in the BHA, with rms and peak values recorded as high as 3g and 8g respectively. Well 1 showed rms and peak values of 11 and 18g and Well 3 showed rms and peak values of 8g and 15g, respectively. These results are shown in **Table 5.2** below.

**Table 5.2 – Peak RMS Lateral BHA Accelerations for each well**

<b>Vibration Type</b>	<b>Well 1 Bit Run 1</b>	<b>Well 1 Bit Run 2</b>	<b>Well 2 Bit Run 1</b>	<b>Well 3 Bit Run 1</b>
Peak RMS Lateral BHA Acceleration	11g	8g	3g	7g

The roller reamers incorporated in Well 1 and the integral blade stabilizers incorporated in Well 3 are both 5-7/8-in in outside diameter (OD), which means they should have comparable lateral acceleration values due to having the same clearance between their gauge and the wellbore wall. A possible explanation for the discrepancy between the two wells is the addition of the LMS tool in Well 1, which is a 10.84-ft long “limber” addition to the BHA that could promote higher lateral acceleration, due to extending the distance between the roller reamer directly above it and the roller reamer below it.

The increase in lateral accelerations experienced in the BHA with increasing WOB is expected. This is because when the drill string is put in compression with an axial load, it has a tendency to want to bow or displace laterally and eccentrically in the borehole is increased. This increase in lateral displacement is generally not considered detrimental to performance. Typically as axial load (WOB) is increased, the bit’s DOC increases proportionally. This provides lateral stabilization at the most crucial location, the bit/rock interface. However, in the case of the wells included in this study, higher lateral instability in the BHA, which can be compounded by increased WOB, means the

greater the potential for whirl-like beachmark damage. This damage comes from impacts and increased side cutting during sustained periods of low DOC such as experienced during unstable stick-slip and STO.

### 5.5 Discovery of resonance speeds

In addition to studying the effect of axial loading on the drillstring vibrations, rotational effects were discovered to contribute to the lateral accelerations experienced in the BHA. During the data collection phase of this study, RPM step tests were conducted throughout the bit runs to determine resonant frequencies of the drilling system. Somewhat repeatable results were produced that highlighted possible resonant and non-resonant rotational speeds. **Fig. 5.20**, **Fig. 5.21**, and **Fig. 5.22** below show resonant frequencies corresponding to rotational speeds between 30 and 60 rotations per minute.

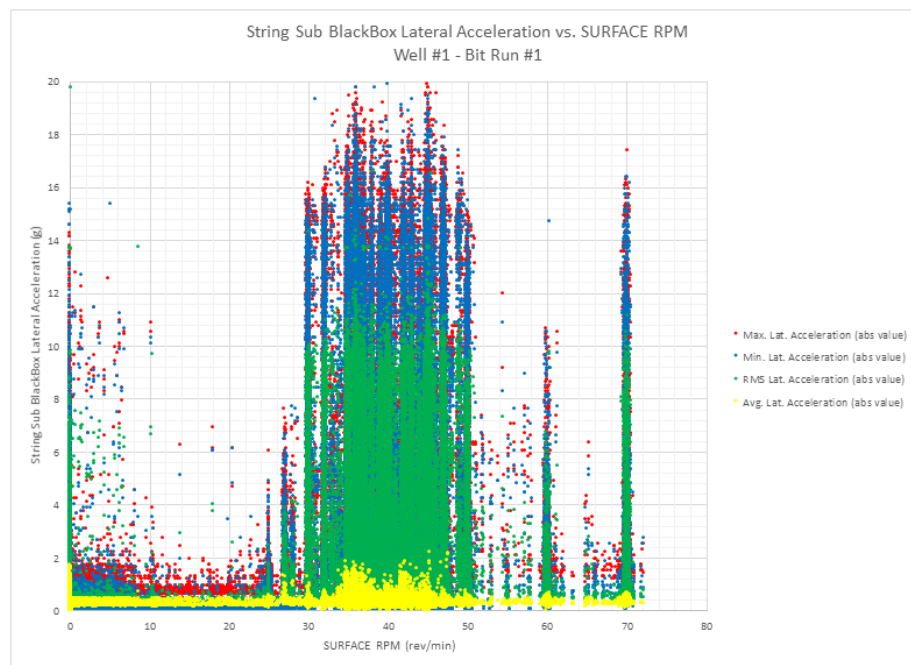


**Fig. 5.20 – Lateral BHA accelerations versus rotary speed Well 1 Bit Run 1**

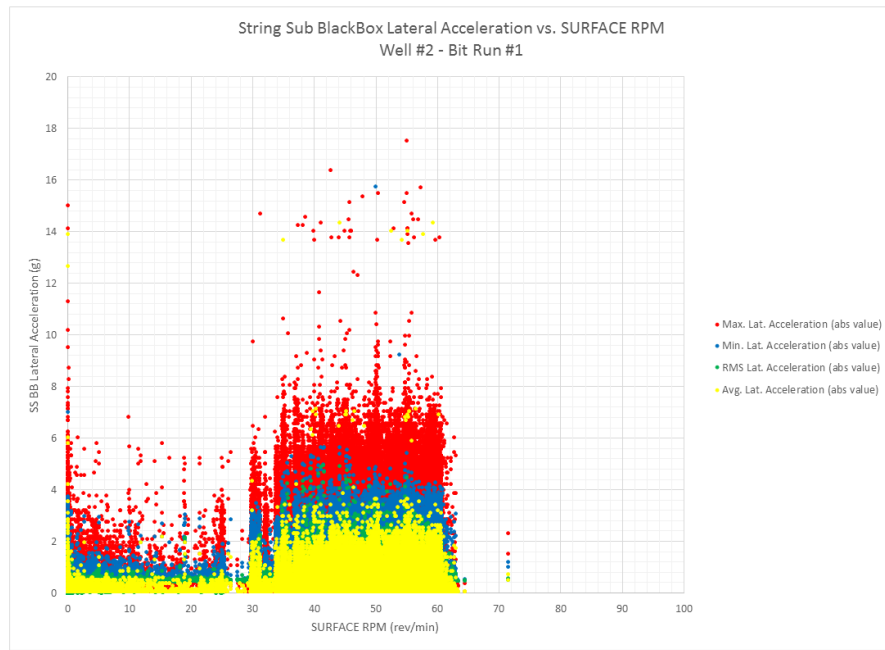


**Fig. 5.21 – Lateral BHA accelerations versus rotary speed Well 2 Bit Run 1**

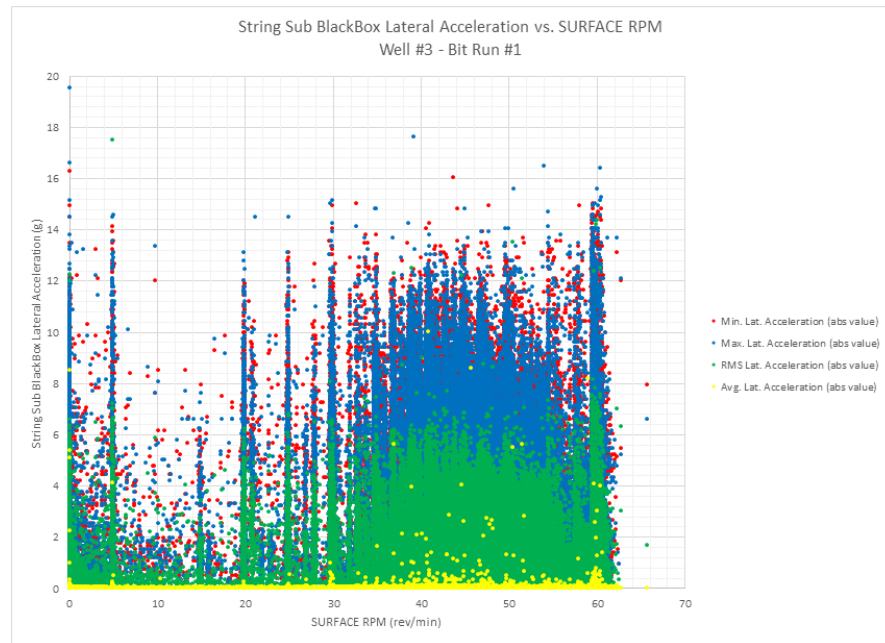


**Fig. 5.22 – Lateral BHA accelerations versus rotary speed Well 3 Bit Run 1**

**Fig. 5.20** shows that high levels of sustained lateral accelerations occur between 30 and 50 rotations per minute, which correspond to periods where unstable stick-slip and STO were observed to exist. It could be suggested from this plot that it might be beneficial to rotate the drillstring at either 55 or 65 revolutions per minute as those speeds appear to be non-resonant or “quiet.” **Fig. 5.21 and Fig. 5.22**, however show that excited vibrations occurred at rotational speeds over the entire range of 30 to 60 revolutions per minute. These results seem to contradict the non-resonant speeds believed to be observed in Well 1 at 55 and 65 revolutions per minute. This discrepancy is believed to be attributed to drill string resonance being a function of drill string length which changes with depth. The author suggests that further investigation be performed to model drill string resonance with depth, similar to the work done by Ertas et al. (2013). He believes from review of their work that operating at higher rotational speeds will suppress the occurrence of unstable stick-slip and STO, and will likely promote a less damaging mode of torsional oscillation such as stick-slip, or even less damaging simple torsional oscillation if the depth of cut can be managed below the stick-slip threshold. The observation of resonance and changing of drilling parameters to operate at non-critical speeds should be actively managed, while looking at mechanical specific energy to ensure more efficient and less damaging drilling operation.

#### 5.6 *Finding the onset of torsional oscillation*

To determine the threshold at which the onset of synchronous torsional oscillation and stick-slip occur, a series of plots were constructed to represent the characteristic phenomena that exists during these vibrations, which include elevated

lateral and tangential bit accelerations and negative or reverse rotation. These characteristics were ultimately captured as a function of surface and downhole torque when available and downhole stick-slip index (DSSI). Several sets of these plots were created to represent each well in the study and produced repeatable results when roller reamers were incorporated in the BHA design. These plots show that the onset of unstable stick-slip and STO exists around 4.0 to 4.5 kft-lbs of surface torque, while full and well-developed stick-slip was shown to exist at higher torque ranges, where the vibration shows lower lateral bit accelerations and lower DSSI values.

**Fig. 5.23, Fig. 5.24, Fig. 5.25, and Fig. 5.26** below show the measured torque on surface and downhole at which the bits vibrational state becomes excited and shows high lateral accelerations during the first and second bit run on the first well in the study. It was important to capture the difference in measured torque between the surface and downhole measurement for this well as it provides insight into the torque loss as a results of drillstring material compliance and lost to wellbore friction for a given interval such that the operator could potentially use these loss values to determine the expected bit torque based off of the surface torque measurement in real-time on future wells.



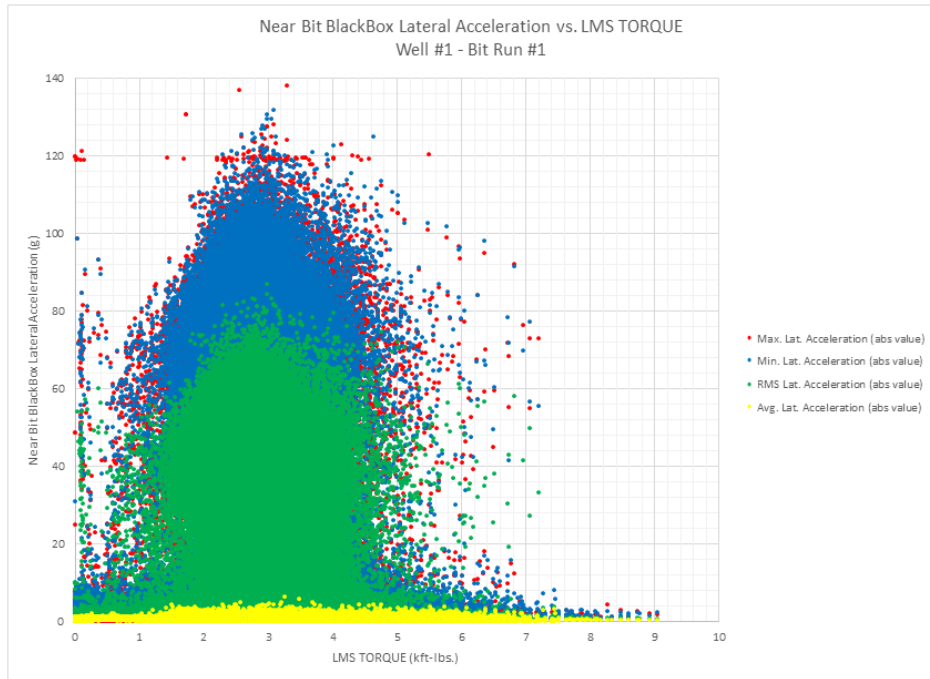


**Fig. 5.23 – Lateral bit acceleration versus downhole torque for Well 1 Bit Run 1**

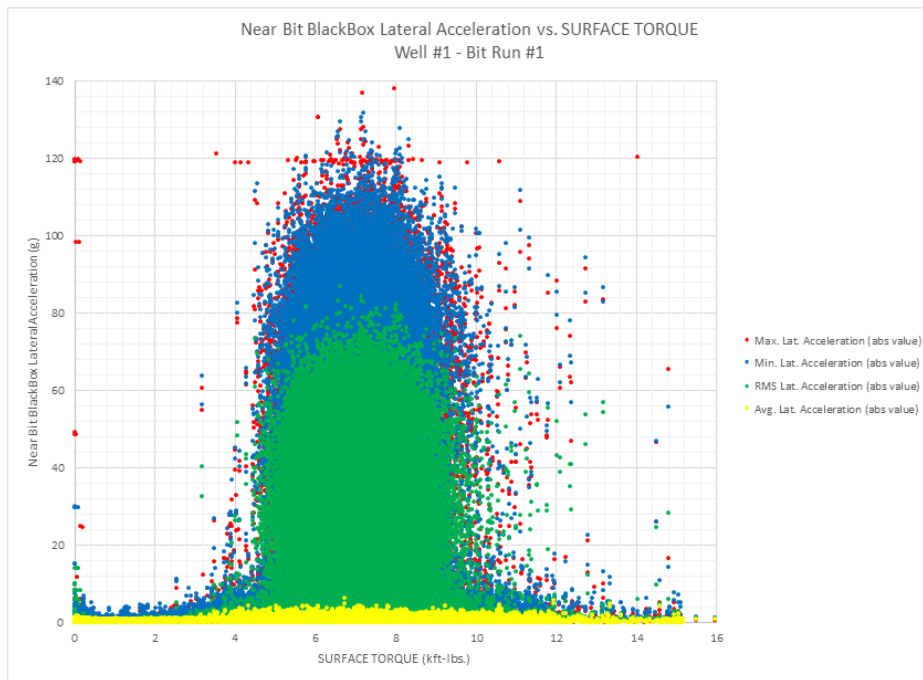


**Fig. 5.24 – Lateral bit acceleration versus surface torque for Well 1 Bit Run 1**

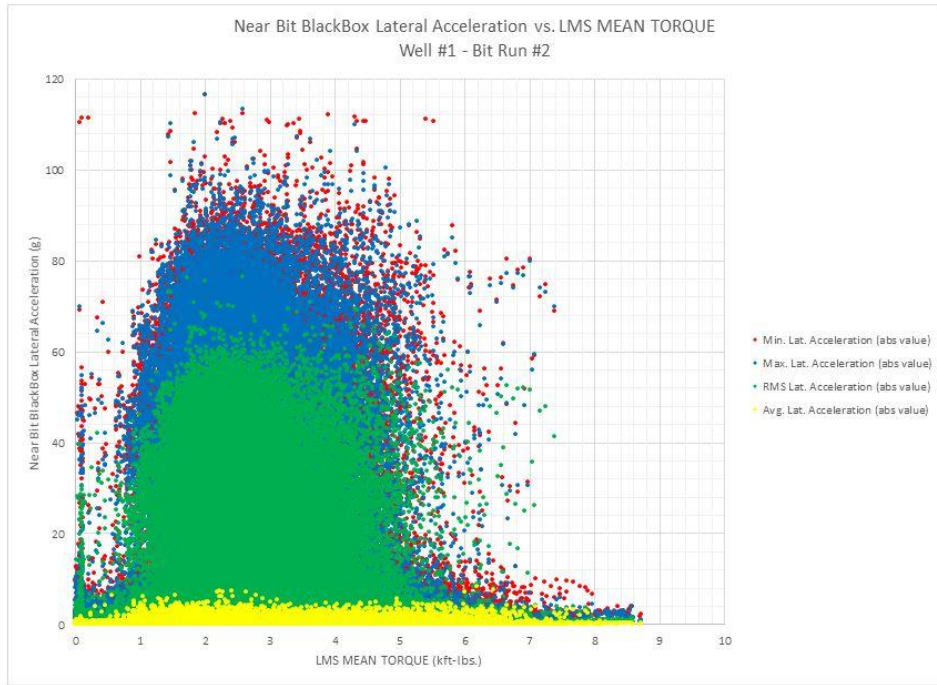


**Fig. 5.25 – Lateral bit acceleration versus downhole torque for Well 1 Bit Run 2**

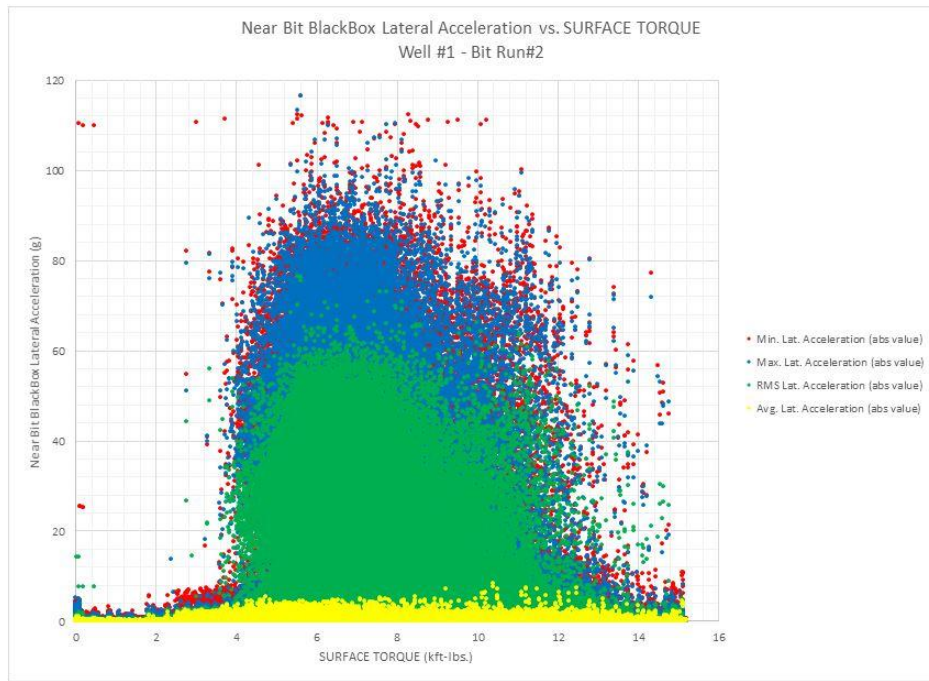


**Fig. 5.26 – Lateral bit acceleration versus surface torque for Well 1 Bit Run 2**

These results show that there is a discrepancy of roughly 2,000 ft-lbs between the measured surface torque and measured downhole torque at which the bit dysfunction becomes excited. It also shows that the onset of dysfunction occurs at relatively unaggressive torque levels, which can be attributed to the limber drillstring in use to drill these wells as well as the characteristics of the unstable stick-slip and STO vibrations present in these wells, which tend to show high levels of coupled lateral and tangential accelerations at low torque corresponding to low DOC. The onset of this excited vibrational state is very acute, showing that the lateral bit accelerations increase greatly in magnitude over a very short range in torque, attributed to synchronous torsional oscillation over the lower end of the torque range. Full stick-slip can be observed over the entire torque range, where the sticking phase torque levels are shown at high torque values with decreasing lateral bit accelerations as torque increases, and the slip phase torque values are intermingled with the STO at the lower torque range, but are observed to primarily occur in a range where the lateral bit accelerations do not appear to be excited, having much lower values than the values associated with unstable stick-slip and STO.

Observing the surface and downhole torque measurements associated with the onset of unstable stick-slip and STO shows that the excitation torque is very similar with depth, although it does decrease about 300-500 ft-lbs. from the first to the second bit run. This slight decrease in the torque required for the onset of the vibration is related to the increased amount of drag loss as the drill string becomes longer with the increasing hole

depth. The increased drillstring and BHA friction due to longer lengths of tubulars tends to promote excitation of unstable stick-slip and STO.

A comparison of the lateral bit vibrations as a function of measured surface torque for the second and third wells included in this study show that the torque values for the onset of the excited vibrational states of STO and stick-slip are roughly the same for Well 2 as for Well 1, occurring around 4.0 to 4.5 kft-lbs. of surface torque, however, Well 3 shows that the use of integral blade stabilizers, which produce higher levels of contact friction between the blades and the borehole wall, can promote the occurrence of unstable stick-slip and STO at a lower torsional threshold. With the use of integral blade stabilizers, the amount of WOB that can be applied before the onset of dysfunction is lower than with the use of roller reamers as shown in a comparison between **Fig. 5.28** and **Fig. 5.28** on the next few pages, which results in less efficient rock cutting and slower penetration rates.

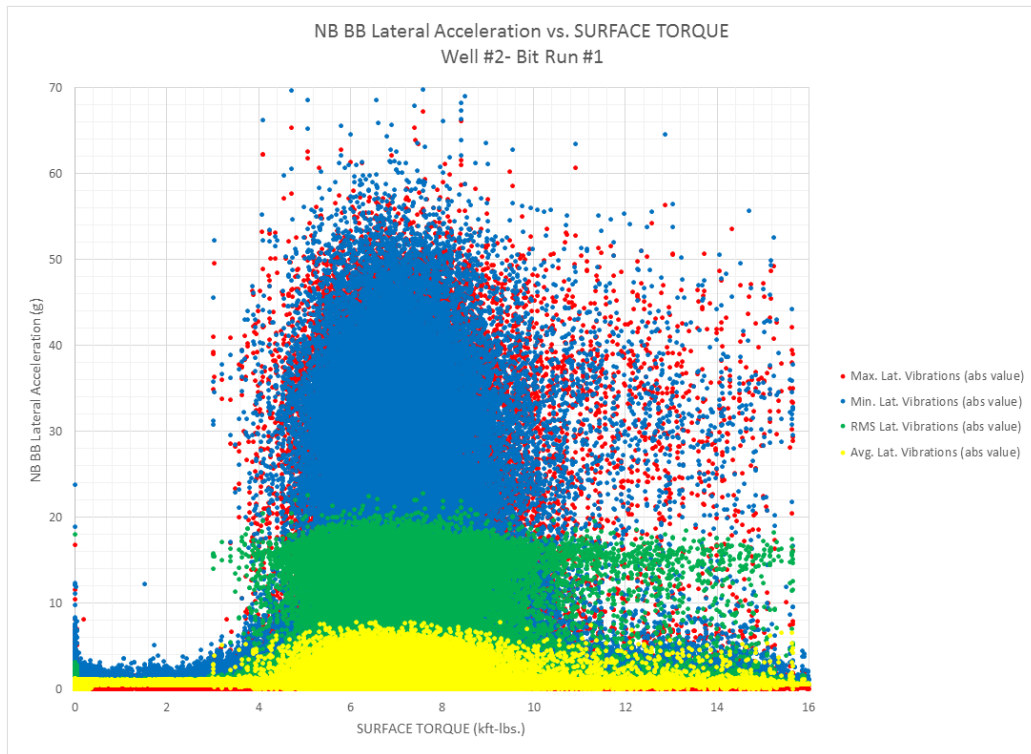


**Fig. 5.27 – Lateral bit acceleration versus surface torque for Well 2 Bit Run 1**

The second well has roughly the same torsional profile as the first well, showing that excited torsional oscillation with coupled high lateral accelerations starts to occur over the same range around 4.0 to 4.5 kft-lbs. torque on surface. However, it should be noted that the lateral acceleration levels are roughly 3 times less than Well 1 during the peak excitation range of torque, with sustained RMS lateral bit acceleration levels peaking at around 20g versus 60g in Well 1. From these plots it can be inferred that the larger roller reamers incorporated in the BHA design on Well 2 were more effective at containing lateral motion than the smaller roller reamers on Well 1, while simultaneously not providing any excess torque or drag loss in transmission of torque

from surface to the bit. This is likely due the creation of a less severe borehole pattern and thus a less severe overgauge hole, while the larger rolling elements of the roller reamers maintaining their functionality in preventing excess drag.

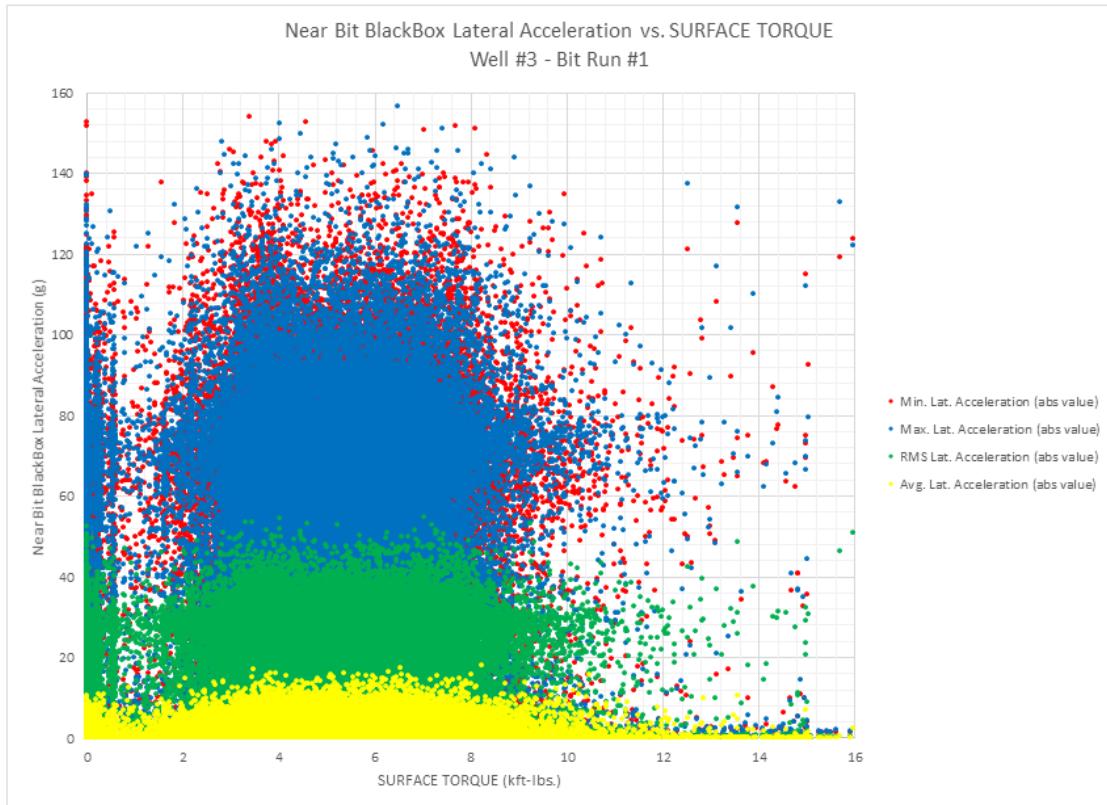


**Fig. 5.28 – Lateral bit acceleration versus surface torque for Well 3 Bit Run 1**

Well 3 shows the onset of unstable stick-slip and STO occurs around 2 kft-lbs. surface torque, which is about half the onset surface torque values of Wells 1 and 2. This can be attributed to the integral blade stabilizers creating excess BHA drag, which promotes the excitation of those vibrations. However, Well 3 did show that torque operating ranges higher than 10 kft-lbs. experienced low levels of lateral bit acceleration,

whereas Wells 1 and 2 showed this range to contain some elevated acceleration events. This can possibly be attributed to the depth of cut controlling features of the bit suppressing torsional oscillation at higher torque.

To prove the existence of zero or reverse bit rotation, in addition to showing the lateral bit accelerations profile as a function of rate of change in bit rotational speed, plots were constructed showing the downhole stick-slip index versus measured surface torque, and downhole torque when available, to investigate the onset of torsional oscillation. The downhole stick-slip index (DSSI) is given by the following equation:

Downhole Stick-Slip Index (Lai et al. 2014):

$$DSSI = \frac{\omega_{max} - \omega_{min}}{2 * \omega_{avg}} \dots \dots \dots \text{Eqn. 5}$$

- where:
- $DSSI$  = downhole stick-slip index (unitless)
  - $\omega_{max}$  = maximum angular velocity during the sampling range
  - $\omega_{min}$  = minimum angular velocity during the sampling range
  - $\omega_{avg}$  = average angular velocity over the sampling range

A DSSI greater than 1.0 signifies the onset of full stick-slip or torsional oscillation in which the bit exhibits zero or negative rotation. Showing the lateral bit accelerations as a function of the DSSI also helps to prove that full stick-slip, unstable stick-slip, and STO are responsible for the excited vibrational state of the bit by confirming that the values of torque associated with elevated lateral bit accelerations are also associated with high DSSI values. This explains why negative bit rotation is observed during periods of high lateral bit accelerations. **Fig. 5.29** and **Fig. 5.30** below show the measured torque on surface and downhole at which the DSSI shows that the vibrational state becomes

excited and shows the existence of zero or negative bit rotation during the second bit run on the first well in the study.

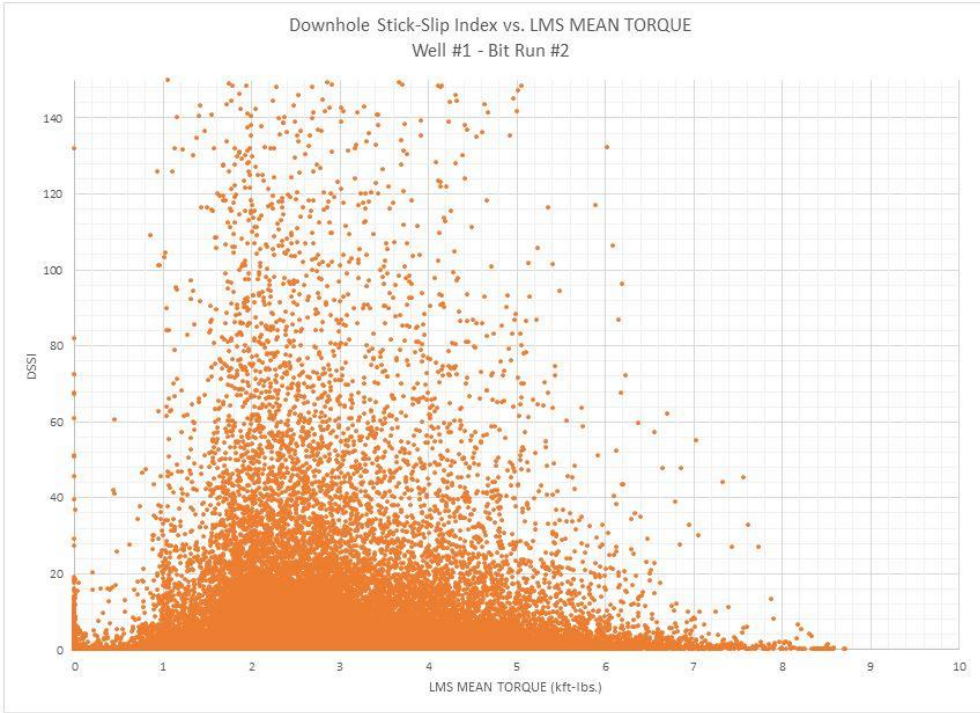


**Fig. 5.29 –DSSI versus downhole torque for Well 1 Bit Run 2**



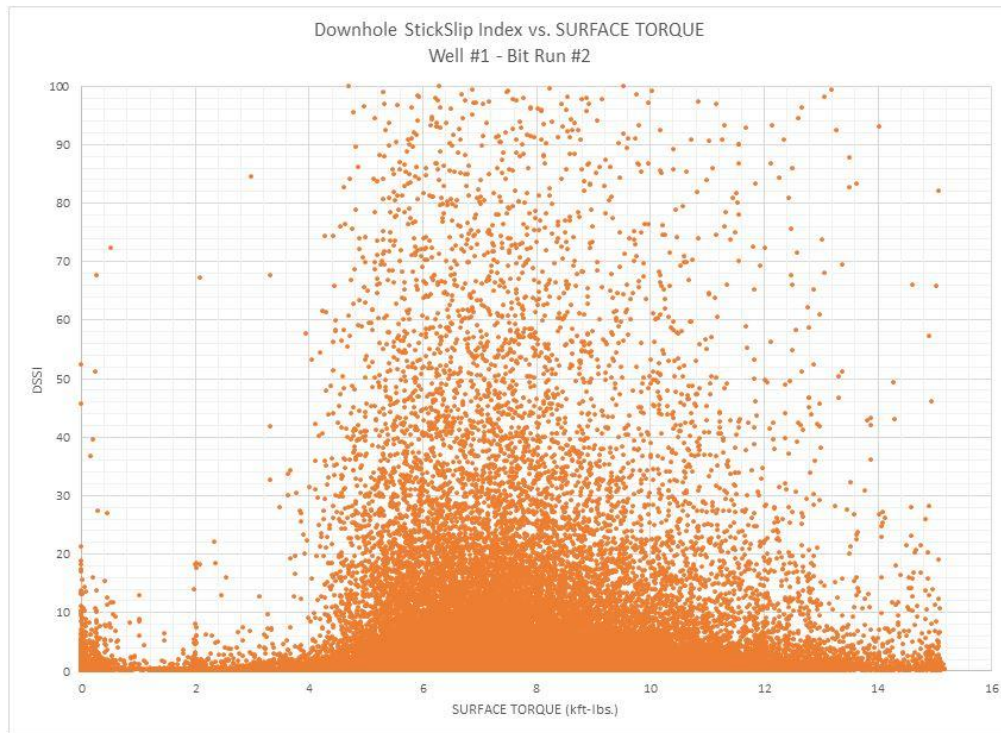


**Fig. 5.30 –DSSI versus surface torque for Well 1 Bit Run 2**

These plots show that there is again a discrepancy of about two thousand pounds between the surface and downhole torque measurements for the onset of bit dysfunction due to torque and drag. They also tend to confirm the trends in **Fig. 5.23**, **Fig. 5.24**, **Fig. 5.25**, **Fig. 5.26**, **Fig. 5.27** and **Fig. 5.28** showing lateral bit accelerations as a function of torque, in that the onset of the excited vibrational state during STO and stick-slip is acute, elevating the DSSI from relatively low values to high values greater than 100. These plots also confirm the observation that STO is associated with higher tangential accelerations than full stick-slip. The DSSI equations are more dependent on the difference between minimum and maximum angular velocities recorded over the sampling range, which in this case is 0.5 seconds. The higher the DSSI value the greater

the difference is between the minimum and maximum angular velocities experienced, and thus the higher tangential acceleration. Looking at the **Fig. 5.29** and **Fig.5.30** one can see that higher DSSI values are observed over the torque range that correspond to STO, than were observed over the full stick-slip range, which is similar to what was described by the lateral bit accelerations versus torque plots. This further confirms that STO has a higher potential for whirl-like bit damage than stick-slip in these wells.

A comparison of DSSI as a function of measured surface torque for the first bit runs of the second and third wells included in this study also shows that the excitation torque for the excited vibrational states of STO and stick-slip are roughly the same for Well 2 as for Well 1, but Well 3 shows again that the use of integral blade stabilizers can promote the occurrence of unstable stick-slip and STO at a lower torsional threshold. **Fig. 5.31** and **Fig. 5.32** on the next page display the DSSI as a function of surface torque for Wells 2 and 3.

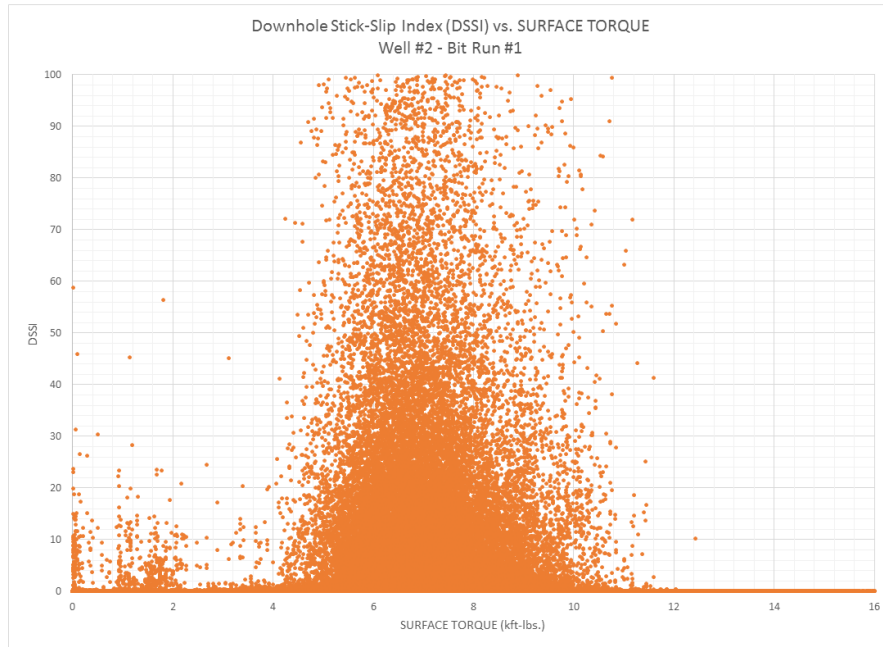


**Fig. 5.31 –DSSI versus surface torque for Well 2 Bit Run 1**

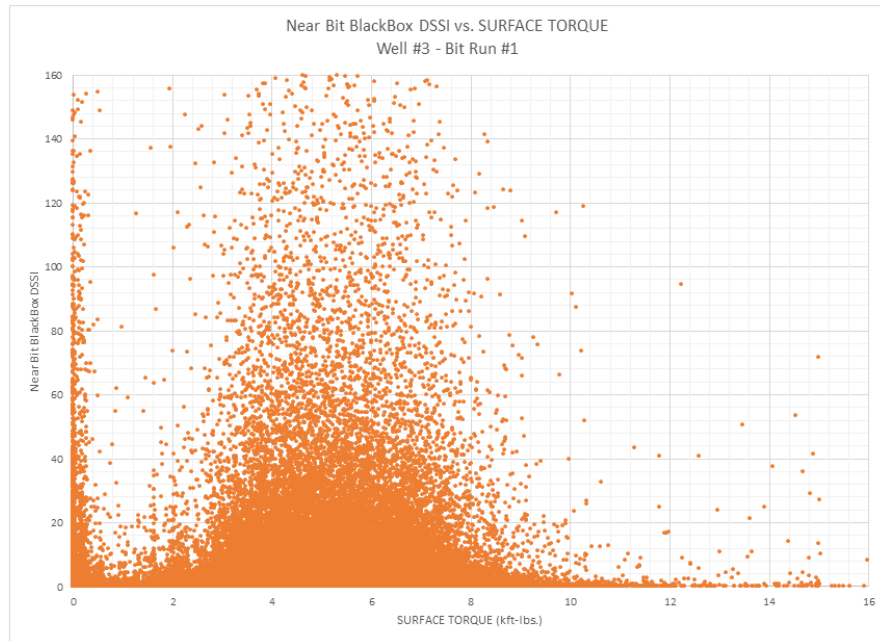


**Fig. 5.32 –DSSI versus surface torque for Well 3 Bit Run 1**

The second well has roughly the same torsional profile as the first well which shows the excited torsional oscillation over the same range around 4.0 to 4.5 kft-lbs. torque on surface. However, it should be noted that the DSSI values observed in Well 2 are slightly higher than in Well 1, which may have a variety of explanations. One explanation could be that the larger roller reamers incorporated in the BHA of Well 2 helped to promote less lateral deflection and side force at the bit, which in turn promoted less side cutting and more efficient angular bit speed transfer, thus creating larger DSSI values. Well 3 also shows a similar torsional profile to Wells 1 and 2, except that the torque required to initiate unstable stick-slip and STO is lower.

Finally, in order to confirm the onset torque values associated with STO and full stick-slip and to show that negative bit rotation was occurring during these bit runs, plots showing bit rotational speed as a function of torque were created. These plots tend to agree with the plots created showing lateral bit accelerations and DSSI as a function of torque, in that the observed onset of unstable stick-slip and STO is shown to be at the same torque value, and can be visible with zero or negative bit rotational speed. The other measure that this plot gives insight into is the data density of near zero or negative instantaneous bit rotational speeds throughout the bit runs. **Fig. 5.33** and **Fig. 5.34** show the measured torque on surface and downhole at which the bit rotation begins to oscillate, showing that the vibrational state becomes excited and shows the existence of zero or negative bit rotation during the first and second bit run on the first well in the study. The rotational speed shown in these **Fig. 5.33** and **Fig. 5.34** is called a

“composite rpm” meaning that it shows a combination of the minimum and maximum rotational speed measured at 2Hz.

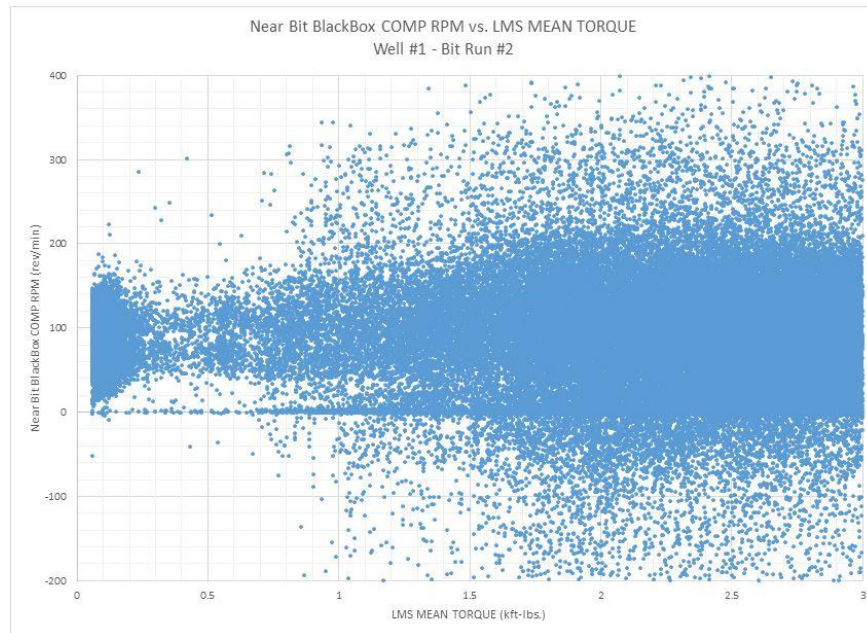


**Fig. 5.33 – Bit RPM versus downhole torque for Well 1 Bit Run 2**

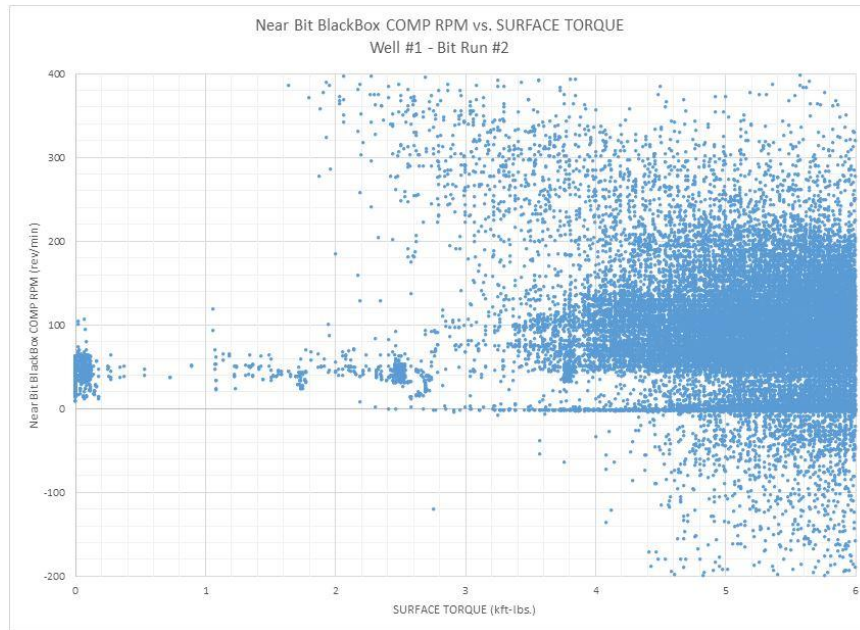


**Fig. 5.34 – Bit RPM versus surface torque for Well 1 Bit Run 2**

The **Fig. 5.35** and **Fig. 5.36** show the rotational speed of the bit for Wells 2 and 3 as a function of surface torque and agree with the previous plots showing lateral bit acceleration and DSSI as a function of surface torque, in that negative instantaneous bit rotation is observed at the onset of unstable stick-slip and STO corresponding to the same torque values as the previous plots.

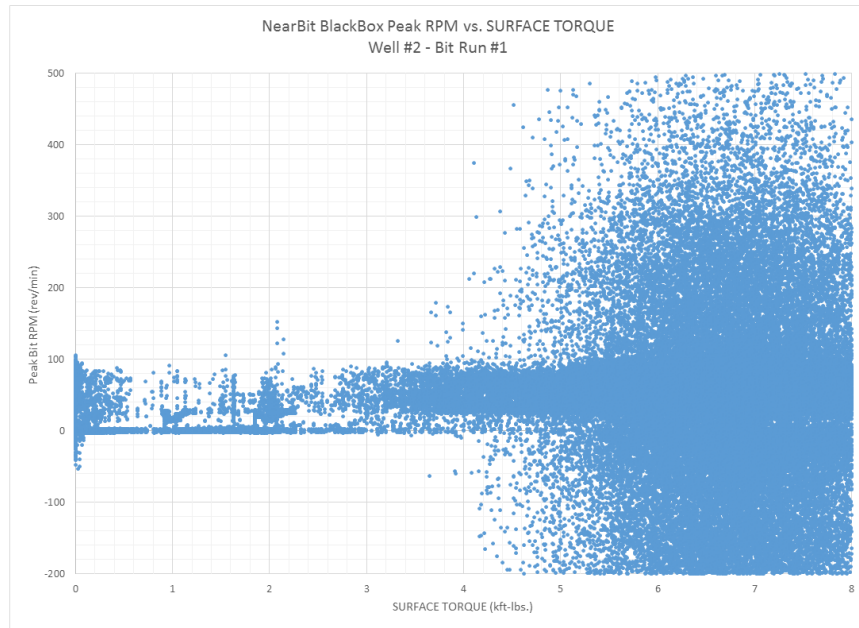


**Fig. 5.35 – Bit RPM versus surface torque for Well 2 Bit Run 1**

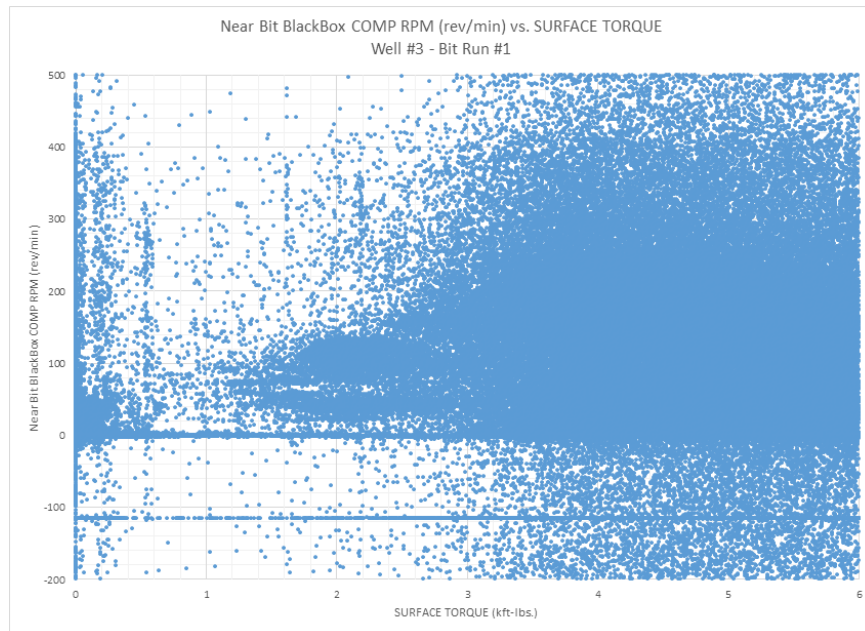


**Fig. 5.36 – Bit RPM versus surface torque for Well 3 Bit Run 1**

## 5.7 Closer look at STO

Following the discovery of the bit and BHA dysfunction profiles with respect to surface operational parameters including WOB, RPM, and torque, a closer look was taken at the vibrational wave profiles of STO and stick-slip to understand their relative magnitudes and dependency on factors such as rock strength or gamma ray, and depth of cut. In this effort high frequency data was loaded into the Excel program and plots were made to attempt to highlight the delicate relationship between STO and fully developed stick-slip. **Fig. 5.37** below shows an example of a period of time when STO was seen while drilling the second bit run on Well 1.

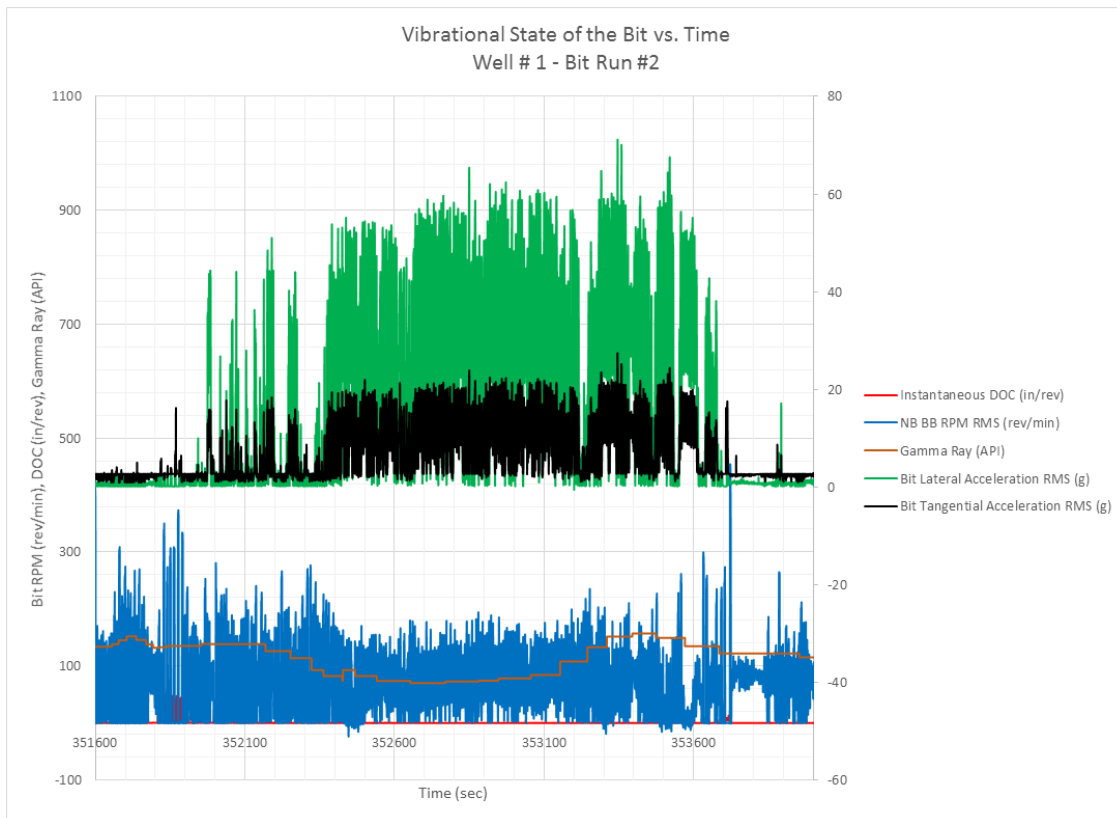


**Fig. 5.37 – Vibrational state of the bit during a period of STO**



The plot shows the bit rotational speed and the lateral and tangential bit accelerations over time, while also displaying the open hole gamma ray log signature, which is measured as a function of depth. From the plot there is strong correlation between the gamma ray value and the initiation of STO. API gamma ray values are typically correlated with clay content in the formation. The lower the gamma ray value, the less clay that is contained in the material, and thus a perceived higher rock strength, as high clay contents are typically associated with shale, which is a soft rock. It is believed that STO occurs during periods of drill string resonance, but from the plot it appears that STO can also occur with sustained loss in depth of cut from drilling the harder interfaces that have lower gamma ray values. The bit never comes to a complete stop, although it may exhibit zero and even reverse bit rotation, and as a result there is a massive increase in coupled lateral and tangential bit acceleration for sustained periods of time. This coupling of the lateral and tangential bit accelerations was very interesting as the conventional view of these vibrational types is that they typically do not exist simultaneously, instead they typically exhibit peak values during periods where the other vibration type exhibits its lowest values. **Fig. 5.38** below shows the DOC range for a period of STO and displays the long period of loss in DOC, with instantaneous gains in DOC related to the bit suddenly biting the formation and the just as suddenly losing hold on the formation and continuing to skim the top of the formation in an unconstrained and chattering manner.

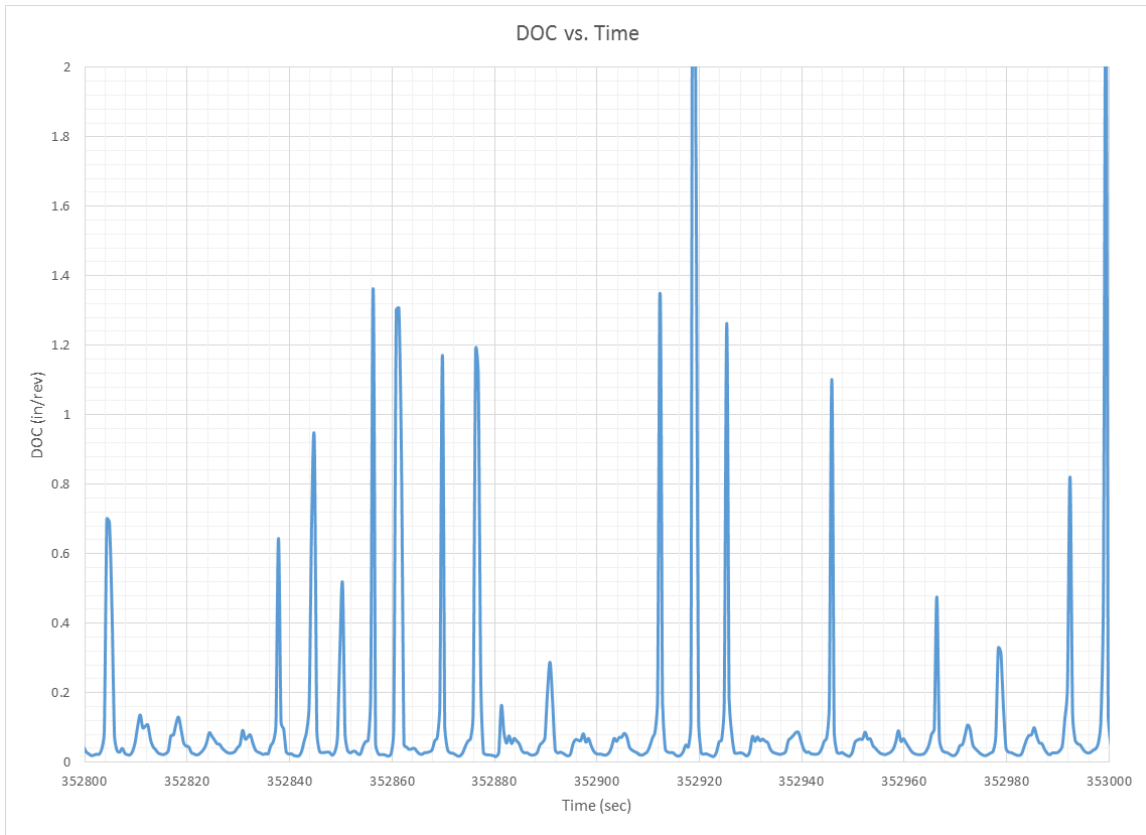


**Fig. 5.38 – DOC versus time for a period of STO**

It was very interesting to observe that oftentimes, periods of well-developed stick-slip, occurring before and after periods of STO, exhibited little lateral and tangential accelerations at all and the lateral and tangential vibrations behaved in their conventional nature with peak values of each acceleration type occurring out of phase with the other. **Fig. 5.39** below shows a period of well-developed stick-slip that precedes an extended period of STO, where gains in tangential bit acceleration were observed to occur during the sticking phase and gains in lateral bit acceleration occurred during the slip phase of stick-slip.

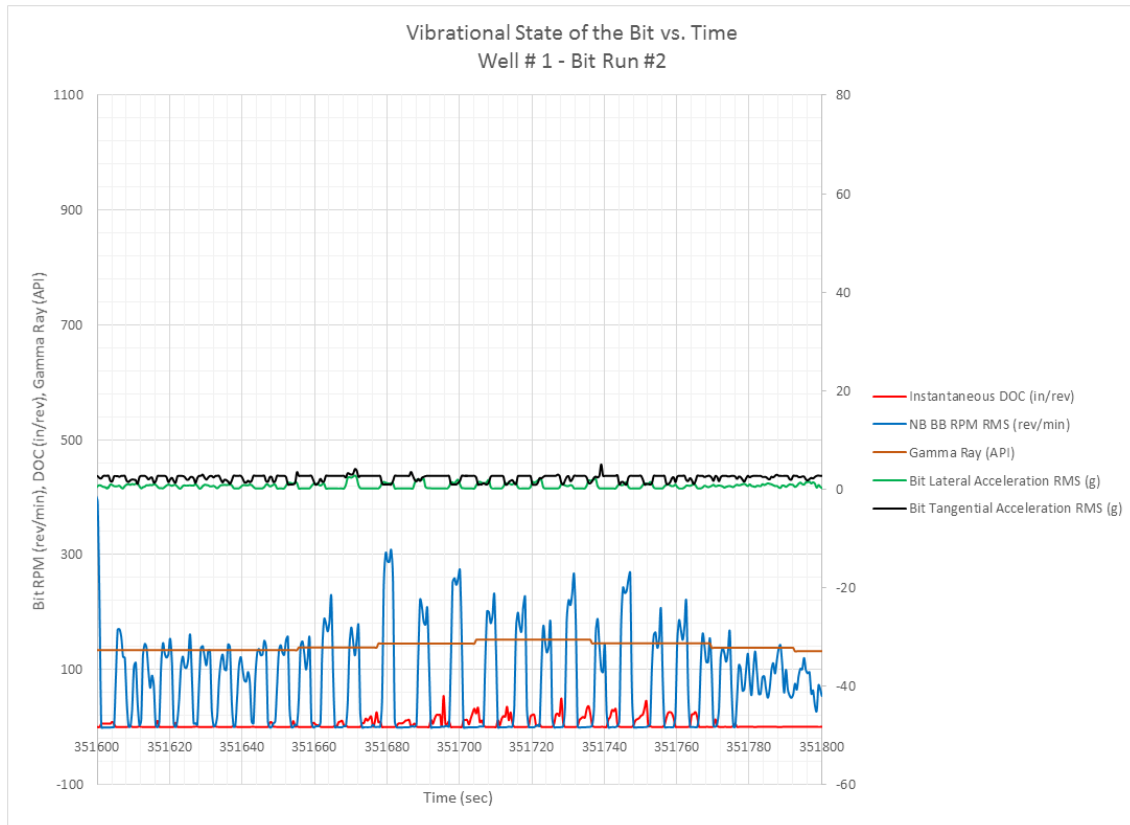


**Fig. 5.39 – Well-developed full stick-slip preceding a period of STO**

The plot shows that very minimal amounts of lateral and tangential bit acceleration oscillation occur during periods of stick-slip. It also shows the highest levels of tangential vibration are experienced during the sticking phase, which are associated with elevated values of instantaneous DOC during the period where instantaneous bit speed is zero or near-zero. The highest levels of lateral acceleration are experienced during the slip phase of stick-slip, where bit angular speed is at a maximum and instantaneous DOC is at a minimum.

When the shift from well-developed stick-slip to unstable stick-slip or STO occurs, the vibrational state of the bit changes dramatically. The bit will no longer stop rotating for periods of time, and will instead only briefly come to a stop or simply slow down to a near zero rotational speed before accelerating forward. During this period, there exists extended periods of time in which little or loss of DOC occurs, which facilitates a loss in containment of the drill bit and allows the bit to react to side forces and vibrational forces that are propagated towards the bottom of the hole from the BHA and drillstring. When these vibrational waves arrive at the bit they allow the bit to violently vibrate around in the hole, which can rapidly create whirl-like bit damage. The **Fig. 5.40** below shows a period of time in which short periods of STO are observed between periods of well-developed and stable stick-slip.

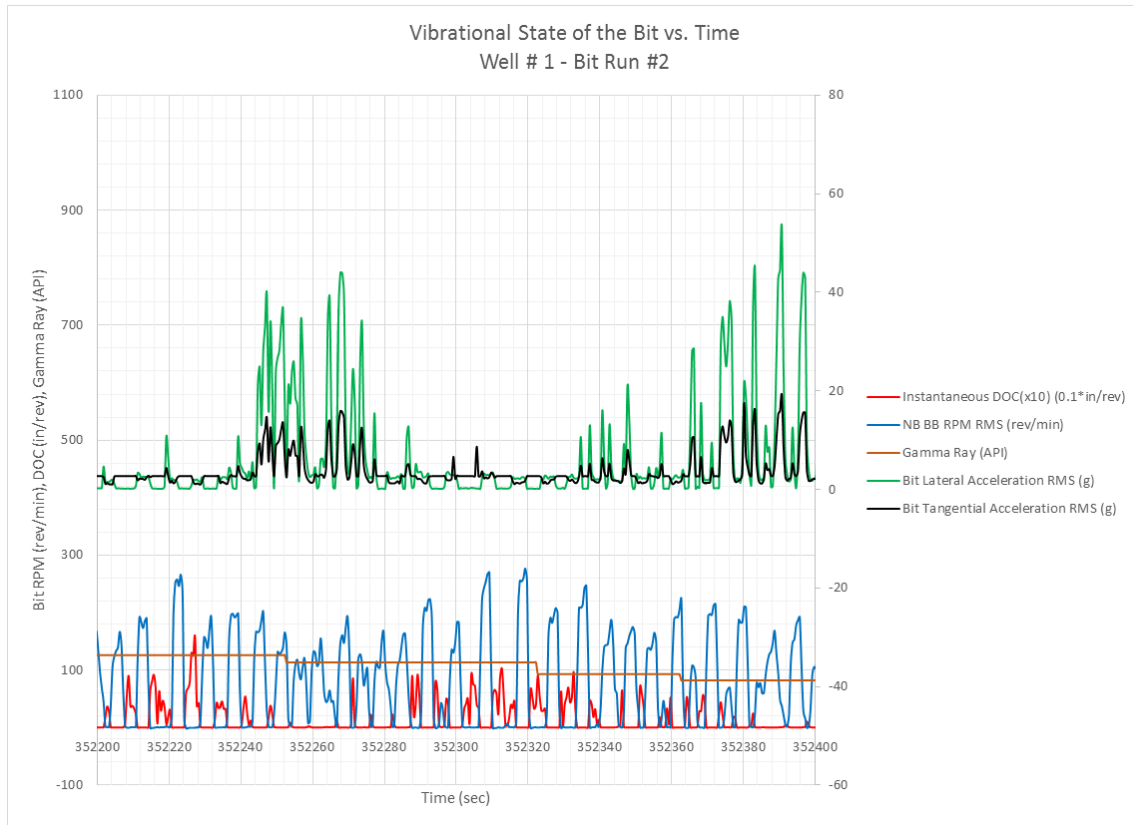


**Fig. 5.40 – Onset and periods of STO between periods of stick-slip**

Periods of stable stick-slip are shown to have periodic high gains in DOC (red), with simultaneous periodic zero bit RPM (blue), as well as opposing, and low in magnitude, lateral (green) and tangential (black) vibrational patterns, where each respective acceleration shows peaks and valleys out of phase with the other. During periods of the STO vibration, periods of low or near-zero DOC are experienced, while the bit rotational speed never comes to a sustained stop. Also, the magnitudes of the lateral and tangential accelerations are much higher and also synchronous, occurring in phase or simultaneously with respect to each other. It is important to note that during this period, high WOB in the average range of 18.5 k lbs is being applied to the bit,

which is in the upper range for WOB applied during the bit run, while also the gamma ray value is decreasing as time increases, which can be correlated to an increase in rock strength that would likely decrease the attainable DOC for a given WOB.

Sustained periods of unstable stick-slip and STO show sustained periods of loss in depth of cut, sustained periods of oscillating bit rotational speed with non-sustained periods of zero bit speed, and elevated and coupled lateral and tangential bit accelerations. **Fig. 5.41** displays these characteristics over a 200 second interval.

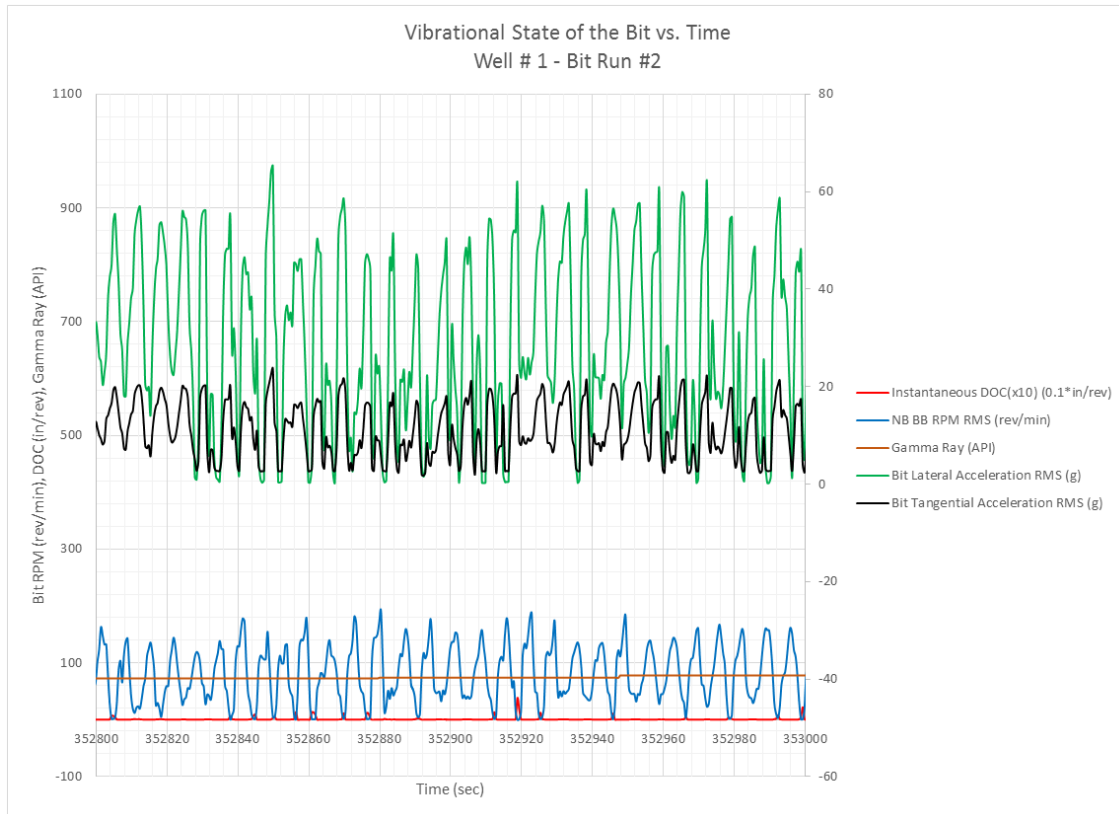


**Fig. 5.41 – Sustained period of STO**

During this extended period of STO the magnitudes of the lateral and tangential accelerations are very high and also synchronous, with peak values as high as 60g. This period shows high WOB in the average range of 20 klbs being applied to the bit and also low gamma ray values throughout the time interval. It is believed that this hard lamination, as shown by the gamma ray reading, compounded the loss in depth of cut experienced at the bit and helped, along with other factors, to promote the bits unconstrained motion. During this period, the bit rarely comes to a rest for any length of time with zero rotational speed, and tends to exhibit only instantaneous zero RPM, which helps provide an explanation for the low sustained DOC, where the bit fails to bite the formation being drilled and constrain itself with cutter indentation to prevent lateral movement.

When synchronous torsional oscillation occurs it is believed to be excited by a vibrational resonance that is a function of rotary speed, drillstring length, and torsional compliance of the drilling system (Ertas 2013). The shift from full stick-slip to unstable stick-slip or STO results in sustained periods of low DOC, which is likely a function of both rock strength and drill string resonance, but also increases the lateral displacement and side force experienced by the bit. In addition, the existence of STO has been correlated with higher WOB, which is likely applied during the drilling operation in an attempt to maintain higher torque levels and efficient DOC. The higher WOB levels during this dysfunction promote higher lateral accelerations during high levels of forward synchronous whirl or backwards whirl, which can result in higher angles of bit tilt when the bit is unconstrained and larger side forces. The **Fig. 5.42** displays a set of

drilling logs that show local periods without STO and low simultaneous WOB, resulting in high ROP.



**Fig. 5.42 – STO and its relationship with WOB (Courtesy of NOV)**

The log tracks, which show, from left to right, time, MD, ROP, WOB, torque, bit RPM, string RPM, lateral bit vibrations, lateral string vibrations, differential pressure, and pump flow rate, tend to represent that the STO vibration can be mitigated by reducing WOB similar to stick-slip, which agrees with **Fig. 5.16**, **Fig. 5.17**, **Fig. 5.18**, and **Fig. 5.19** showing lateral string vibrations as a function of downhole and surface WOB. As WOB increases, the likelihood of high bit and BHA lateral vibrations



increases due to higher lateral displacement, bit tilt, and higher levels of BHA whirl. While WOB has been shown to suppress bit whirl by achieving higher DOC, it also increases the lateral displacement of the drill string and BHA, which in events of low bit containment due to loss in DOC can trigger whirl-like events at the bit that behave with high lateral bit accelerations. It is assumed that during the time interval shown in **Fig. 5.42**, the driller observed a few instances of elevated MSE levels from what appeared to be stick-slip and reduced the WOB to attempt to mitigate the vibrations. When the WOB was reduced during prolonged periods of STO, ROP increased (as shown in green), which is believed to be a function of gaining DOC due to reduced resonance amplitude and speed oscillation in the BHA from borehole contact and friction during elevated BHA whirl from higher WOB, in turn promoting less bit tilt and side force.

In addition to reducing the WOB, another technique to mitigate unstable stick-slip and STO is to rotate the drill string at non-resonant speeds due to the torsional oscillation being related to torsional vibrational resonance that is excited at different speeds that change with depth. This work has provided evidence that rotational resonance or excited rotational speeds exist and that STO severity is related to the drillstring RPM. Specifically, **Fig. 5.20** shows the existence of “quiet” rotatory speeds at which low levels of lateral accelerations occur. These speeds are believed to be non-resonant for the given depth, and tend to promote more efficient drilling. An attempt was made to associate the existence of STO with the existence of lateral or torsional resonance rotary speeds and is shown in **Fig. 5.43** below using a Fast Fourier Transform.

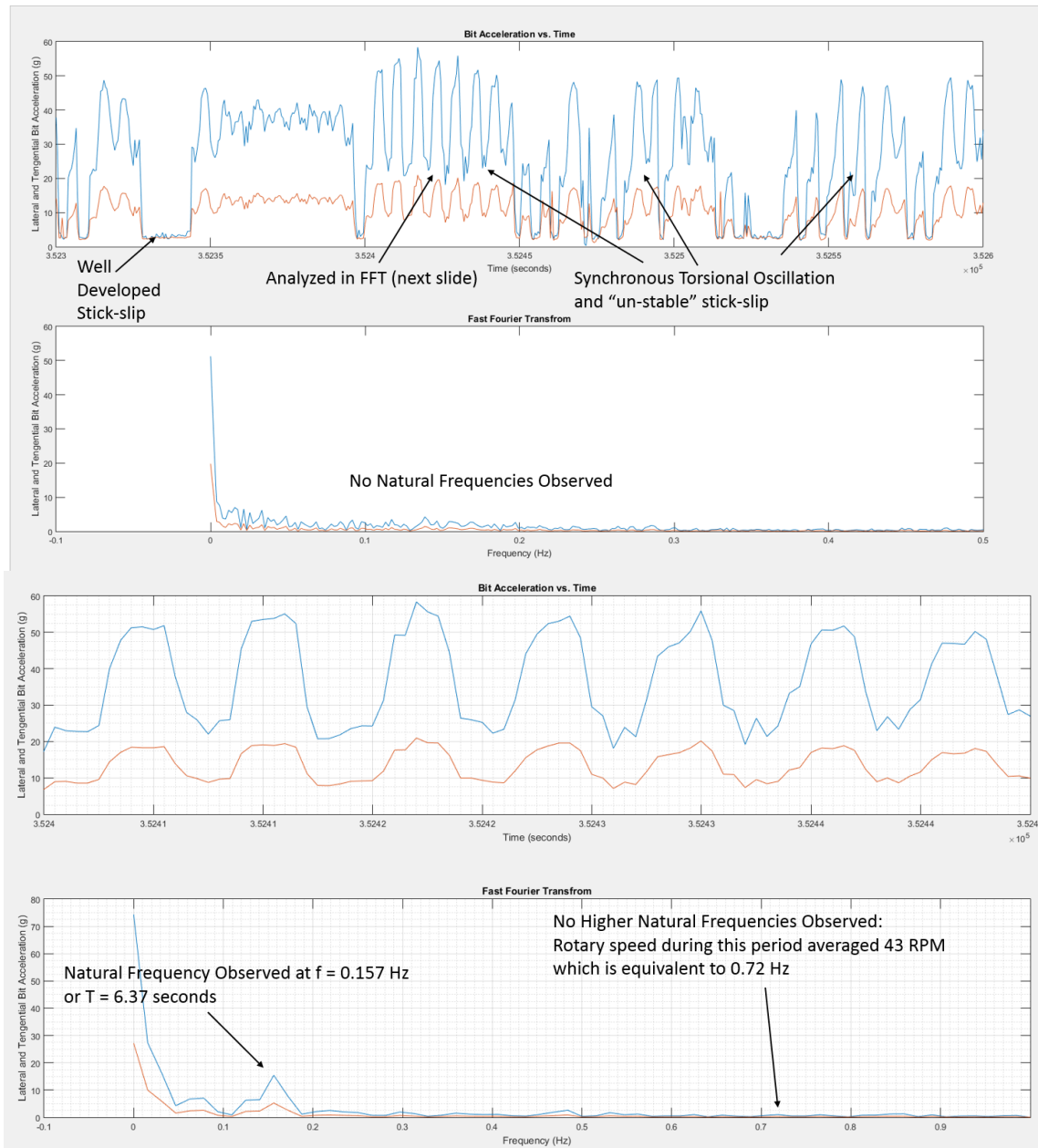


**Fig. 5.43 – Fast Fourier Transform analysis of a period of STO**

Unfortunately this relationship could not be proved with Fast Fourier Transform analysis or it does not exist. It is believed that the resonance relationship between STO and rotary speed exists, but that the data frequency was not fast enough to capture it.

The tools used to collect this data provided high enough measurement frequency to capture this phenomenon, however, the data recording frequency used to write these measurements to memory is only 2Hz and in the absence of the ability to sample and record burst data, provided an insufficient frequency to make definitive conclusions.

A major conclusion of this study is that STO is likely the most damaging vibration present in these wells for creating whirl-like bit damage due to its severe coupled and synchronous lateral and torsional bit accelerations, which promote the creation of beach marks during periods of lateral instability. Severe stick-slip, typically occurring in a single or limited number of cycles at the end of extended periods of STO, and sustained periodic stick-slip occurring near the end of bit runs when the bit is highly damaged, is considered to be a very damaging vibration due to its tendency to display long periods of zero rotation and sometimes reverse rotation during the stick phase. This motion promotes tearing and flaking of the cutters from the reverse direction, as well as elevated and coupled levels of lateral and tangential bit accelerations during the slip phase. Well-developed and stable stick-slip, which occurs with lower vibration levels, is also considered to be a significant and potentially damaging vibration occurring in these wells because it shows periods of zero and reverse bit rotational speeds, which can promote tearing and flaking of the cutters from the reverse direction, but it occurs with only moderate lateral and tangential acceleration levels which are non-coupled and non-synchronous. Simple torsional oscillation, although rare, was concluded to be the least damaging vibration as it promotes the lowest levels of lateral and tangential bit accelerations which are non-coupled and non-synchronous. **Fig. 5.44** shows a time

interval in which each of these vibrations is experienced, when the bit comes out of an extended period of STO.

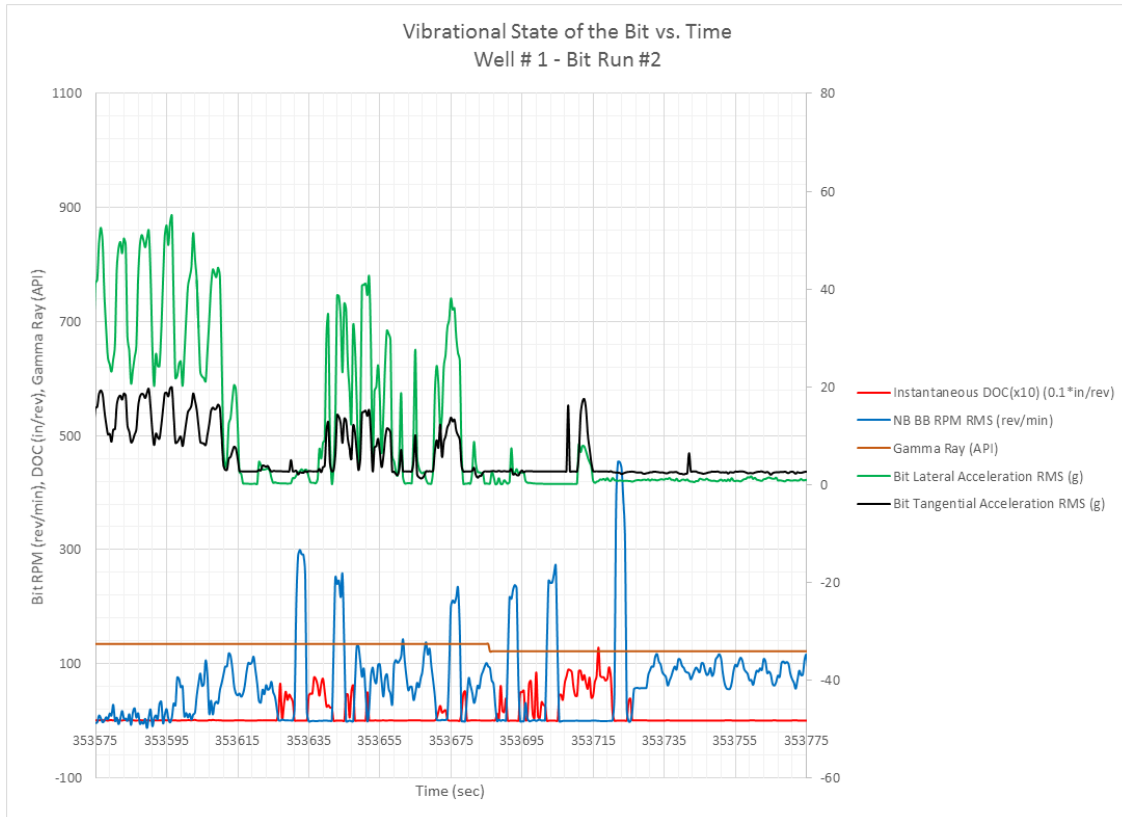


**Fig. 5.44 – Period in which various dysfunction occurs**

Starting from left to right, the bit starts off in STO, where it displays an extended period of low DOC, while simultaneously showing the highest levels of lateral and tangential acceleration during the time interval. The STO is then followed by two to three periodic cycles of stable stick-slip in which the bit shows low lateral and tangential accelerations during periodic DOC oscillation. Following the stable stick-slip is another period of STO, where similar phenomena and dysfunction is observed as the first period

of STO. After the second occurrence of STO, the bit exhibits two periodic cycles of stable stick-slip with low vibration levels, however, this is then followed by a single, non-periodic, and likely damaging cycle of severe stick-slip, where there is a non-periodic DOC oscillation. During the slip phase of this severe stick-slip cycle, which follows the longest sticking phase of this vibration period, nearing 15 seconds in length, the bit exhibits a violent release of energy in energy or a kick. During this kick, the lateral and tangential accelerations become coupled, showing that the kick is primarily tangential in nature with a high magnitude of tangential acceleration, and much less severe lateral acceleration, differentiating it from STO which primarily shows extreme increases in lateral accelerations. Finally, on the right side of the plot the drill bit shows a period of simple torsional oscillation, where the lowest, near-zero values of lateral and tangential accelerations are observed.

## 6. DISCUSSION AND SUMMARY

### 6.1 *Bit wear and modes of failure*

The PDC drill bits that are continuing to be pulled out of the wells the operator is drilling for either inadequate penetration rates or because they wouldn't drill any further show a unique type and location of bit wear that is prevalent in these wells with hard laminated formations. The location of the recurring bit wear is interesting because it predominantly occurs on the last two outside cutter rows and only occasionally on other cutters. Typically, this location is associated with axial vibrations such as bit bounce, while the locations of damage generally seen for lateral vibrations such as whirl occurs along the bit shoulder and gauge, and damage from tangential vibrations occurs on the inner-most cone cutters.



**Fig. 6.1 – Unique location of bit wear**

**Fig. 6.1** shows the distinct and contained location of wear on the drill bits used in these wells. The damage is almost completely contained in the last two outside cutter rows, with only minimal and seemingly normal wear occurring to the trim and gauge cutters just above the concentrated wear region, which is believed to be associated with whirl-like events. It is also very rare to see damage to the cone cutters on bits pulled from these wells, although the bits typically experience torsional vibrations throughout the majority of each bit run.

The combination of damage modes shown to be existent on the cutter faces and behind the diamond table into the substrate are of mixed origin. **Fig. 6.2** shows a cutter face that is perceived to have experienced both lateral and torsional motion due to the presence of beachmarks and wear patterns associated with thermal degradation along the cutter edge during periods of high angular velocity during the slip phase of stick-slip and STO.



**Fig. 6.2 – Close up of lateral impact damage**

When looking at center of the cutter face in the center of the **Fig. 6.2**, there appears to be clear signs of impact wear in the form of beachmarks, which have a center



of focus along the worn leading edge, at an angle of roughly 150 degrees, where the center of the diamond face is the origin. It is believed that during periods of unstable stick-slip and STO, the bit exhibits a periodic whirl-like motion and release of energy during the slip phase of the torsional oscillation while sustaining low DOC levels, which promotes higher lateral accelerations at the bit than the tangential accelerations experienced as a result of the rotational speed oscillations. The magnitudes of lateral and tangential accelerations experienced during periods of dysfunction serve as an indication of the relative motion of the bit and can be used to estimate the severity of impact and side cutting. During unstable stick-slip and STO the drill bit is unconstrained laterally due to extended periods of limited DOC, allowing it to develop a periodic and coupled vibration pattern that allows for the greatest lateral accelerations experienced in the well to occur. The lateral accelerations are accentuated by the stored rotational energy in the drill string, which allows the bit to spin faster than the designed rotational speed during the slip phase of the STO cycle and promotes higher speed impact than drilling that does not experience torsional oscillations. Although the maximum observed bit speed occurs during severe stick-slip, the maximum lateral and tangential accelerations occur during periods of STO, and are significantly larger than during periods of full stick-slip. It is believed that the overwhelming majority of the whirl-like bit damage occurs during impacts in STO.

The direction of the beachmarks on the diamond face are indicative of the direction of impact and also the direction of cutting. From **Fig. 6.2** and the orientation of the impact wear that is visible, it would appear that during episodes of unstable stick-slip

and STO the bit is primarily cutting sideways rather than towards the target. This side cutting motion is often associated with whirl and the creation of borehole patterns which can subsequently amplify the severity of this motion in overgauge hole. The side-cutting motion is clearly present in these wells giving an explanation for the high lateral accelerations experienced and the low penetration rates during periods of this dysfunction.

While unstable stick-slip and STO were not found to occur exclusively in harder rocks, it was found that hard rocks could help to promote these types of damaging motions, while also providing for a more abrasive impact surface. With conventional forwards and backwards non-coupled whirl being non-existent in these wells, it is very likely that the entirety of the impact damage was created as the result of unstable stick-slip and STO. Further it is very possible that the majority of that damage occurred in the harder laminations of the formations being drilled.

The large wear flat that is present on the edges of the cutters show signs that there are also wear contributions from torsional vibrations. However, this wear is not likely the result of reverse rotation, which has been proven to be capable of shearing, flaking, or tearing the diamond cutter face off from the back side. Instead, this wear appears more likely attributed to thermal degradation of the cutters leading edge, which is common in harder rocks, where lower cutter face contact area and higher heat from friction between the rubbing surfaces is promoted. Due to the resonance characteristics of the STO events and the extended periods over which the vibration shows the most elevated levels of lateral and tangential accelerations that are present in these wells, it is

most likely that this wear from thermal degradation occurs during STO. This is because STO facilitates low DOC and does not provide a distinct sticking phase, where enough time would be likely be provided to allow mud flow to cool the bit at a rate which can keep pace with the excessive amounts of heat generated during the slip phase. This non-uniform wear to the cutter face and substrate appears to work in combination with the whirl-like damage that accumulates from impact and from rubbing during side cutting, because it tends to show damage in the same location. The location of the thermal wear is also likely compounded by the increased travel distance that the two outside rows of cutters experience when compared to the inner-most nose cutters, which comparatively travel a much shorter distance per revolution, thus generating less heat from friction. The lack of wear to the inner nose cutters could be another indication that wear from reverse bit rotation, which is conventionally associated with stick-slip and torsional oscillation due to the inner nose cutters carrying the highest axial load and thus being more prone to damage from cutter flaking during reverse rotation, is rare in this application. **Fig. 6.3** shows a set of outside cutters that have experienced wear and degradation from torsional oscillation that has advanced into the matrix of the bit.



**Fig. 6.3 – Close up of thermal wear and degradation on PDC cutters from Well 2  
(Courtesy of Ultra Petroleum)**

It seems clear from this work that the bit damage seen in these wells is primarily, if not exclusively, occurring during long periods of STO, where high temperatures and damage from severe impacts occur. However, it is not necessarily clear how quickly the damage can occur and it would seem to be a function of the strength of the rock being drilled, the level of indentation depth of the leading cutters over time, the severity of the vibrations resonance, and the amount of heat generated during sliding.



**Fig. 6.4 – Thermal damage starting on PDC cutter (Courtesy of Ultra Petroleum)**

**Fig. 6.4** above shows an example of the development of thermal wear on a bit used to drill a short interval of 120-ft to target depth in the Lower Mesaverde formation. STO was observed to be the dominant vibration experienced during this period and bit wear associated with its existence developed in only a short amount of drilling time.

#### *6.2 Stick-slip, STO and operations management*

Based on the results of this study, it would appear to the author that the best practices to mitigate STO are the same as the best practices for mitigating stick-slip and other torsional oscillation. The STO that was observed during this study has resonance

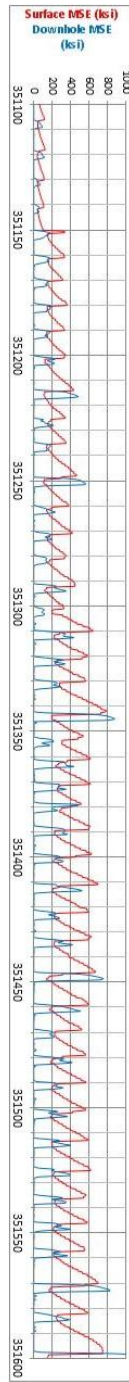
characteristics based on depth, rotary speed, and WOB. The depth intervals that are associated with developing and sustaining the STO resonance can be hundreds of feet of drilling time for a given rotary speed. These resonance bands are typically wider, in both depth range and in the range of rotary speeds which can sustain them, at lower rotary speeds. In addition, STO seems to occur more often and occur more violently at higher levels of WOB, similar to stick-slip. In light of these observations, it was determined that real time response mitigation techniques for STO are to increase the rotary speed, reduce WOB, and manage whirl in the stabilizers until a reduction in the mean MSE value displayed in real time is achieved. Design changes for the mitigation of STO are also similar to those for stick-slip and include increasing the torsional stiffness of the drill string, using roller reamers, BHA redesign to mitigate whirl, using DOCC bits, using lubricants to reduce drill string torque, and using active torque control such as Soft Torque™ or Soft Speed™. Some of these redesign opportunities will be discussed later in this section.

The response in mechanical specific energy to periods of STO is slightly different than its response to stick-slip. The mean value of MSE during STO is slightly higher than it is during periods of well-developed stick-slip. The variance in MSE is very different for the two vibrations. For full stick-slip, where there is a distinct sticking phase and larger torque and WOB oscillations, MSE tends to track these parameters and MSE oscillates with them. During STO, which is associated with sustained periods of low DOC and limited torque and WOB oscillation, the MSE track tends to produce what

appears to be noise, as there is very little change in any of the surface parameters. **Fig. 6.5** illustrate the differences between the vibrations.

During periods of full stick-slip, the MSE track also tends to represent the asymmetric trend that the torque track follows, while STO does not show any asymmetric shape due to the lack of a distinct sticking phase in which the bit comes to a full rest for any period of time.

While the MSE trends of the two vibration types are different when closely examined while using a system with the ability to capture data at 1-second intervals, these differences may not be distinguishable with lower resolution capture. Also, it may be advantageous to use a data acquisition system that is capable of sampling data at 10 Hz, such that the small variations and oscillations during each cycle of the waveform can be observed and the specific vibration type can be confirmed. It may be confusing or too time consuming for drillers to analyze the MSE waveform during drilling to distinguish the differences between the two vibrations such that he knows which dysfunction is occurring downhole. Because of this complication the author suggests that the driller instead be cognizant of the relative MSE range at which full stick-slip occurs, and then observe STO by noticing that the MSE value is equal to or greater than the MSE value for stick-slip, and to look for near zero oscillation in the surface torque and WOB measurements.



(a)



(b)

**Fig. 6.5 – MSE response to full stick-slip (a) and STO (b)**



It is recommended that the following procedure to identify and mitigate STO be added to the company's workflows and followed at each drilling location to further improve performance:

1. Raise the WOB. If the ROP response is linear (as determined through MSE surveillance), the bit is efficient.
2. Continue raising WOB until non-linear ROP response is observed, or MSE becomes a larger value
3. When torsional oscillation is identified by observing fluctuating values in WOB, Torque, or RPM, determine whether it is either stick-slip due to the presence of asymmetric torsional ramping pattern, or that it is another torsional oscillation that does not exhibit this pattern
4. If stick-slip, follow procedure for mitigating stick-slip and note the min, max, and mean MSE values during its existence
5. If it is not stick-slip, and the MSE mean value is larger than the stick-slip mean MSE value, then synchronous torsional oscillation (STO) is likely occurring
6. If STO is identified, reduce WOB until a reduction in MSE is observed, then change the rotary speed to avoid resonance speed for STO, by first increasing the rotary speed to a speed outside the predicted range of resonance for STO
7. Apply additional WOB at the non-resonant rotary speed until torsional oscillation is observed, at which point, record the values of

each drilling parameter and the measured depth at which STO started to occur

8. Redesign the system appropriately to extend the identified limiter and repeat steps 1-8.

### 6.3 *Roller reamers*

During the study, it was shown that the use of roller reamers in the BHA was highly effective at both delaying the onset of harmful torsional oscillations and when used in the full gauge configuration were shown to be very effective at reducing lateral accelerations in the BHA and at the bit. The roller reamers that were incorporated on two of the wells in this study were added in an effort to reduce torsional oscillation and proved to be effective at doing so. The torque required to initiate STO when using the roller reamers was proven to be almost double the torque required when using IBS in the BHA. In addition, the difference between the onset torque for STO when using full gauge roller reamers compared to the under gauge roller reamers was shown to be negligible. It is therefore the author's recommendation that full gauge roller reamers be incorporated on every well drilling these formations, due to their characteristic of allowing for higher WOB to be applied before dysfunction occurs, which will lead to higher performance and greater penetration rates.

#### 6.4 *Extending the gauge on drill bits*

Due to the lateral impact damage that is perceived to be occurring during severe torsional oscillation with coupled lateral acceleration, it is recommended that the gauge length be extended on drill bits used to drill the remaining wells in this field. Extending the gauge length limits the lateral displacement of the bits center of mass and reduces the associated angle of bit tilt that accompanies the displacement. Constraining the bit laterally by minimizing the lateral distance available for displacement between the gauge cutters and the top of the gauge section allows extended gauge bits to further reduce the high levels of lateral bit accelerations observed, in the same manner that the full gauge roller reamers accomplished this. All of the bits included in this study incorporated a 3-in gauge length. While a 3-in gauge length is longer than the industry standard, it is far from being an ideal length for mitigating lateral bit vibrations. It is suggested that longer gauge lengths be tried on subsequent wells starting with a minimum of 4-in, and progressing to lengths of 6 and 8 inches. Due to limited steering requirements of the s-shaped well design with the vertical production hole, the author does not foresee any limitations other than near bit friction or binding preventing the use of extended gauge length. Since steerability is not a limiter in the current well design, it is likely that bits with gauge length of 8 inches or longer can be run without adverse effects from friction.

When choosing an extended gauge length bit to run in these wells there are several key design considerations to minimize side cutting and the negative effects of bit whirl. First, designing the taper or undercut offset profiles to minimize the reduction in diameter in relation to the section of full gauge such that the upper section of the gauge

can make contact with the borehole wall at low angles, which helps to reduce bit tilt. Second, the cutting activity of the gauge and trim cutters should be considered and reduced as much as possible while maintaining the steerability requirements of the well design. For the wells in the study it is recommended that gauge and trim cutters with semi-active or passive activities be incorporated to reduce side cutting and borehole patterning during the acute whirl-like events that occur during STO, which should reduce damage from cutter impact and reduce the likelihood of drilling an overgauge hole.

#### 6.5 *Larger diameter drill pipe*

With the demand for higher penetration rates in wells that are deeper and more difficult, the physical and operational limits of the drilling system itself can be an issue. This can result in excessive loads and drilling vibrations that can damage the drill bit, BHA, and drillpipe (Herbig et al. 2015). Drillpipe comprises up to 95% of the length of the drilling system and behaves as a very long, weak torsional spring which under the right loads can lead to severe torsional vibrations and stick-slip events in addition to lower ROP and reliability of the drilling system (Herbig et al. 2015). Proper design and selection of the drill pipe used can reduce torsional oscillation and mitigate stick-slip, which will improve drilling performance.

During the early stages of analysis it was believed by the author that the torsional compliance of the drill pipe used by the company was a limiting piece of equipment for performance improvement. Significant gains in performance or penetration rates and reduced bit wear could not be achieved without increasing the stiffness of the drill pipe

due to the challenges and dysfunction that these wells present including stick-slip, STO, deep targets, and hard abrasive interbedded rock. Basic calculations were performed (Fig. 6.7 and Fig. 6.7) and presented to the company to illustrate a rough estimate of the perceived gains in stiffness and reductions in torsional deflection that could be attained by increasing the size of the drill pipe.

$$\Theta = \frac{TL}{GJ}$$

**Where:**  $\Theta$  = torsional deflection between the top drive and BHA  
 T = resultant torque acting at the cross section  
 L = length of the pipe  
 J = polar moment of inertia of the cross-sectional area  
 G = transverse elastic modulus of the pipe

$$J = \frac{\pi}{2} (r_o^4 - r_i^4)$$

**Where:** J = polar moment of inertia of the cross-sectional area  
 $r_o$  = outer radius of shaft  
 $r_i$  = inner radius of shaft

**Fig. 6.6 – Torsional deflection and polar moment of inertia equations for a hollow circular shaft (Davis et al. 2012)**

$$J_{4 \text{ in} - 14.0 \text{ ppf}} = \frac{\pi}{2} \left( \frac{4^4}{2^4} - \frac{3.34^4}{2^4} \right) = 12.915 \text{ in}^4$$

$$J_{4.5 \text{ in} - 16.6 \text{ ppf}} = \frac{\pi}{2} \left( \frac{4.5^4}{2^4} - \frac{3.826^4}{2^4} \right) = 19.221 \text{ in}^4$$

$$J_{4.5 \text{ in} - 20.0 \text{ ppf}} = \frac{\pi}{2} \left( \frac{4.5^4}{2^4} - \frac{3.64^4}{2^4} \right) = 23.023 \text{ in}^4$$

**Fig. 6.7 – Polar moment of inertia results for various drill pipe sizes and weights**

The results of these calculations showed that by increasing the drill pipe by one half of an inch or one size, the company could gain up to a 78.3% increase in torsional stiffness and up to a 43.9% reduction in torsional deflection, or number of wraps experienced while drilling, given the same material properties and length. This improvement would allow more weight on bit to be applied to the bit before experiencing dysfunction due to torsional oscillation and consequently higher penetration rates with increasing WOB. The increase in drill pipe stiffness also promotes shorter sticking phases during stick-slip and lower maximum values of bit rotational speed given the same operating parameters (Herbig et al. 2015).

While it has been recommended that the use of roller reamers and larger diameter drill pipe be incorporated in the drilling system, it is not recommended that the use of larger BHA components, such as larger heavy weight drill pipe or drill collars, be used without first increasing the size of the drill pipe. Adding mass and size to the end of the torsional pendulum has been shown to increase the maximum rotational speed downhole

created from torsional oscillation (Herbig et al. 2015). Using a simplified lumped mass model with two degrees of freedom to represent the drill string, it is can be shown that the severity of downhole maximum rotational speed is largely a function of the fourth order diameter ratio of the BHA and drillpipe (Herbig et al. 2015). This ratio is shown below along with results (Fig. 6.8) from calculation using two sizes of heavy weight drill pipe:

Fourth-order diameter ratio of BHA and drill pipe:

$$R = \left( \frac{d_{BHA,outer}^4 - d_{BHA,inner}^4}{d_{DP,outer}^4 - d_{DP,inner}^4} \right) \dots \dots \dots \text{Eqn. 6}$$

where:  $d$  = diameter  
 $BHA$  = bottom hole assembly  
 $DP$  = drill pipe

$$R_{4 \text{ in HWDP}} = \left( \frac{4^4 - 2.56^4}{4^4 - 3.34^4} \right) = 1.620$$

$$R_{4.5 \text{ in HWDP}} = \left( \frac{4.5^4 - 2.75^4}{4^4 - 3.34^4} \right) = 2.682$$

**Fig. 6.8 – Results of fourth-order diameter ratio calculation**

From this rough calculation, it can be expected that the replacement of the currently used 4-in heavy weight drill pipe with 4.5-in heavy weight drill pipe (HWDP), without also increasing the diameter of the rig drill pipe, will produce higher maximum angular velocities at the bit due to the fourth-order diameter ratio of the BHA or HWDP and rig drill pipe increasing with increasing HWDP size. These higher maximum

angular velocities would be the result of higher severity torsional oscillation that could potentially be more damaging to the bit and downhole tools, especially if the coupled lateral accelerations during these torsional oscillations is not reduced with increasing the size of the HWDP. It is the author's belief that the lateral accelerations will likely not be reduced, due to the greater effect of the stabilization equipment on reducing these vibrations in addition to the tendency of stiffer BHA to promote whirl and the creation of borehole patterns given that it contains the same number of stabilizing elements or contact points (Pastusek and Brackin 2003). It is therefore not recommended to increase the size of the HWDP used in the BHA on these wells because doing so will likely be more damaging than the current design.

#### *6.6 Soft-Speed™ response system*

The Soft-Speed™ active torque control system is an active damping system that varies the top drive rotary speed to reduce torsional oscillation and vibration downhole. Without the use of Soft-Speed™, the top drive wants to maintain a constant speed, and thus applies more power in the form of torque to the drill string to compensate for the resistance as a result of torsional oscillation, which in turn adds more power to the motion. The use of Soft-Speed™ allows for the top drive to slow down when it measures a greater resistance during dysfunction, which allows the deceleration of the string's mass to absorb the excess torsional energy.

It is recommended that Soft-Speed™ be incorporated in the drilling system for the remaining wells due to its proven ability to extend the founder point of torsional



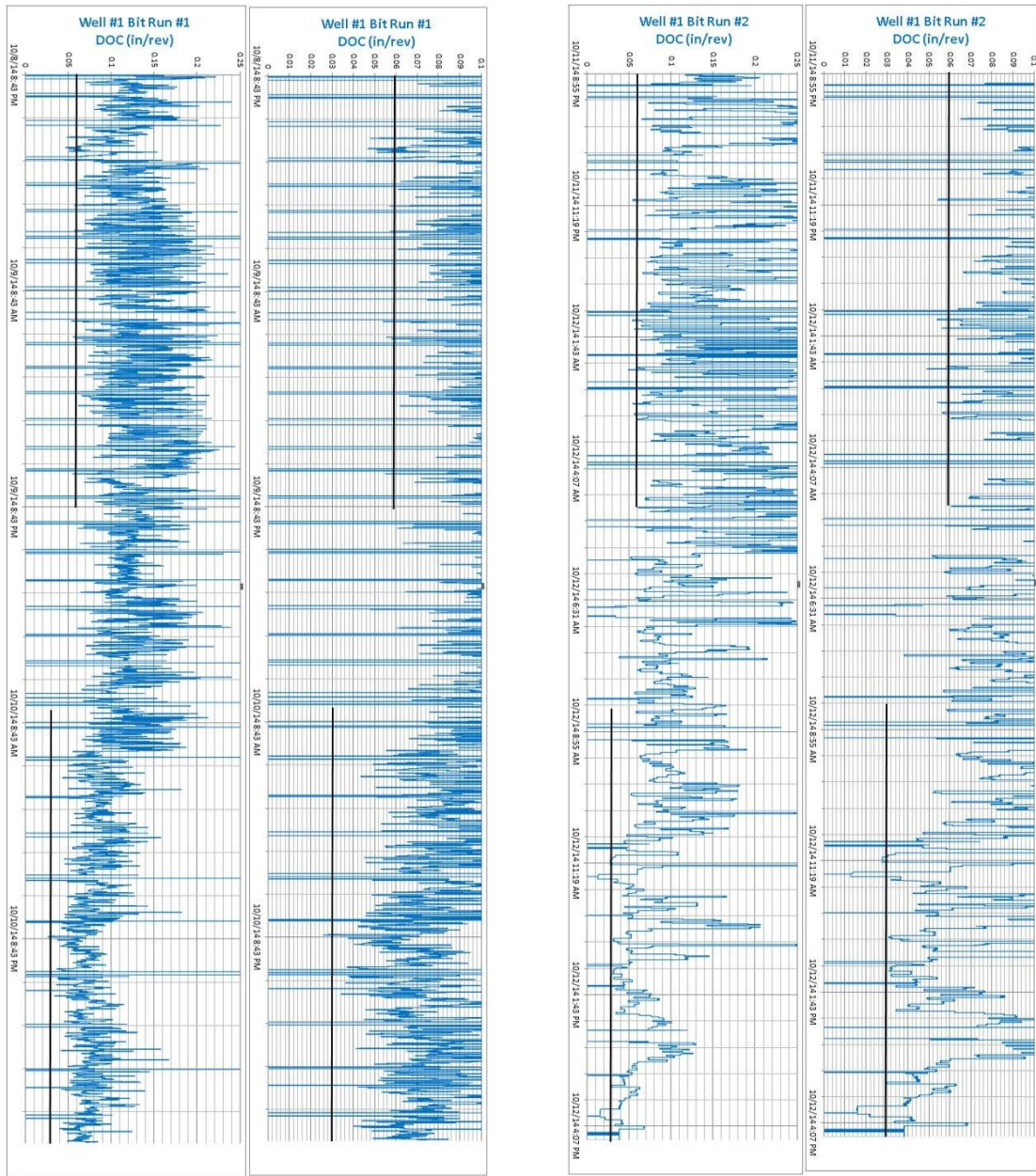
dysfunction, allowing greater WOB to be applied and results in higher downhole torque before the onset of dysfunction. It is important if this equipment is installed to measure the increase in performance gained through its addition by measuring and observing the downhole vibrations with the use of NOV Data Loggers, such that the torque at which the onset of STO occurs can be observed. The onset of STO is acute and can be easily seen with a plot showing lateral bit acceleration as a function of torque, whether it be measured from surface or downhole. The author would recommend incorporating the LMS into this trial such that the most accurate measurement of the onset of STO can be taken at the bit, thus eliminating the chance of error in the measurement from excess drill string drag or other source of increased wellbore friction. It is also recommended that if installed, the Soft-Speed™ system response should be tuned to respond to the first torsional mode, meaning it would be attempting to mitigate stick-slip rather than the second torsional mode, which is the resonance in the drill string promoting STO.

It is the author's belief that the addition of Soft-Speed™ to the rigs' capabilities will result in significant performance improvements as it has been consistently shown to do so in applications where the drilling system is torsionally limited in literature (Jansen and Van den Steen 1995), (Nessjoen et al. 2011), (Runia et al. 2013), (Attar et al. 2014), (Efteland et al. 2014), and (Dwars 2015).

### *6.7 Depth of cut control effectiveness*

The effectiveness of the depth of cut control bits at reducing torsional oscillation could not be directly compared during the study because of the differences in

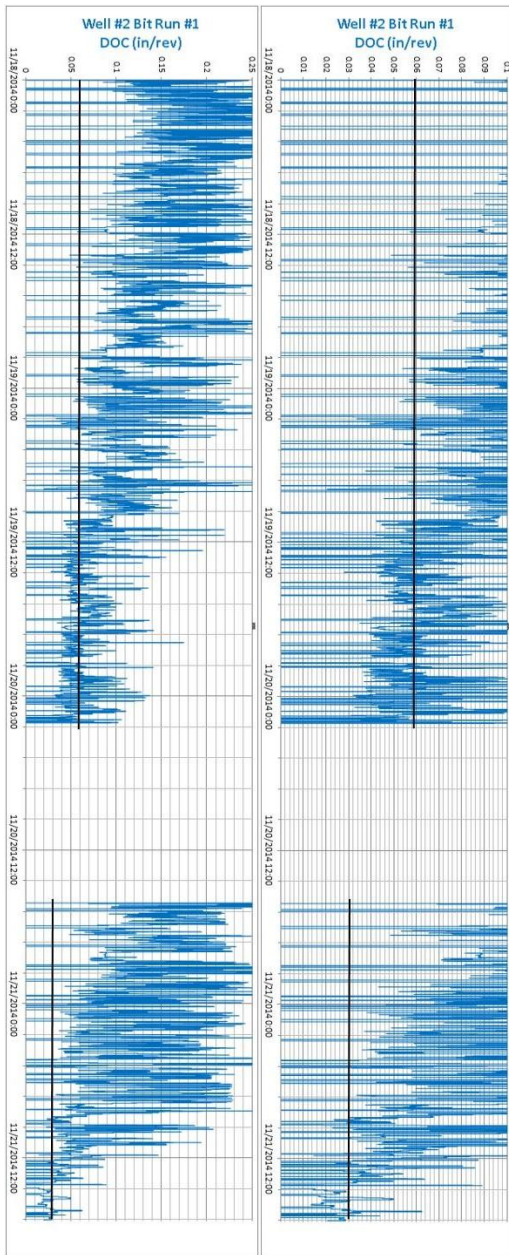
stabilization equipment incorporated on the various wells. Because the use of integral blade stabilizers increased the frictional losses due to drag, reduced the efficiency of weight transfer to the bit, and promoted torsional oscillation and dysfunction at lower torque, it is unfair to directly compare the dynamics of the depth of cut control bit to the dynamics of the non-depth controlling bits. However, an attempt was made to quantify the ideal or appropriate design setting for the rubbing surfaces that manage the over-engagement of the bit to the formation. A series of plots were constructed to illustrate the proper design and location of rubbing surface engagement by showing DOC as a function of time for each of the bit runs included in the study. Somewhat repeatable results were achieved and can be found in the **Fig. 6.9** and **Fig. 6.10** on the next two pages.



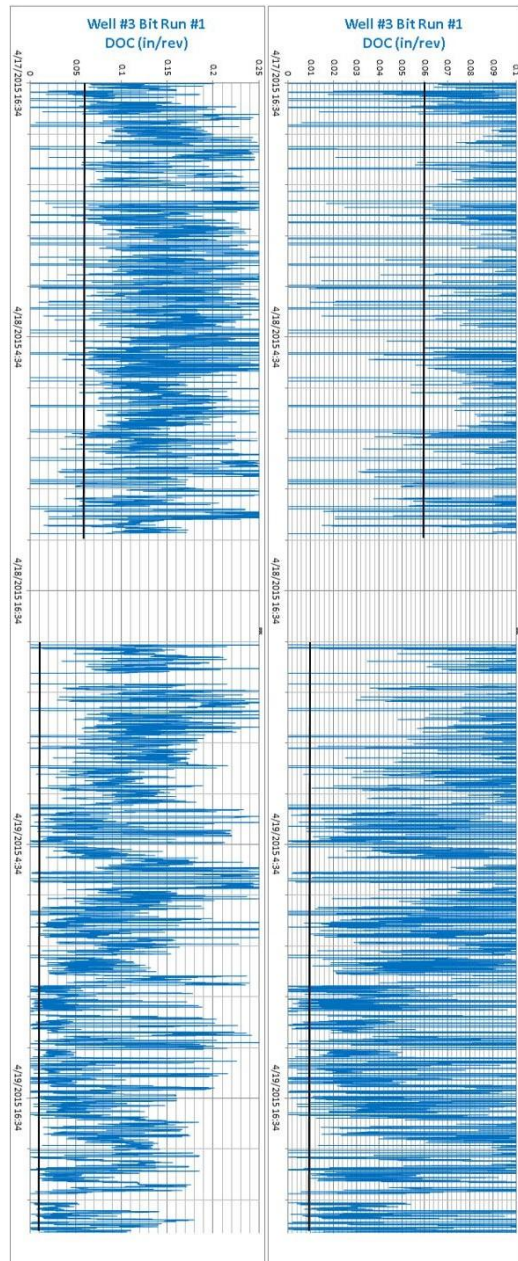
(a)

(b)

**Fig. 6.9 – DOC versus time Well 1 Bit Run 1 (a) and Bit Run 2 (b)**



(a)



(b)

**Fig. 6.10 – DOC versus time Well 2 Bit Run 1 (a) and Well 3 Bit Run 1 (b)**

**Fig. 6.9** and **Fig. 6.10** show two distinct regions where DOC and torsional oscillation start to exist which correspond to both rock type and bit wear. At the beginning of each bit run, with a fresh bit and at higher depths with lower strength rock, where higher drill rates have been observed, the DOC at which oscillation is initiated is slightly higher than 0.06 in/rev for every bit included in the study. While later in each bit run, with a worn and damaged bits, and at lower depths with higher rock strengths, the DOC at which oscillation is initiated varies by bit type. The Hughes Christiansen bit shows the onset of oscillation at 0.03 in/rev, while the NOV Reed Hycalog bit shows the onset of oscillation at 0.01 in/rev, although this low DOC value could be the result of the excess stabilizer drag. Rotating at 100 revolutions per minute, a depth of cut value of 0.06 inches per revolution results in a drill rate of 30 feet per hour, which would be the location of the bit's "knee" or the point at which the rubbing surfaces start to engage and the torque profile changes as a function of WOB; the bit's coefficient of friction becomes less aggressive with further increases in WOB. When running a depth of cut controlling bit, it is important to apply enough WOB to operate at a DOC that is greater than the value at the knee to ensure that the beneficial effects of the DOCC bit are taken advantage of, such as limited torsional oscillation and suppressed bit whirl.

It is recommended that if the company would like to pursue the use of DOCC bits, with the current drilling system limitations and without the addition of any improvements to the system such as larger drill pipe or Soft-Speed™, that the rubbing surface setting height should be such that they engage at 0.06 in/rev DOC, or just below an agreed upon minimum ROP, for example 100 ft/hr, such that they promote efficient

cutting without dysfunction. It is important to remember that as much weight as possible should be applied to the bit past the knee to gain the maximum possible drill rate without dysfunction past the knee. It is also recommended that the rubbing surface be moved further towards the center of the bit, such that they carry a higher axial load and prevent torque loss from their placement. Changing the material of the torque control components (TCC) or rubbing surface from tungsten carbide to diamond is also recommended, especially in the hard abrasive formations present in these wells to prevent wear and ensure that their engagement is at a uniform DOC throughout the bit run.

#### 6.8 *Managing vibrations levels*

After significant improvement is made in the drilling system, which allows for longer periods of drilling time spent in the stable drilling region between torsional oscillation and whirl, management practices should be incorporated to consistently improve drilling efficiency through vibrations reduction. It has been shown in literature that there exists an operating region with a non-zero DSSI in which lateral vibrations are natural dampened, due to the “mistuning” effect (Reckmann et al. 2010), in which moderate, non-damaging torsional oscillation reduces the possibility of a constant lateral excitation frequency, thus preventing the lateral accelerations from reaching steady state with high amplitudes. **Fig. 6.11** below shows an example of a quiet drilling region present at a non-zero value of the DSSI from the second bit run of Well 1.

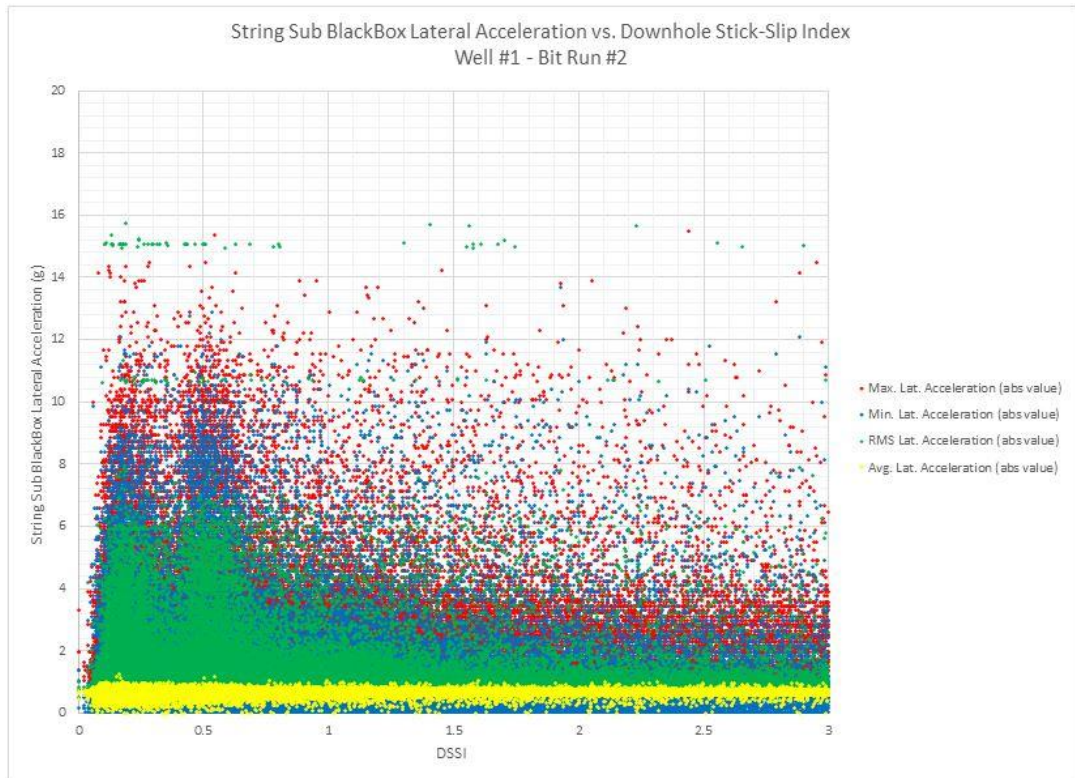


**Fig. 6.11 – BHA lateral accelerations versus DSSI**

The optimal DSSI shown in Well 1 to reduce the lateral accelerations present and provide a healthy benefit for drilling with the specific BHA configuration is around 0.35. It is suggested that future downhole data sets be studied in this manner to determine ideal operating parameters once issues of severe torsional oscillation, such as STO which produce DSSI values greater than 100, are mitigated. Once ideal DSSI levels are determined for the current revision of the BHA design, it is suggested that the use of the surface stick-slip index (SSSI) be incorporated and scaled to accurately represent the DSSI value (Lai et al. 2014), such that through this process drillers can actively manage to the downhole condition of the bit to reduce damaging lateral vibrations.

## 6.9 *Further research*

Suggestions for further research to better comprehend the dysfunction and bit wear present in these wells are related to understanding the dysfunction through surveillance, understanding other potentially contributing drilling limiters, and redesigning drilling equipment to be more withstanding of the punishment the dysfunction imposes on it.

Understanding the nature of the STO present in these wells is dependent on the quality and resolution of the downhole data gathered while using memory based downhole dynamics measurement tools. Data collected at 2-Hz, while diagnostic in determination of the vibrations existence, does not allow a detailed study of the frequency response and resonance tendencies of STO. Analysis of higher frequency data, either sampled continuously at finer resolutions such as 10-Hz or sampled in burst formats, where extremely high frequency data is collected and stored during short time intervals multiple times throughout the drilling process should provide much more diagnostic results. It is the author's belief that analysis of burst datasets will provide the most meaningful results and could provide additional information about how the vibration is triggered and why the lateral and tangential accelerations associated with it are coupled.

It has also been suggested by a member of the committee that the vibrations present in the wells included in this study resemble Mode Coupling Chatter (MCC), which is a common vibration present in certain types of industrial manufacturing. MCC most notably occurs during end milling and lathe cutting processes (Altintas 2000),



which are both mechanically different than rotary drilling because they differ in the direction of cutting and forces involved during cutting. The size, scale, and system torsional rigidity of end milling and lathe cutting also differ greatly when compared to rotary drilling. In MCC, inconsistencies in the material surface being cut drives high frequency resonant vibrations that can become coupled both in the lateral and tangential directions (Altintas 2000). The changes in material profile that drives the vibrational resonance of MCC appear to behave similarly to the manner in which the three lobed bottomhole pattern that can be created when rotary drilling with a roller cone bit drives vibrational resonance in the axial direction of a drillstring. These high frequency MCC vibrations also occur at frequencies that are multiples of HFTO and multiple magnitudes larger than the frequencies at which STO was observed to occur during this study. However, there could be a possible connection between the vibrations observed in this study and MCC. It is suggested that if higher frequency data is collected in future wells, that the frequency at which data is recorded to memory be sufficient to capture the potential existence of MCC, such that stability lobes could potentially be created as a function of WOB and bit speed. This sampling frequency would likely need to be upwards of 3000 Hz to capture the very high chatter frequency (Altintas 2000).

Identifying all of the potential limitations of the drilling system is fundamental to making performance improvements and reducing dysfunction caused by vibrations and other inefficient phenomena. To improve the efficiency and damping characteristics of the BHA it is suggested that a dynamic modal analysis be performed to determine ideal locations for stabilizer placement given the characteristics of the equipment and

components incorporated. The objective of the modal analysis would be to increase the operating window or the stable region between the stick-slip region, where insufficient bit rotational speed is supplied for the applied axial load and the whirl region, where insufficient WOB is applied for the given bit speed. It is also suggested that in moving forward, an in-depth buckling analysis is performed to understand the magnitude of the side force and angle of bit tilt that is associated with the current well design and BHA configuration. If these wells are determined to be buckling limited and preventing efficient weight transfer without severe lateral displacement, then redesigning the BHA to include components less prone to buckling should be considered. As previously discussed, if more mass is added to the BHA, then consideration should be given to increasing the size of the rig drill pipe to prevent increasing the fourth-order diameter ratio of BHA and drill pipe, which can result in larger torsional oscillation. The downhole mud motor should also be given consideration for further research during analysis of the BHA as it may actually help to promote the STO vibration by accentuating the bits motion during periods of sustained loss in depth of cut. The motor has also shown to rotate the drill string in the reverse direction and then stall during periods of full stick-slip during the sticking phase. This motion adds energy to the torsional vibration and can make the associated damage worse. If Soft-Speed™ is planned to be added to the drilling system, analysis should be performed to determine if the current BHA design using a downhole motor could be outperformed by a BHA not containing a motor in combination with Soft-Speed™ and operating at more aggressive parameters, which could potentially promote quieter drilling.

Redesigning the drilling equipment incorporated in the current well design to be more withstanding of the punishment the dynamic dysfunction imposes on it should also be concern for further research. This research could include but is not limited to improved cutter geometry to reduce torsional oscillation and tendency to whirl, improved cutter face design and cutter material processing design for temperature and impact damage resistance, improved operation and reliability of the near bit rotary steerable system in cases of torsional oscillation, and improved motor design and reliability of the pressure containing sealing elements.

## NOMENCLATURE

AEG	= Altered edge geometry
AKO	= Adjustable kick-off
AVAZ	= Amplitude versus angle and azimuth
BHA	= Bottom hole assembly
CCS	= Confined compressive strength (psi)
COF	= Coefficient of friction (dimensionless) [Tangential force]/[Normal force]
d	= Diameter (in.)
D	= Diameter (in.)
DLS	= Dogleg severity
DOC	= Depth of cut (in/rev)
DP	= Drill pipe
DSSI	= Downhole stick-slip index
FFT	= Fast Fourier Transform
HFTO	= High frequency torsional oscillation
HTI	= Horizontally transverse isotropic
HWDP	= Heavy weight drill pipe
IADC	= International Association of Drilling Contractors
IBS	= Integral blade stabilizer
LMS	= Lower mechanical sub
MCC	= Mode coupling chatter

MD	= Measured depth (ft.)
MSE	= Mechanical specific energy (psi)
MSE <sub>adj.</sub>	= Adjusted mechanical specific energy (psi)
MWD	= Measurement while drilling
N/A	= Not applicable
NAF	= Non-aqueous fluid
NPT	= Non-productive time
OBM	= Oil-based mud
OD	= Outer diameter (in.)
PDC	= Polycrystalline diamond compact
PDM	= Positive displacement motor
psi	= Pounds per square inch
$Q_{pump}$	= Total flow rate through the mud pumps and standpipe (gpm)
RMS	= Root mean square
ROP	= Rate of penetration (ft./hr)
RPM	= Rotations per minute (rev/min)
$RPM_{bit}$	= Instantaneous bit rotational speed (rev/min)
$RPM_{bit,pump}$	= Estimated downhole bit rotational speed (rev/min)
$RPM_{rotary}$	= Rotational speed of the topdrive or Kelly (rev/min)
SPE	= Society of Petroleum Engineers
SSSI	= Surface stick-slip index
STO	= Synchronous torsional oscillation

TCC	= Torque control component
T	= Torque (ft-lbs.)
TD	= Target depth
TK	= Tertiary-Cretaceous
UCS	= Unconfined compressive strength (psi)
$\mu_{motor}$	= Motor specific ratio of revolutions to flow volume (rev/gal)
VSPC	= Visual single point cutter
WBM	= Water-based mud
WOB	= Weight on bit (lbs.)
$\omega_{avg}$	= Average angular velocity over the sampling range (rev/min)
$\omega_{min}$	= Minimum angular velocity during the sampling range (rev/min)
$\omega_{max}$	= Maximum angular velocity during the sampling range (rev/min)

## REFERENCES

- Altintas, Y. 2000. Manufacturing Automation: Metal Cutting Mechanics, Machine Tool Vibrations, and Cnc Design. In, 1:14. Original edition, Cambridge University. 0521650291
- Attar, F., Grauwmans, R., and Ikhajiagbe, O. 2014. Soft Torque Impact on Drilling Performance in Qatar. Paper presented at the International Petroleum Technology Conference, Doha, Qatar. DOI: 10.2523/17651-MS.
- Azizov, A.A., Davila, W., Nnanna, O.C. et al. 2011. Positive Displacement Motor Innovation Drives Increased Performance with Pdc Bits in Unconventional Plays. Paper presented at the SPE/IADC Middle East Drilling Technology Conference and Exhibition, Muscat, Oman. Society of Petroleum Engineers. DOI: 10.2118/148262-MS.
- Bailey, J.R., Wang, L., Tenny, M. et al. 2010. Design Tools and Workflows to Mitigate Drilling Vibrations. Paper presented at the SPE Annual Technical Conference and Exhibition, Florence, Italy. Society of Petroleum Engineers. DOI: 10.2118/135439-MS.
- Barton, S.P., Setlur, D.R., and Clegg, J.M. 2008. Testing of New Pdc Cutter Edge Geometry Doubles Penetration Rate and Reduces Torque. Paper presented at the SPE Annual Technical Conference and Exhibition, Denver, Colorado. Society of Petroleum Engineers. DOI: 10.2118/116173-MS.
- Bowker, K.A. and Robinson, J.W. 1997. Jonah Field: A Shallow Sweetspot in the Basin-Centered Gas Accumulation of the Northern Green River Basin. *AAPG Rocky Mountain Sect. Mtg. (Denver, 8/24-27/97) PAP; AAPG Bull.* **81** (7): 1219-1220.
- Brett, J.F. 1992. The Genesis of Bit-Induced Torsional Drillstring Vibrations. *SPE Drilling Engineering*: 7. DOI: 10.2118/21943-PA.
- Brett, J.F., Warren, T.M., and Behr, S.M. 1990. Bit Whirl - a New Theory of Pdc Bit Failure. *SPE Drilling Engineering*: 7. DOI: 10.2118/19571-PA.
- Caicedo, H.U., Calhoun, W.M., and Ewy, R.T. 2005. Unique Rop Predictor Using Bit-Specific Coefficient of Sliding Friction and Mechanical Efficiency as a Function of Confined Compressive Strength Impacts Drilling Performance. Paper presented at the SPE/IADC Drilling Conference, Amsterdam, The Netherlands. Society of Petroleum Engineers. DOI: 10.2118/92576-MS.
- Chen, D.C.K., Comeaux, B.C., Gillespie, G.M. et al. 2006. Real-Time Downhole Torsional Vibration Monitor for Improving Tool Performance and Bit Design.

Paper presented at the IADC/SPE Drilling Conference, Miami, Florida, USA. Society of Petroleum Engineers. DOI: 10.2118/99193-MS.

Cooley, C.H., Pastusek, P.E., Christensen, H. et al. 1992. The Design and Testing of Anti-Whirl Bits. Paper presented at the Annual Technical Conference and Exhibition of the Society of Petroleum Engineers, Washington, DC, USA. Society of Petroleum Engineers. DOI: 10.2118/24586-MS.

Davis, J., Smyth, G.F., Bolivar, N. et al. 2012. Eliminating Stick-Slip by Managing Bit Depth of Cut and Minimizing Variable Torque in the Drillstring. Paper presented at the SPE/IADC Drilling Conference and Exhibition, San Diego, California. Society of Petroleum Engineers. DOI: 10.2118/151133-MS.

Detournay, E. and Defourny, P. 1992. A Phenomenological Model for the Drilling Action of Drag Bits. *International Journal of Rock Mechanics and Mining Sciences* **29** (1): 14. DOI: 10.1016/0148-9062(92)91041-3.

DiGiovanni, A., Stockey, D., Fuselier, D. et al. 2014. Innovative Non-Planar Face Pdc Cutters Demonstrate 21% Drilling Efficiency Improvement in Interbedded Shales and Sand. Paper presented at the IADC/SPE Drilling Conference and Exhibition, Fort Worth, Texas, USA. Society of Petroleum Engineers. DOI: 10.2118/168000-MS.

Drillstring Vibrations and Vibration Modeling. 2010. *Brochure*.  
[https://www.slb.com/~media/Files/drilling/brochures/drilling\\_opt/drillstring\\_vib\\_br.pdf](https://www.slb.com/~media/Files/drilling/brochures/drilling_opt/drillstring_vib_br.pdf).

Dufeyte, M.P. and Henneuse, H. 1991. Detection and Monitoring of the Slip-Stick Motion: Field Experiments. Paper presented at the SPE/IADC Drilling Conference, Amsterdam, The Netherlands. Society of Petroleum Engineers. DOI: 10.2118/21945-MS.

Dupriest, F.E. 2006. Comprehensive Drill Rate Management Process to Maximize Rop. Paper presented at the SPE Annual Technical Conference and Exhibition, San Antonio, Texas, USA. Society of Petroleum Engineers. DOI: 10.2118/102210-MS.

Dupriest, F.E. and Koederitz, W.L. 2005. Maximizing Drill Rates with Real-Time Surveillance of Mechanical Specific Energy. Paper presented at the SPE/IADC Drilling Conference, Amsterdam, The Netherlands. Society of Petroleum Engineers. DOI: 10.2118/92194-MS.

Dupriest, F.E. and Sowers, S.F. 2010. Maintaining Steerability While Extending Gauge Length to Manage Whirl. *SPE Drilling & Completion*. DOI: 10.2118/119625-PA



- Dwars, S. 2015. Recent Advances in Soft Torque Rotary Systems. Paper presented at the SPE/IADC Drilling Conference and Exhibition, London, United Kingdom. Society of Petroleum Engineers. DOI: 10.2118/173037-MS.
- Efteland, F., Coit, A., and McKenna, K.I. 2014. Surface Control Software Dramatically Mitigates Downhole Torsional Vibration in the Eagle Ford Shale Play as Validated by High-Speed Downhole Dynamics Data. Paper presented at the SPE Annual Technical Conference and Exhibition, Amsterdam, The Netherlands. Society of Petroleum Engineers. DOI: 10.2118/170925-MS.
- Ertas, D., Bailey, J.R., Wang, L. et al. 2013. Drillstring Mechanics Model for Surveillance, Root Cause Analysis, and Mitigation of Torsional and Axial Vibrations. Paper presented at the SPE/IADC Drilling Conference and Exhibition, Amsterdam, The Netherlands. Society of Petroleum Engineers. DOI: 10.2118/163420-MS.
- Falconer, I.G., Burgess, T.M., and Sheppard, M.C. 1988. Separating Bit and Lithology Effects from Drilling Mechanics Data. Paper presented at the IADC/SPE Drilling Conference, Dallas, Texas, USA. Society of Petroleum Engineers. DOI: 10.2118/17191-MS.
- Fear, M.J., Abbassian, F., Parfitt, S.H.L. et al. 1997. The Destruction of Pdc Bits by Severe Slip-Stick Vibration. Paper presented at the SPE/IADC Drilling Conference, Amsterdam, The Netherlands. Society of Petroleum Engineers. DOI: 10.2118/37639-MS.
- Freeman, D. 1999. 3-D Helps Cut Costs at Jonah Field. *AAPG Explorer* **20** (5): 14,16-14,16.
- Gent, J., Isenhour, J.D., Freeman, M. et al. 2009. Advanced Pdc Technologies Deliver Significant Performance Improvements in the Pinedale Anticline Production Interval. Paper presented at the SPE/IADC Drilling Conference and Exhibition, Amsterdam, The Netherlands. Society of Petroleum Engineers. DOI: 10.2118/119423-MS.
- Gibson, R.I. 1997. Greater Green River Basin. *Rocky Mountain Oil Journal*.
- Gray, D., Boerner, S., Marinic, D.T. et al. 2003. Fractured Reservoir Characterization Using Avaz on the Pinedale Anticline, Wyoming. *Canadian Society of Exploration Geophysicists Recorder* **2003** (5): 7.
- Gray, D., Boerner, S., Todorovic-Marinic, D. et al. 2003. Analyzing Fractures from Seismic for Improved Drilling Success. *WORLD OIL* **224** (10): 62-66,69.

- Gray, D., Marinic, D.T., and Lahr, M. 2002. Seismic Fracture Analysis on the Pinedale Anticline: Implications for Improving Drilling Success. Paper presented at the SEG International Exposition and 72nd Annual Meeting, Salt Lake City, Utah. Society of Exploration Geophysicists.
- Guerrero, C.A. and Kull, B.J. 2007. Deployment of an Serop Predictor Tool for Real-Time Bit Optimization. Paper presented at the SPE/IADC Drilling Conference, Amsterdam, The Netherlands,. Society of Petroleum Engineers. DOI: 10.2118/105201-MS.
- Han, G., Lemesany, L., Azizov, A.A. et al. 2013a. Bottomhole Assembly Result Analysis to Improve Drilling Performance in Pinedale Field, Wyoming, USA. Paper presented at the SPE Unconventional Resources Conference-Canada, Calgary, Alberta, Canada. Society of Petroleum Engineers. DOI: 10.2118/167140-MS.
- Han, G., Lemesany, L., Azizov, A.A. et al. 2013b. Practical Directional Drilling Techniques in Pinedale Field Wyoming to Improve Drilling Performance. Paper presented at the SPE Unconventional Resources Conference-Canada, Calgary, Alberta, Canada. Society of Petroleum Engineers. DOI: 10.2118/167141-MS.
- Herbig, C., Oueslati, H., Hohl, A. et al. 2015. Drillpipe Influence on Drilling Performance. Paper presented at the SPE/IADC Drilling Conference and Exhibition, London, United Kingdom. Society of Petroleum Engineers. DOI: 10.2118/173015-MS.
- Jain, J.R., Ledgerwood, L.W., Hoffmann, O.J.-M. et al. 2011. Mitigation of Torsional Stick-Slip Vibrations in Oil Well Drilling through Pdc Bit Design: Putting Theories to the Test. Paper presented at the SPE Annual Technical Conference and Exhibition, Denver, Colorado, USA. Society of Petroleum Engineers. DOI: 10.2118/146561-MS.
- Jain, J.R., Oueslati, H., Hohl, A. et al. 2014. High-Frequency Torsional Dynamics of Drilling Systems: An Analysis of the Bit-System Interaction. Paper presented at the IADC/SPE Drilling Conference and Exhibition, Fort Worth, Texas, USA. Society of Petroleum Engineers. DOI: 10.2118/167968-MS.
- Jansen, J.D. and Van den Steen, L. 1995. Active Damping of Self-Excited Torsional Vibrations in Oil Well Drillstrings. *Journal of Sound and Vibration* **179** (4): 22.
- Jogi, P.N. and Zoeller, W.A. 1992. The Application of a New Drilling Model for Evaluating Formation and Downhole Drilling Conditions. Paper presented at the SPE Petroleum Computer Conference, Houston. Texas, USA. Society of Petroleum Engineers. DOI: 10.2118/24452-MS.

- Jorden, J.R. and Shirley, O.J. 1966. Application of Drilling Performance Data to Overpressure Detection. *SPE Drilling*: 8. DOI: 10.2118/1407-PA.
- Kneller, S.R., Zinke, S.G., McDermott, R.W. et al. 2006. Unlocking the Potential of a Tight Gas Sand Giant: Pinedale Field, Wyoming. *Rocky Mountain Natural Gas Geology and Resources Conference (Denver, CO, 8/7-9/2006) Expanded Abstracts; The Mountain Geologist* **43** (3): 181-186.
- Kriesels, P.C., Keultjes, W.J.G., Dumont, P. et al. 1999. Cost Savings through an Integrated Approach to Drillstring Vibration Control. Paper presented at the SPE/IADC Middle East Drilling Technology Conference, Abu Dhabi, UAE. Society of Petroleum Engineers. DOI: 10.2118/57555-MS.
- Lai, S.W., Wood, M.J., Eddy, A.J. et al. 2014. Stick-Slip Detection and Friction Factor Testing Using Surface-Based Torque and Tension Measurements. Paper presented at the SPE Annual Technical Conference and Exhibition, Amsterdam, The Netherlands. Society of Petroleum Engineers. DOI: 10.2118/170624-MS.
- Law, B.E. and Spencer, C.W. 1989. *Geology of Tight Gas Reservoirs in the Pinedale Anticline Area, Wyoming, and at the Multiwell Experiment Site, Colorado*. U.S. Geological Survey Bulletin: 1886: [Reston, Va.?] : Dept. of the Interior, U.S. Geological Survey ; Denver, CO : For sale by the Books and Open-File Reports Section, 1989. Original edition. ISBN.
- Ledgerwood, L.W., Hoffmann, O.J.-m., Jain, J.R. et al. 2010. Downhole Vibration Measurement, Monitoring, and Modeling Reveal Stick/Slip as a Primary Cause of Pdc-Bit Damage in Today. Paper presented at the SPE Annual Technical Conference and Exhibition, Florence, Italy. Society of Petroleum Engineers. DOI: 10.2118/134488-MS.
- Ledgerwood, L.W., Jain, J.R., Hoffmann, O.J. et al. 2013. Downhole Measurement and Monitoring Lead to an Enhanced Understanding of Drilling Vibrations and Polycrystalline Diamond Compact Bit Damage. *SPE Drilling & Completion*. DOI: 10.2118/134488-PA.
- Leine, R.I. and van Campen, D.H. 2002. Stick-Slip Whirl Interaction in Drillstring Dynamics. *Journal of vibration and acoustics* **124** (2): 209-220.
- Lubinski, A. 1950. A Study of the Buckling of Rotary Drilling Strings. American Petroleum Institute.
- Medley, G.H., Jr., Shook, R.A., and Hansen, J.T. 1997. State-of-the-Art Slim-Hole Drilling in the Green River Basin in Wyoming: A Three Well Case History.

- Paper presented at the SPE Rocky Mountain Regional Meeting, Casper, Wyoming, USA. Society of Petroleum Engineers. DOI: 10.2118/38361-MS.
- Nelson, P.H., Ewald, S.M., Santus, S.L. et al. 2009. Gas, Oil, and Water Production from Jonah, Pinedale, Greater Wamsutter, and Stagecoach Draw Fields in the Greater Green River Basin, Wyoming. *U.S. Geological Survey Open-File Report*: 19.
- Nessjoen, P.J., Kyllingstad, A., Dambrosio, P. et al. 2011. Field Experience with an Active Stick-Slip Prevention System. Paper presented at the SPE/IADC Drilling Conference and Exhibition, Amsterdam, The Netherlands. Society of Petroleum Engineers. DOI: 10.2118/139956-MS.
- Oueslati, H., Jain, J.R., Reckmann, H. et al. 2013. New Insights into Drilling Dynamics through High-Frequency Vibration Measurement and Modeling. Paper presented at the SPE Annual Technical Conference and Exhibition, New Orleans, Louisiana, USA. Society of Petroleum Engineers. DOI: 10.2118/166212-MS.
- Overview: Kymera Fsr Directional Hybrid Drill Bit. 2014. *Brochure*.  
[http://public.bakerhughes.com/fastcurve/pdf/40820\\_Kymera\\_directional\\_OV.pdf](http://public.bakerhughes.com/fastcurve/pdf/40820_Kymera_directional_OV.pdf)
- Pastusek, P. and Brackin, V. 2003. A Model for Borehole Oscillations. Paper presented at the SPE Annual Technical Conference and Exhibition, Denver, Colorado, USA. Society of Petroleum Engineers. DOI: 10.2118/84448-MS.
- Pastusek, P.E., Brackin, V.J., and Lutes, P.J. 2005. A Fundamental Model for Prediction of Hole Curvature and Build Rates with Steerable Bottomhole Assemblies. Paper presented at the SPE Annual Technical Conference and Exhibition, Dallas, Texas, USA. Society of Petroleum Engineers. DOI: 10.2118/95546-MS.
- Pastusek, P.E., Cooley, C.H., Sinor, L.A. et al. 1992. Directional and Stability Characteristics of Anti-Whirl Bits with Non-Axisymmetric Loading. Paper presented at the Annual Technical Conference and Exhibition of the Society of Petroleum Engineers, Washington, DC, USA. Society of Petroleum Engineers. DOI: 10.2118/24614-MS.
- Pastusek, P.E., Sullivan, E., and Harris, T.M. 2007a. Development and Utilization of a Bit Based Data Acquisition System in Hard Rock Pdc Applications. Paper presented at the SPE/IADC Drilling Conference, Amsterdam, The Netherlands. Society of Petroleum Engineers. DOI: 10.2118/105017-MS.
- Pastusek, P.E., Sullivan, E., and Harris, T.M. 2007b. Development and Utilization of a Bit Based Data Acquisition System in Hard Rock Pdc Applications. Society of Petroleum Engineers. DOI: 10.2118/105017-MS.

- Pessier, R. and Damschen, M. 2010. Hybrid Bits Offer Distinct Advantages in Selected Roller-Cone and Pdc Bit Applications. Paper presented at the IADC/SPE Drilling Conference and Exhibition, New Orleans, Louisiana, USA. Society of Petroleum Engineers. DOI: 10.2118/128741-MS.
- Pessier, R.C. and Fear, M.J. 1992. Quantifying Common Drilling Problems with Mechanical Specific Energy and a Bit-Specific Coefficient of Sliding Friction. Paper presented at the Annual Technical Conference and Exhibition of the Society of Petroleum Engineers, Washington, DC, USA. Society of Petroleum Engineers. DOI: 10.2118/24584-MS.
- Reckmann, H., Jogi, P., and Herbig, C. 2007. Using Dynamics Measurements While Drilling to Detect Lithology Changes and to Model Drilling Dynamics. *ASME 2007 26th International Conference on Offshore Mechanics and Arctic Engineering* Volume 2: Structures, Safety and Reliability; Petroleum Technology Symposium, San Diego, California, USA, June 10–15, 2007.
- Reckmann, H., Jogi, P., Kpetehoto, F.T. et al. 2010. Mwd Failure Rates Due to Drilling Dynamics. Paper presented at the IADC/SPE Drilling Conference and Exhibition, New Orleans, Louisiana, USA. Society of Petroleum Engineers. DOI: 10.2118/127413-MS.
- Richard, T. and Detournay, E. 2000. Stick-Slip Vibrations of Pdc Bits. American Rock Mechanics Association.
- Robinson, J.W. 2000. Discovery of Jonah Field, Sublette County, Wyoming. *Mountain Geologist* **37** (3): 135-143.
- Robnett, E.W., Hood, J.A., Heisig, G. et al. 1999. Analysis of the Stick-Slip Phenomenon Using Downhole Drillstring Rotation Data. Paper presented at the SPE/IADC Drilling Conference, Amsterdam, Holland. Society of Petroleum Engineers. DOI: 10.2118/52821-MS.
- Runia, D.J., Dwars, S., and Stulemeijer, I.P.J.M. 2013. A Brief History of the Shell &quot;Soft Torque Rotary System&quot; and Some Recent Case Studies. Paper presented at the SPE/IADC Drilling Conference and Exhibition, Amsterdam, The Netherlands. Society of Petroleum Engineers. DOI: 10.2118/163548-MS.
- Santos, H., Placido, J.C.R., and Wolter, C. 1999. Consequences and Relevance of Drillstring Vibration on Wellbore Stability. Paper presented at the SPE/IADC Drilling Conference, Amsterdam, Holland. Society of Petroleum Engineers. DOI: 10.2118/52820-MS.

- Sowers, S.F., Dupriest, F.E., Bailey, J.R. et al. 2009. Use of Roller Reamers Improves Drilling Performance in Wells Limited by Bit and Bottomhole Assembly Vibrations. Paper presented at the SPE/IADC Drilling Conference and Exhibition, Amsterdam, The Netherlands. Society of Petroleum Engineers. DOI: 10.2118/119375-MS.
- Spencer, C.W. 1989. Comparison of Overpressuring at the Pinedale Anticline Area, Wyoming, and the Multiwell Experiment Site, Colorado. In *Geology of Tight Gas Reservoirs in the Pinedale Anticline Area, Wyoming, and at the Multiwell Experiment Site, Colorado*: U.S. Geological Survey Bulletin.
- Teale, R. 1964. The Concept of Specific Energy in Rock Drilling. *Int. J. Rock Mech. Mining Sci.* **2**: 57-73.
- Warren, T.M., Brett, J.F., and Sinor, L.A. 1990. Development of a Whirl-Resistant Bit. *SPE Drilling Engineering*. DOI: 10.2118/19572-PA.
- Warren, T.M. and Oster, J.H. 1998. Torsional Resonance of Drill Collars with Pdc Bits in Hard Rock. Paper presented at the SPE Annual Technical Conference and Exhibition, New Orleans, Louisiana, USA. Society of Petroleum Engineers. DOI: 10.2118/49204-MS.
- Waughman, R.J., Kenner, J.V., and Moore, R.A. 2003. Real-Time Specific Energy Monitoring Enhances the Understanding of When to Pull Worn Pdc Bits. *SPE Drilling & Completion*. DOI: 10.2118/81822-PA.

## APPENDIX A: INFORMATION PROVIDED BY ULTRA PETROLEUM

### **Data Received**

The data that has been received to complete this project includes, but is not limited to:

- Well API numbers
- Open hole well logs
- Mud logs and mud reports
- Geologist formation picks
- Well schematics and directional plans
- Final well surveys
- Bit records and pictures
- Daily drilling reports
- NOV BlackBox and LMS data
- Pason 1-second data and access to the U.S. reporting hub
- Schlumberger Power-V data
- Drill bit datasheets
- Third party vibrations analysis